Introduction to Reservoir Geomechanics

1 Introduction

Definitions and some challenges of reservoir geomechanics.
Modeling of coupled phenomena.

2 Constitutive Laws: Behavior of Rocks

Fundamentals of Pore-Mechanics.

3 Constitutive Laws: Behavior of Fractures

Geomechanics of Fractured Media.

4 Reservoir Geomechanics

Elements of a geomechanical model and applications.

5 Unconventional Reservoirs

Naturally fractured reservoirs, hydraulic fracture, proppant and fracture closure model, validation (microseismicity).

6 Advanced Topics

Injection of reactive fluids and rock integrity.

Reservoir Geomechnics

micro

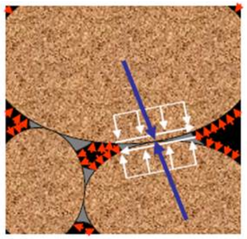

lab

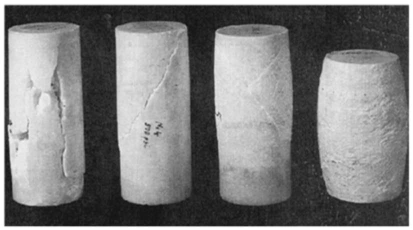

Earth Sciences and Engineering:

Problems Scales

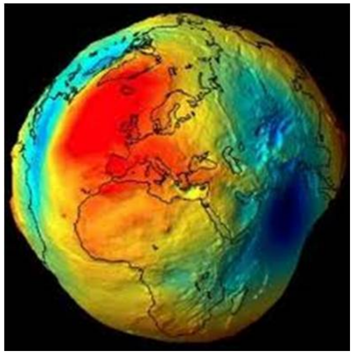

Earth

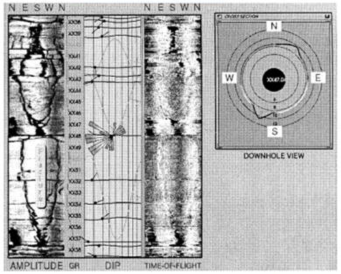

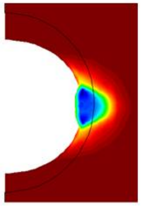

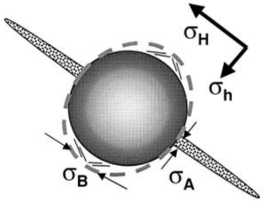

wellbore

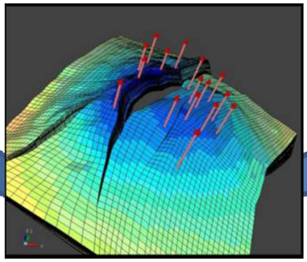

reservoir

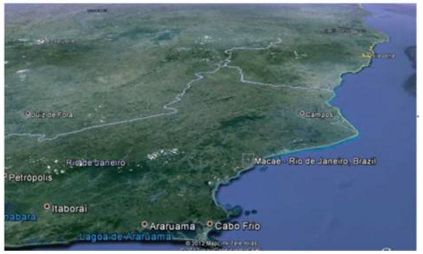

basin

UFPE

Reservoir Geomechnics

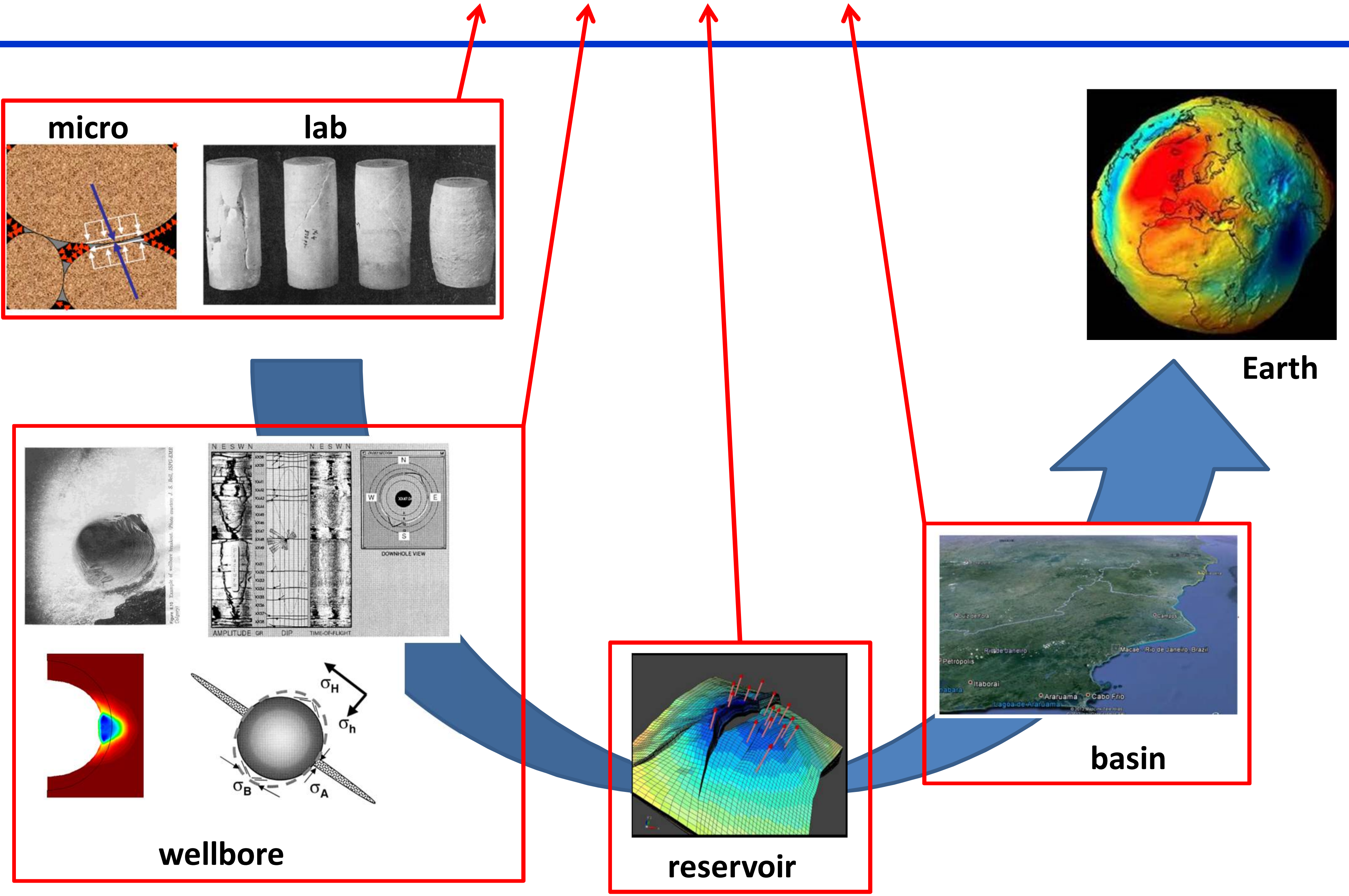

Reservoir Geomechnics

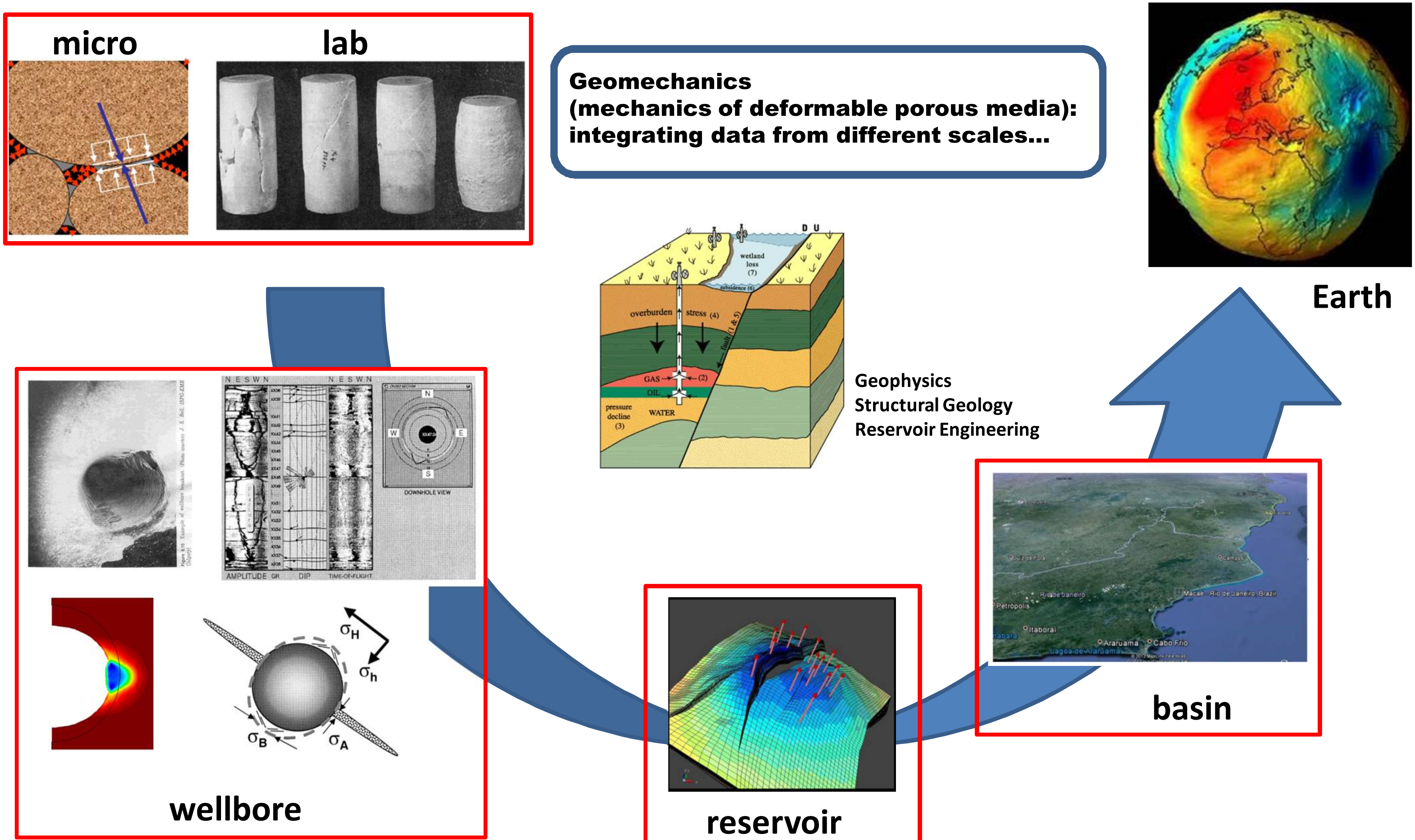

Underground stresses

Normally, an underground formation has to carry the weight of the overlying formations.

The vertical stress at the bottom of a homogeneous column of height z is:

$$\sigma_v = \rho g z$$

where ρ is the density of the material and g is the acceleration of gravity.

If the density varies with depth, the vertical stress at depth D becomes:

$$\sigma_v = \int_0^D \rho(z) g \, dz$$

Off-shore

$$\sigma_v = \rho_w g z_w + \int_{z_w}^D \rho(z) g dz$$

The average density of sediments in the overburden is between 1.8 and 2.2 g/cm3, so as a rough number, the vertical stress increases downwards with about 20 MPa/km (typically 1 psi/ft).

Note: $\rho = (1-\phi)\rho_s + \phi(S_w \rho_w + S_o \rho_o)$

Fluid Pressure

The sedimentary rocks encountered during oil well drilling and production are porous and hence contain fluids. One refers to the pore pressure at depth D as normal if it is given by the weight of a fluid column above, the normal pore pressure p_{fn} is

$$p_{\mathrm{fn}} = \int_0^D \rho_{\mathrm{f}}(z) g \, \mathrm{d}z$$

The pore fluid density in case of brine with sea water salinity is in the range 1.03–1.07 g/cm3, so the pore pressure increase with depth is roughly 10 MPa/km (0.45 psi/ft).

The effective vertical stress, σ'_v, is then also increasing with approximately 10 MPa/km. In many important cases, however, the pore pressure deviates from the normal value p_{fn} (abnormal pore pressures).

Effective stress tensor:

$$\boldsymbol{\sigma}' = \begin{pmatrix} \sigma_1 - P_f & \tau_{12} & \tau_{13} \\ \tau_{21} & \sigma_2 - P_f & \tau_{23} \\ \tau_{31} & \tau_{32} & \sigma_3 - P_f \end{pmatrix}$$

Underground stresses

Vertical stress - Integration of density values (obtained from the density profiles); $\rho(z)$ - Specific weight along the depth.

Pore Pressure - Direct measurement ; Bottom well pressure transducers

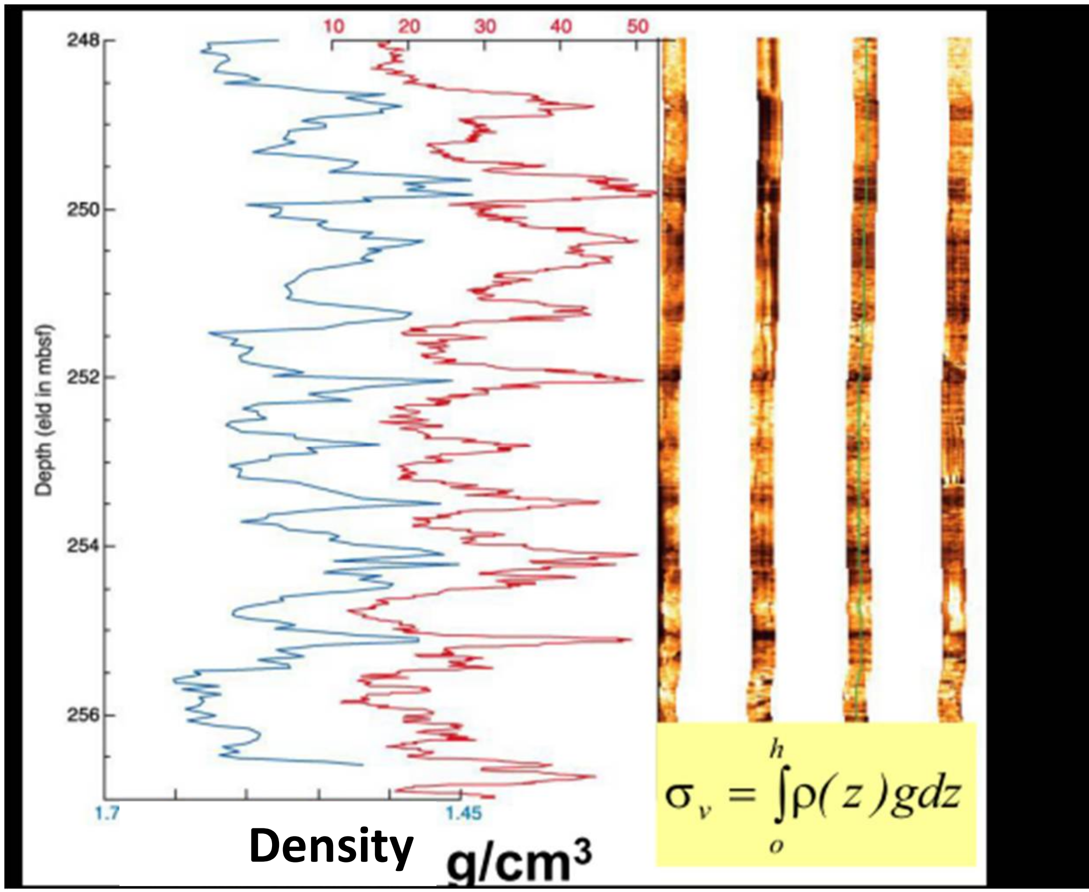

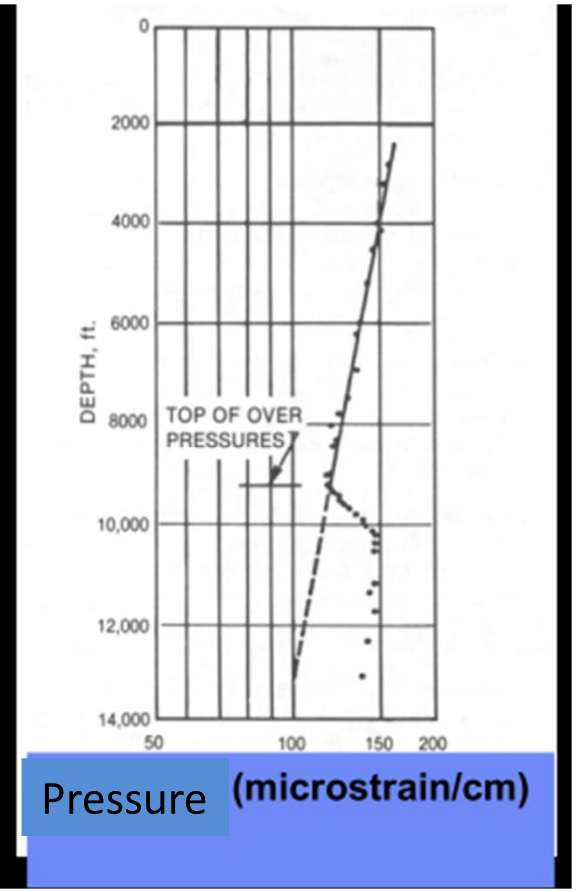

Density Profile L. Cabral (MSc, 2007) **Sonic Profile**

Fluid Pressure

Scenario 1: only sands are deposited in the basin

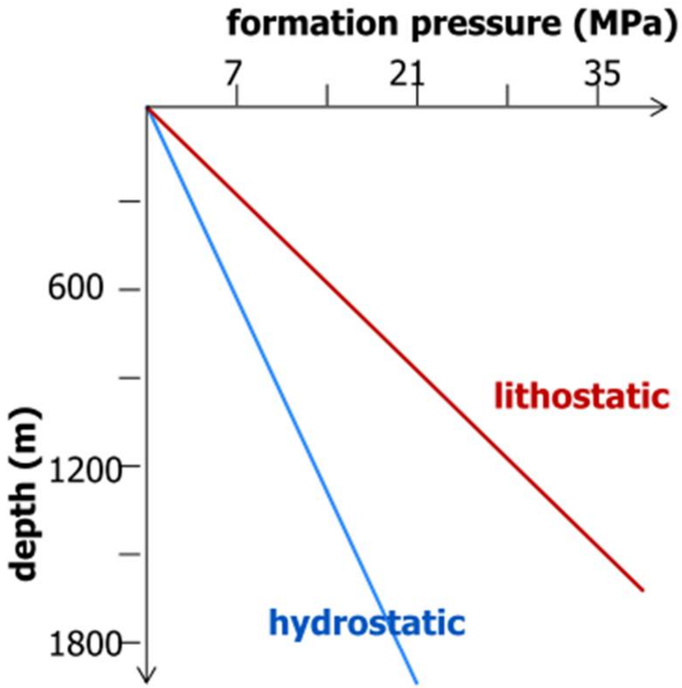

1. draw a curve indicating the pore pressure with depth
2. draw for the deviatoric stress
3. draw 4 Mohr circles showing the 2D state of stress at 0, 600, 1200 and 1800m.
4. do you predict fracturing?

$$\begin{pmatrix} \sigma_1 - P_f & \tau_{12} & \tau_{13} \\ \tau_{21} & \sigma_2 - P_f & \tau_{23} \\ \tau_{31} & \tau_{32} & \sigma_3 - P_f \end{pmatrix}$$

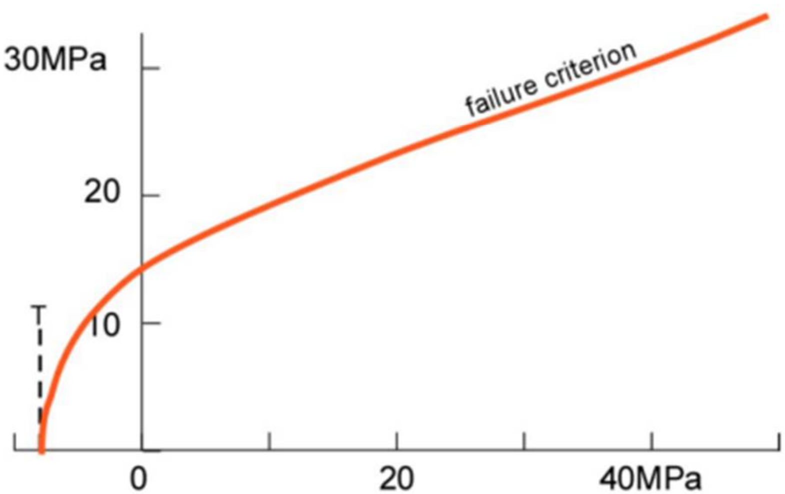

Fluid Pressure

Zones of overpressure

At deposition depths, sediments have 50-80% (sea) water

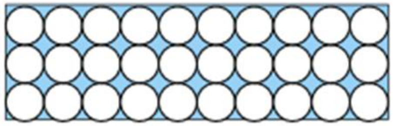

While subsiding the sediments will be covered by other sediments. Two situations are expected depending on the properties of the cover

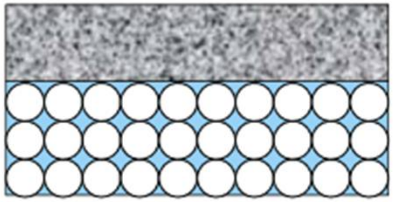

If fluids **can escape**, increasing lithostatic pressure carried by grains = pressure on grain contacts increases

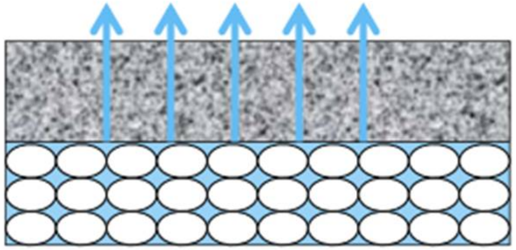

If fluids cannot escape, pore pressure will build and will contribute in carrying the increasing lithostatic pressure.

This decreases the grain-to-grain pressure

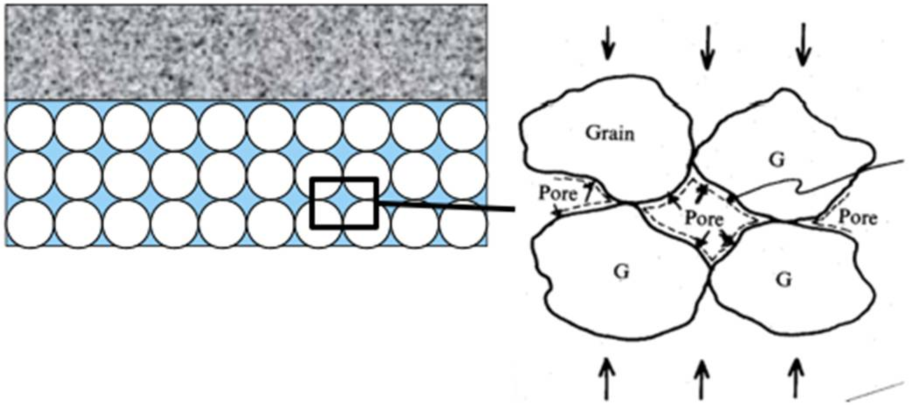

Fluid Pressure

Scenario 2: the first tens of meters of sand are following by a thick layer of impermeable shale

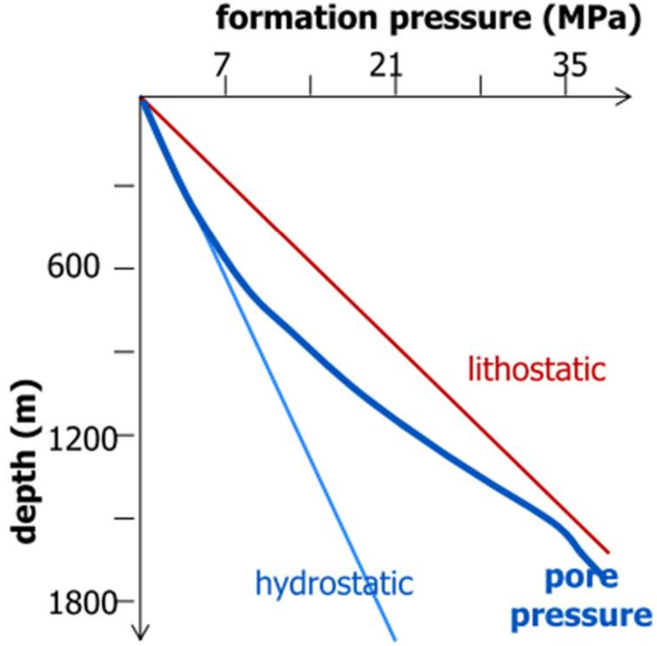

1. Think at the meaning of the pore pressure curve shown in the plot
2. draw for the deviatoric stress
3. draw 4 Mohr circles showing the 2D state of stress at 0, 600, 1200 and 1800m.
4. do you predict fracturing?

$$\begin{pmatrix} \sigma_1 - P_f & \tau_{12} & \tau_{13} \\ \tau_{21} & \sigma_2 - P_f & \tau_{23} \\ \tau_{31} & \tau_{32} & \sigma_3 - P_f \end{pmatrix}$$

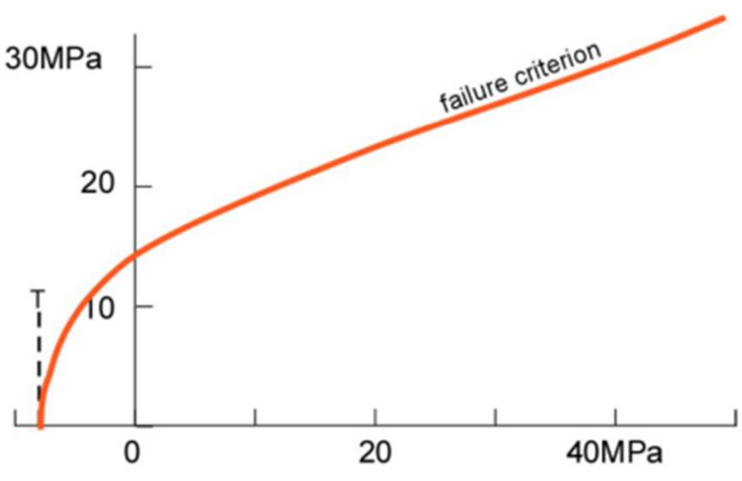

Fluid Pressure

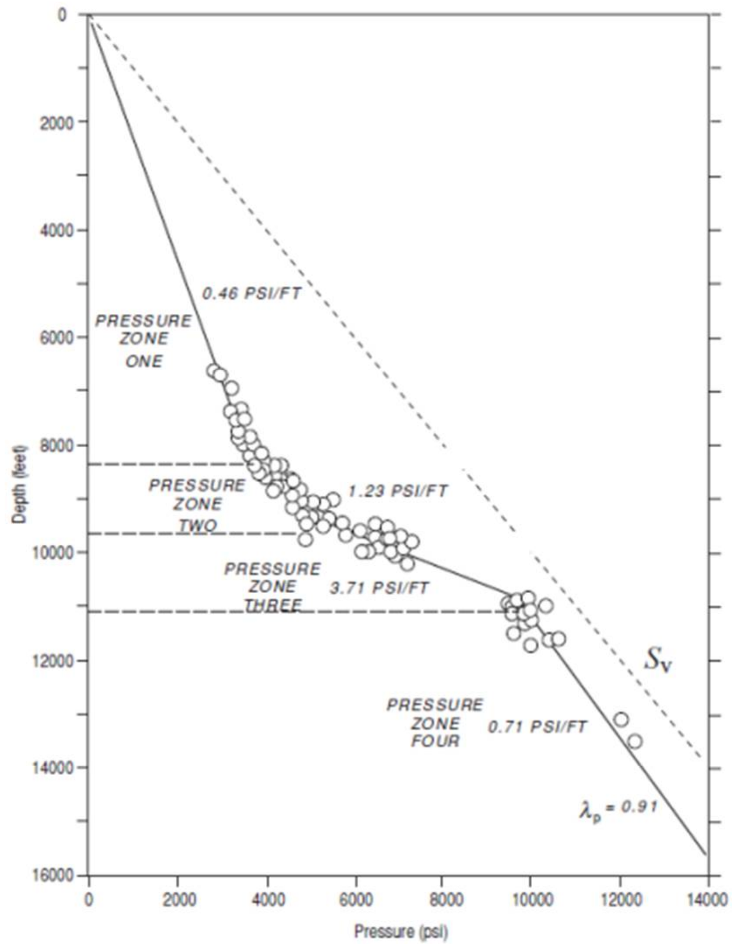

Figura 4.1: *Gráfico da pressão de poros × profundidade do Campo de Monte Cristo-Golfo do México. Na primeira zona de pressão(∼8.300ft) é observada pressão hidrostática. Na segunda e terceira zonas, observa-se uma transição onde a pressão de poros cresce rapidamente (no caso, com um gradiente de ≈3,7psi/ft) e na quarta zona (a partir de ∼11.000ft), nota-se uma pressão de poros extremamente elevada (Zoback, M. D., 2007).*

Underground stresses

Horizontal Stress:

$$\sigma'_h = K'\sigma'_v$$

K' (lateral earth stress coefficient) may vary significantly.

At shallow depths (0–150 m) it may vary from 1 to 10 or even higher.

At larger depths it may vary from 0.2 to 1.5.

Chemical compaction increases in importance at depths below 2–3 km (Bjørlykke and Høeg, 1997). It will contribute to horizontal stresses by altering the trend seen from pure mechanical compaction above this level.

It has been suggested that, with time, $K' \rightarrow 1$, so that the stress state becomes hydro-static (Heim's rule) due to creep (very slow process).

Underground stresses

Models for estimating the in situ stress states:

Formation laterally constrained ($\varepsilon_x = \varepsilon_y = 0$)
rock behaves according to the theory of linear elasticity:

$$\sigma'_{\mathrm{h}} = \frac{\nu_{\mathrm{fr}}}{1 - \nu_{\mathrm{fr}}}\sigma'_{\mathrm{v}}$$

(lateral stress coefficient at rest, $K' = K_0$)

In a fluid, where $\nu_{fr} = 1/2$, $K_0 = 1$. For a rock with $\nu_{fr} = 1/3$, $K_0 = 1/2$

There are many reasons to apply the relationship above with great care...

Stress history analysis must be performed (Warpinski, 1989), incorporating variations in mechanical properties over time:

Consolidation, diagenesis, changes in pore pressure due to gas generation, temperature gradients, and various tectonic and thermal episodes.

Viscoelasticity appeared to be more relevant for stresses in shale than in sandstone (Warpinski, 1989).

Underground stresses

Models for estimating the in situ stress states:

Rock at failure: reasonable assumption in areas of active tectonics.

Mohr-Coulomb:

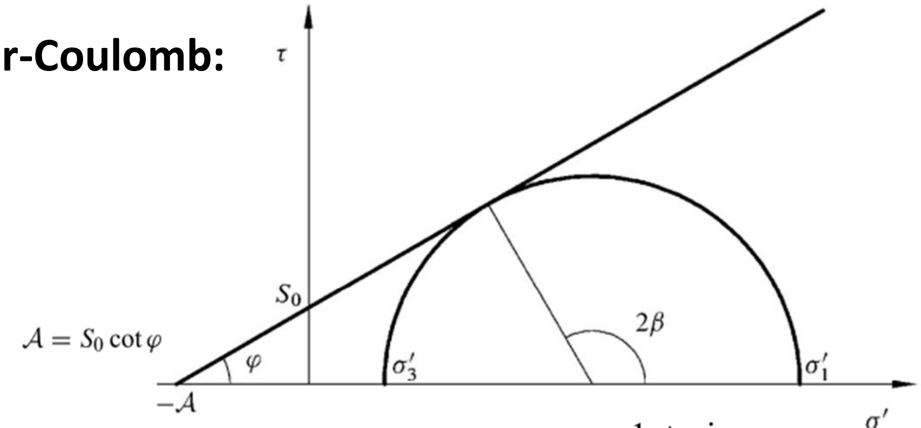

$$\sigma'_1 = 2S_0 \frac{\cos\varphi}{1-\sin\varphi} + \sigma'_3 \frac{1+\sin\varphi}{1-\sin\varphi}$$

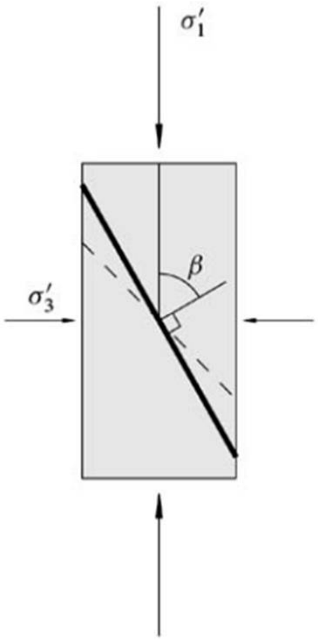

Assuming coesion=0:

$$K' = \frac{1-\sin\varphi}{1+\sin\varphi}$$

If the friction angle is 30°, then $K' = 1/3$**.**
A lower friction angle will result in a higher value for K'**.**

Faults and the stress state: Brittle behaviour leading to fault formation is characteristic of rocks subjected to **low confining pressure**, i.e. in some respect **close to the surface** of the Earth.

Relevant information from the faults: relative magnitude of principal stresses.

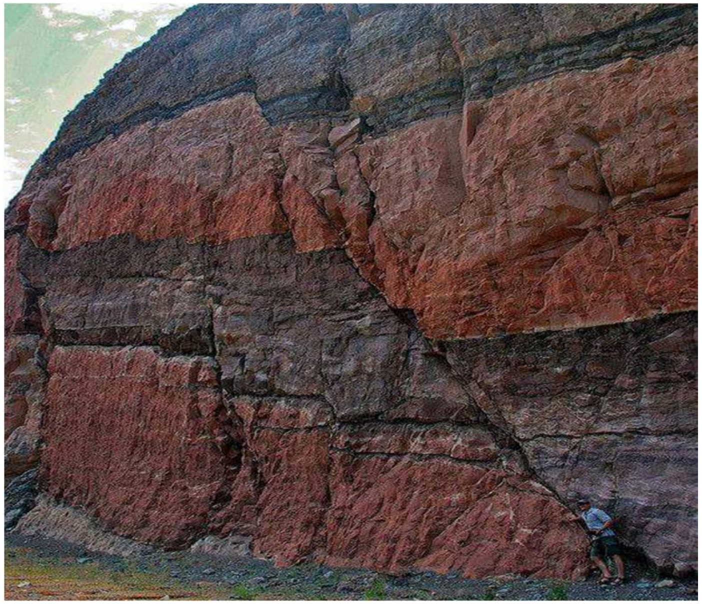

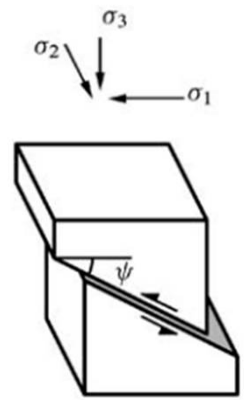

σ_3 vertical

Thrust fault

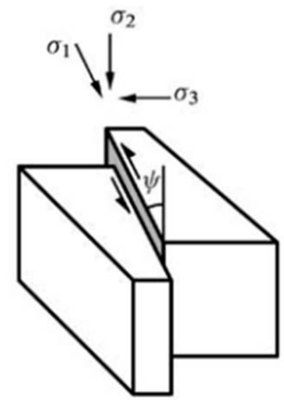

σ_2 vertical

Strike-slip fault

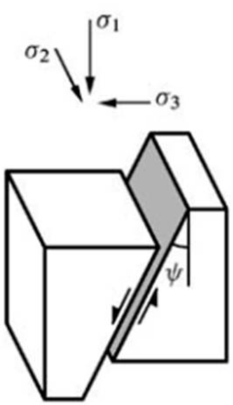

σ_1 vertical

Normal fault

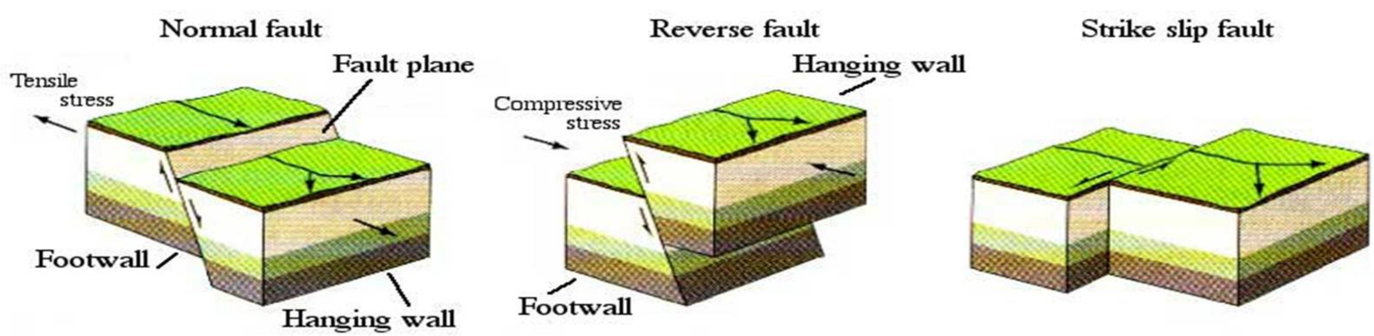

Faults and the stress state: Brittle behaviour leading to fault formation is characteristic of rocks subjected to low confining pressure, i.e. in some respect close to the surface of the Earth.

Relevant information from the faults: relative magnitude of principal stresses.

Anderson, E. M. (1951):

Fracturing will take place in **one or both pairs of conjugate planes** which are **parallel to** the direction of the **intermediate principal stress**, and are **both at equal angles (ψ) of less than 45° to the direction of the maximum principal stress**.

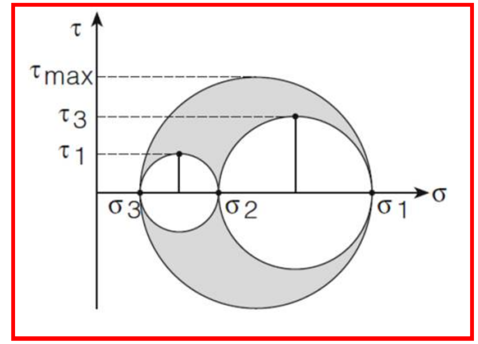

Mohr-Coulumb Criteria (shear failure):

$$\sigma_1' = C_0 + \sigma_3' \tan^2 \beta$$

$$\psi = \pi/2 - \beta$$

35°–20° | 55°–70° sandstone

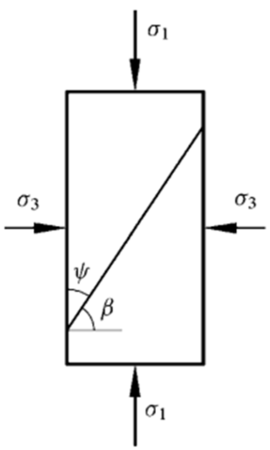

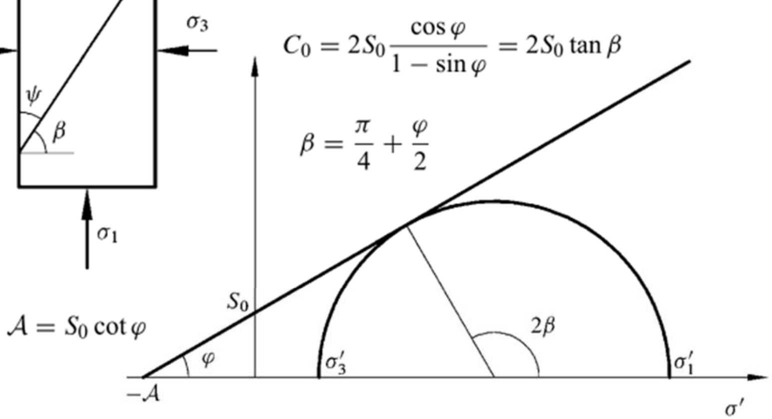

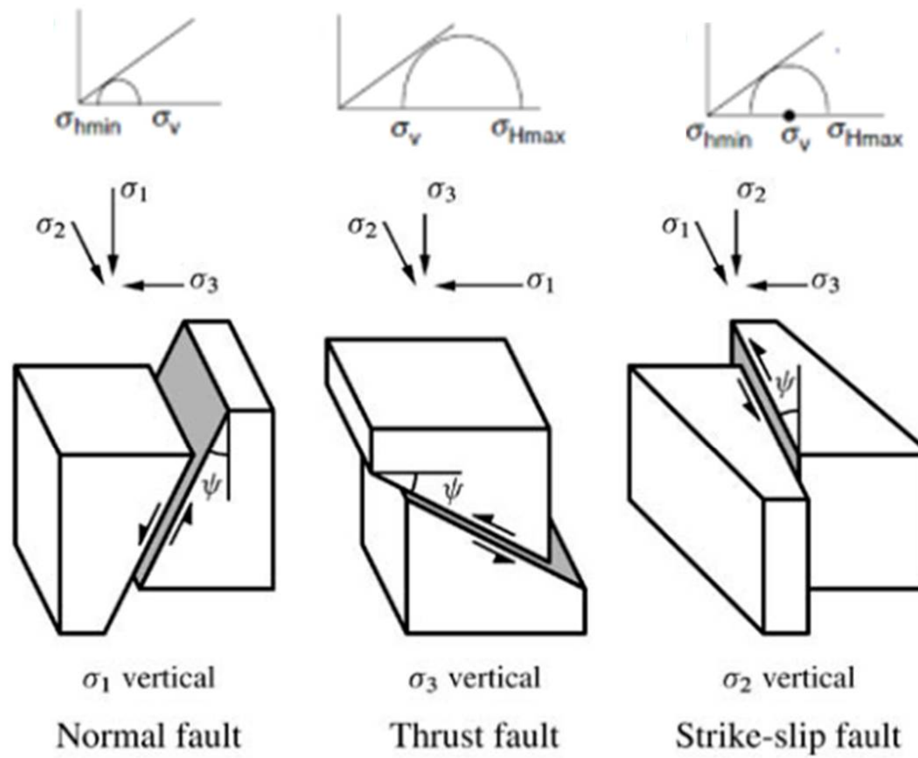

Stress Polygon

(Zoback, M. D., 2007)

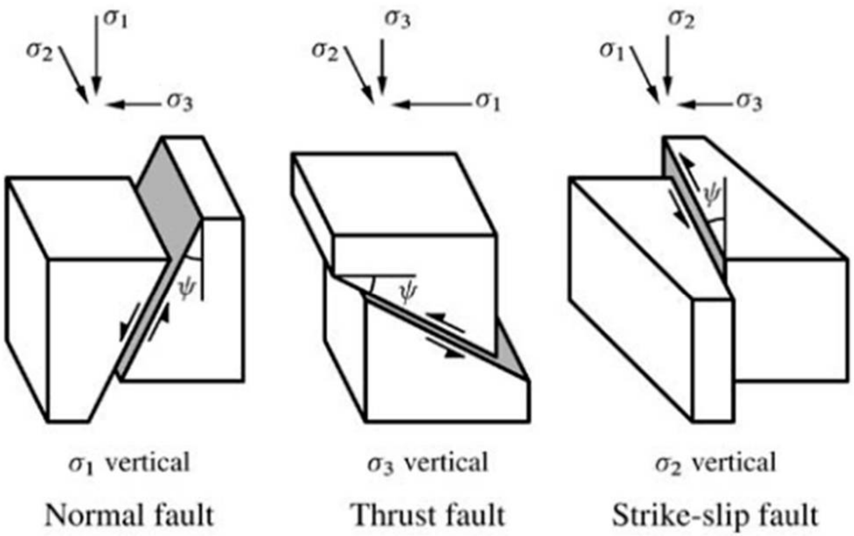

Mohr-Coulomb Failure Surface

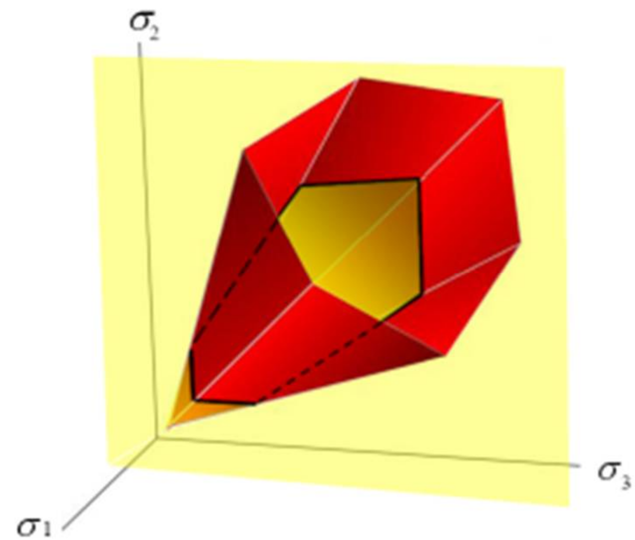

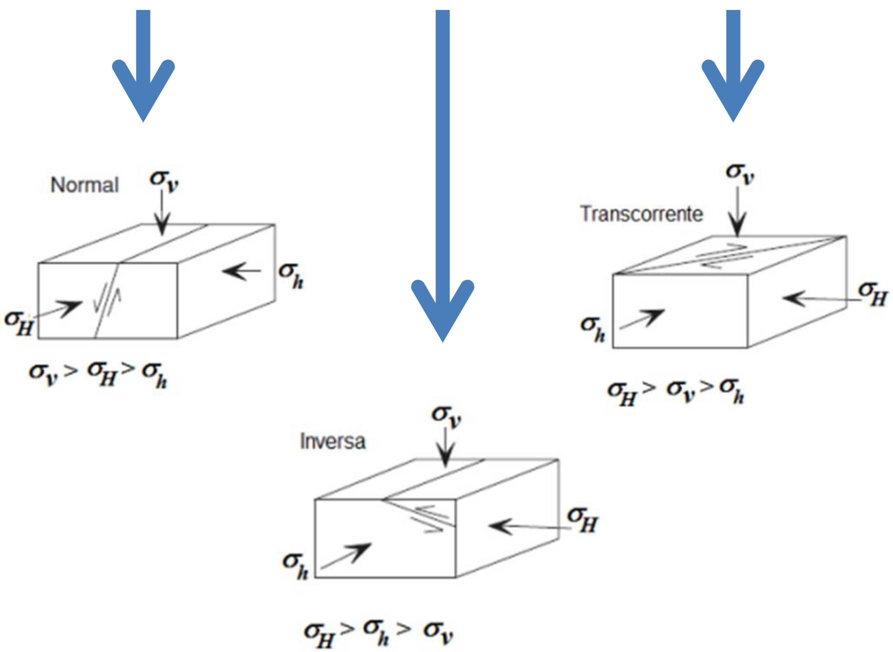

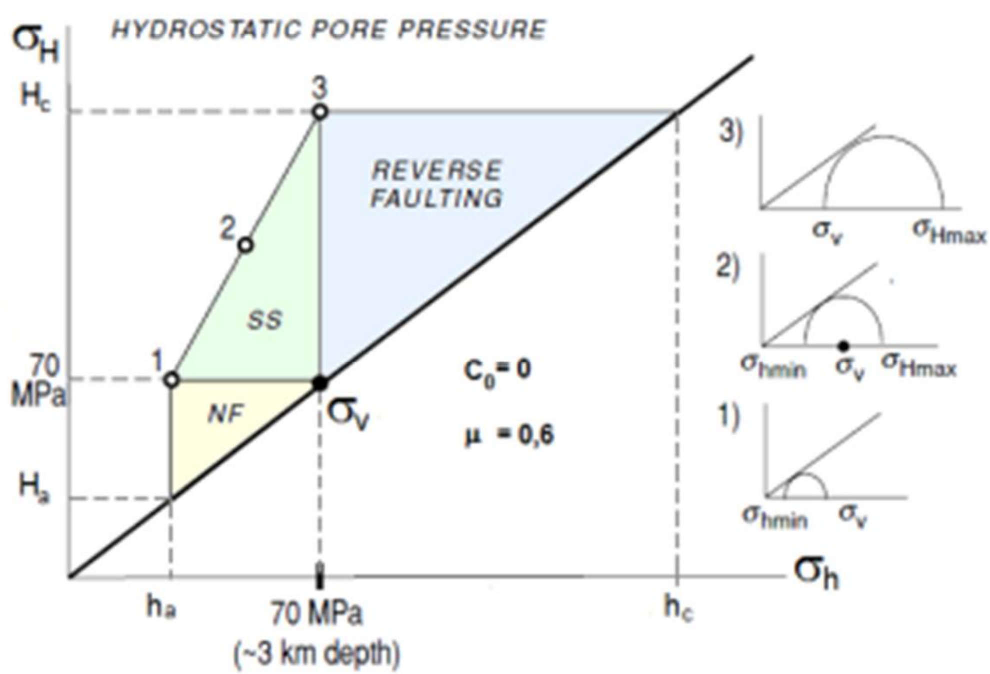

Underground stresses

CONCLUSION: These are very simple examples of models for horizontal stress estimation. In reality, horizontal stresses are difficult to assess from mathematical models. The most direct method of obtaining horizontal stress is to measure it, for instance by a fracturing test of the formation.

Example: Gulf Coast Curve

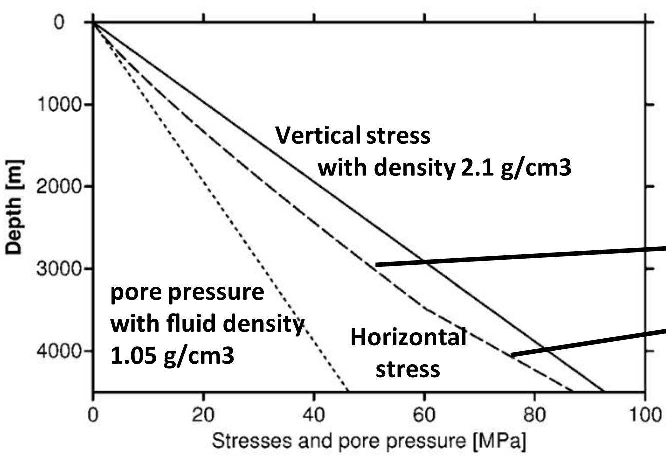

Breckels and van Eekelen (1982) used fracturing data from whole regions, and derived relationships between horizontal stress and depth. They also accounted for possibly abnormal pore pressures. For the US Gulf Coast, Breckels and van Eekelen presented the following relations:

$$\sigma_h = 0.0053 D^{1.145} + 0.46(p_f - p_{fn}) \quad (D < 3500\,\mathrm{m})$$

$$\sigma_h = 0.0264 D - 31.7 + 0.46(p_f - p_{fn}) \quad (D > 3500\,\mathrm{m})$$

"Gulf Coast Curve"

where D is depth in metres, p_f is the pore pressure in MPa, p_{fn} is the *normal* pore pressure (corresponding to a gradient of 10.5 MPa/km) and σ_h is the smallest horizontal stress in MPa. Note that these relations were developed at zero or shallow water depths

Underground stresses

Simple Stress Fields

It is very common (and convenient) in the oil industry.

Assumptions:

- Three mutually orthogonal principal stresses, plus the pore pressure

- Vertical stress is a principal stress, governed by gravity, pointing towards the centre of the Earth.

Reasonable at large depth within a homogeneous Earth, in areas that have NOT been exposed to tectonic activity or are relaxed in the sense that there are no remnant stresses from previous tectonic activity.

Complex Stress Fields

Be aware that there will be cases when this is not fulfilled, such as:

- Near the surface: Because the surface is stress free, the principal stress directions at and near it will be governed by the surface topography. In the case of a strongly sloping surface, even at depth, the principal stress directions may be far from the vertical-horizontal directions.

- Near heterogeneities such as inclusions or faults, near underground openings such as boreholes, or near depleting reservoirs, principal stress directions will differ from the vertical–horizontal orientation.

Leak-off test: obtainig the minimum principal stress (Smin)

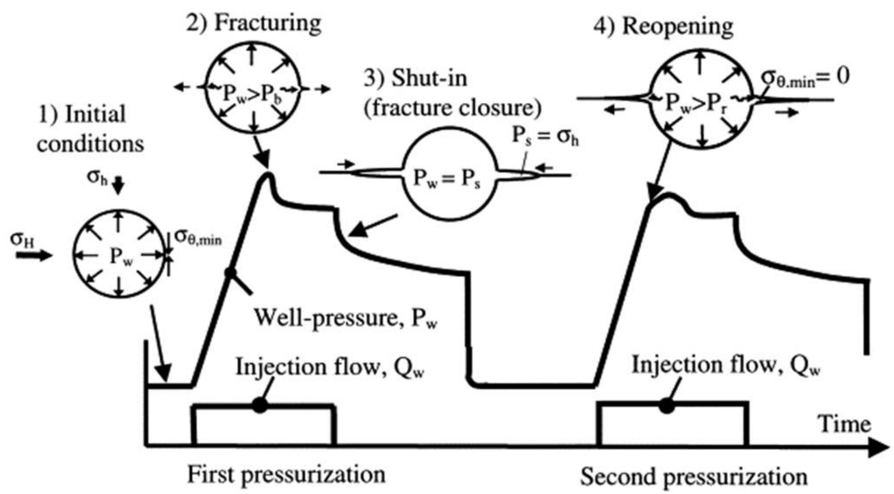

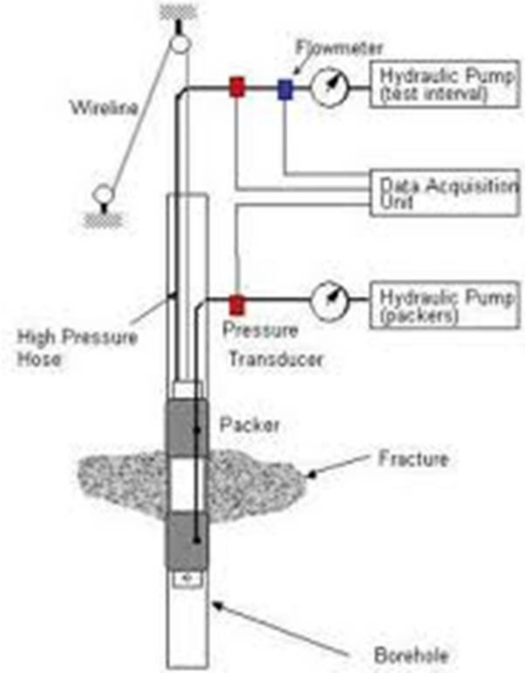

"the only practical and reliable"

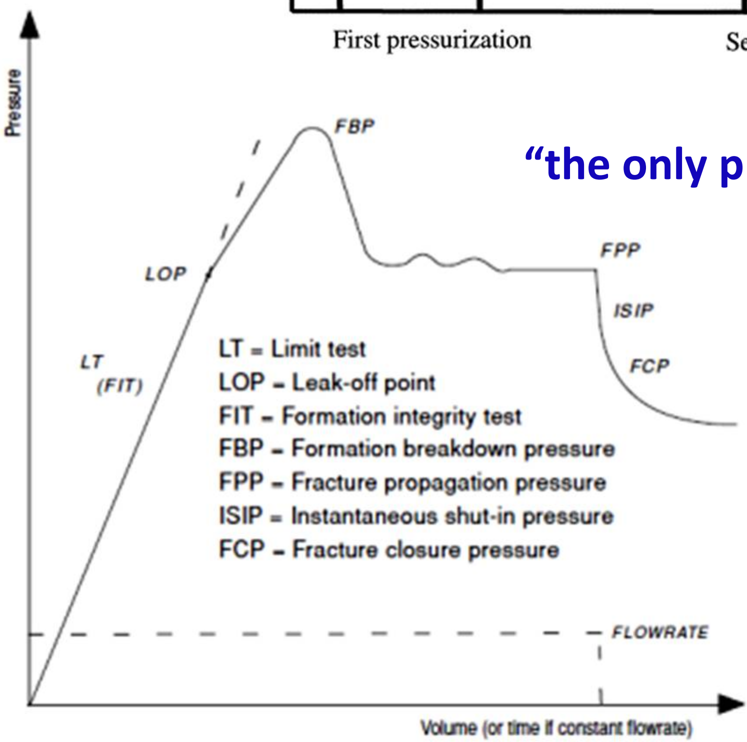

LOP (leak-off point)

FBP (fracture breakdown pressure)

FPP (fracture propagation pressure)

ISIP (instantaneous shut-in pressure)

FCP (fracture closure pressure)

Discontinuities in Reservoir Geomechanics

Shale gas *(Source: The Old Speak Journal, 2011)*

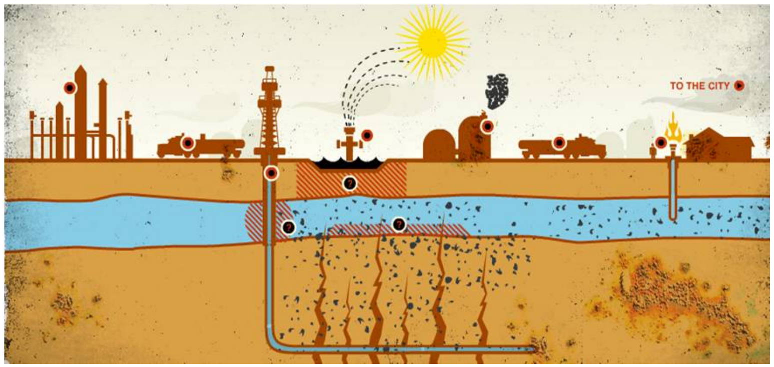

Contamination of an aquifer caused by hydraulic fracturing

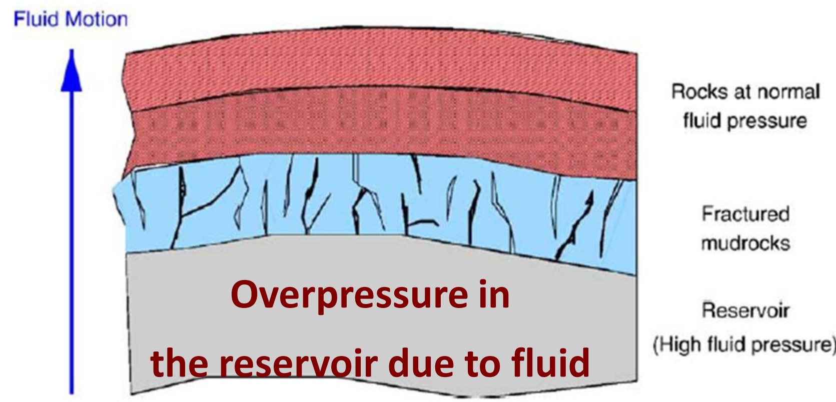

Overpressure in the reservoir due to fluid injection (water, CO_2,...)

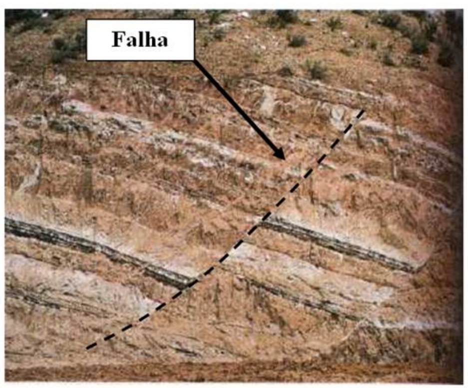

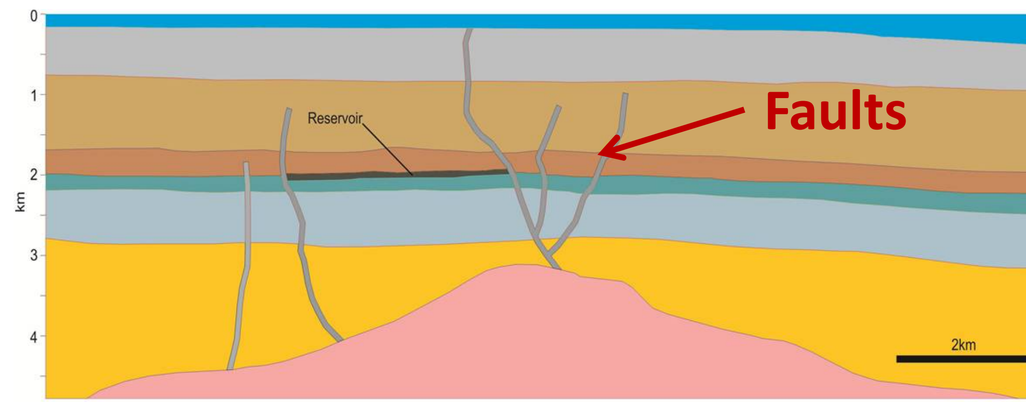

***Enviromental Geomechanics*:**

Geomechnics is often dealing with enviromental problems

Discontinuities in Reservoir Geomechanics

- Hydraulic Fracturing: a subject of great interest of the oil industry

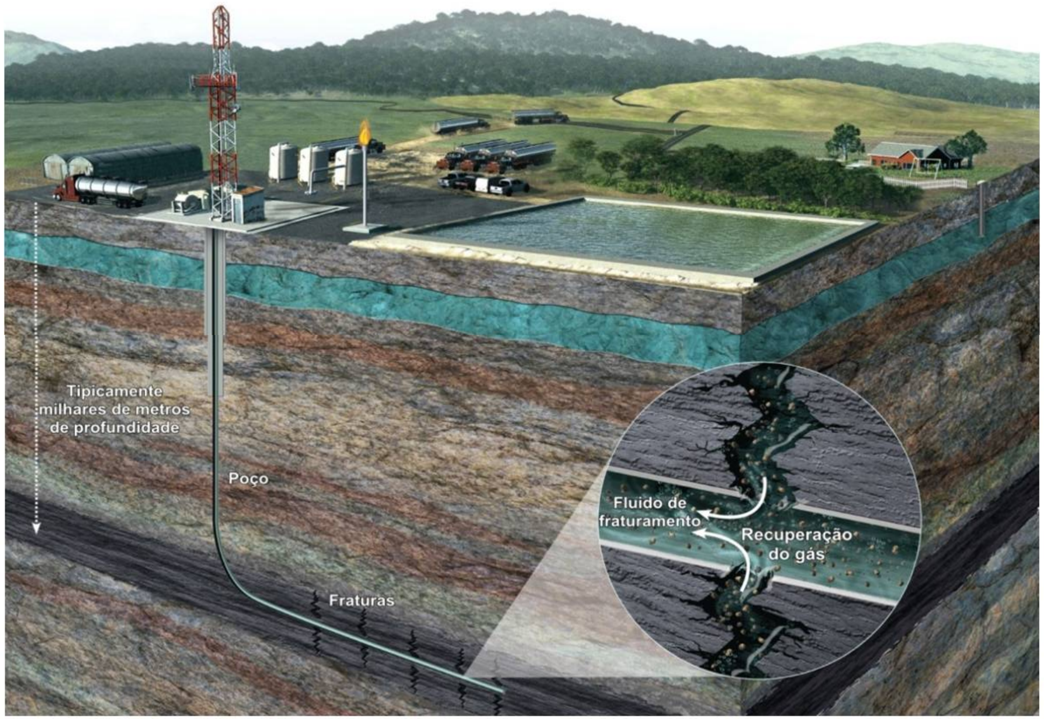

- The Interaction between rock's mechanical properties, in-situ stresses, and heterogeneities such as natural fractures influence the induced fracture.

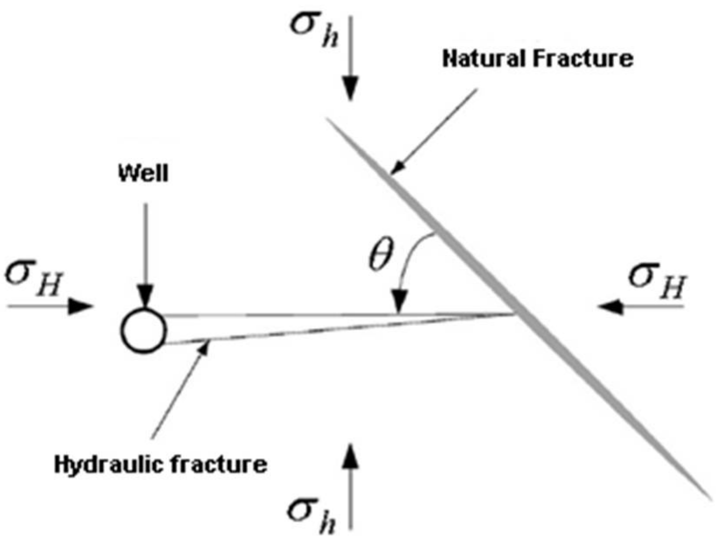

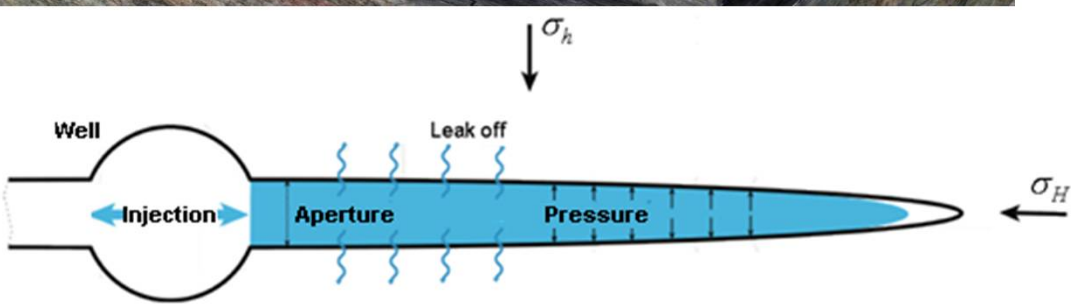

Strong Discontinuity Approach

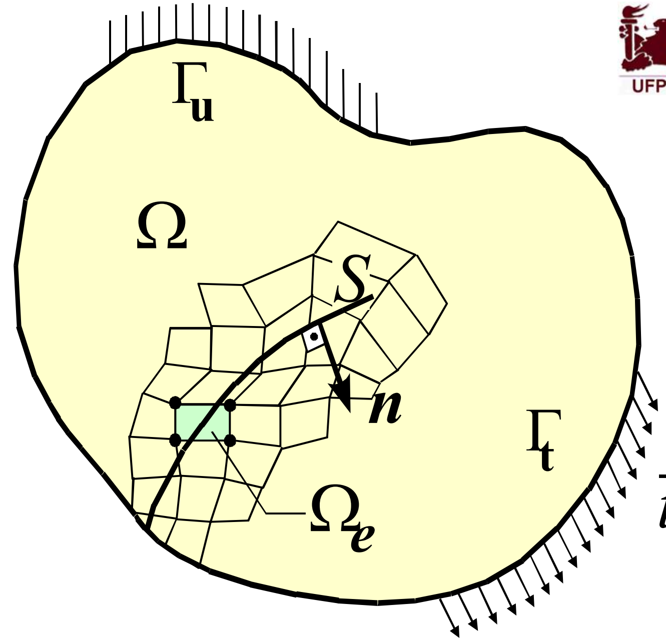

Finite Element with Embedded Discontinuity

- **The discontinuity path is placed inside the elements irrespective of the size and specific orientation.**

Mechanical Problem

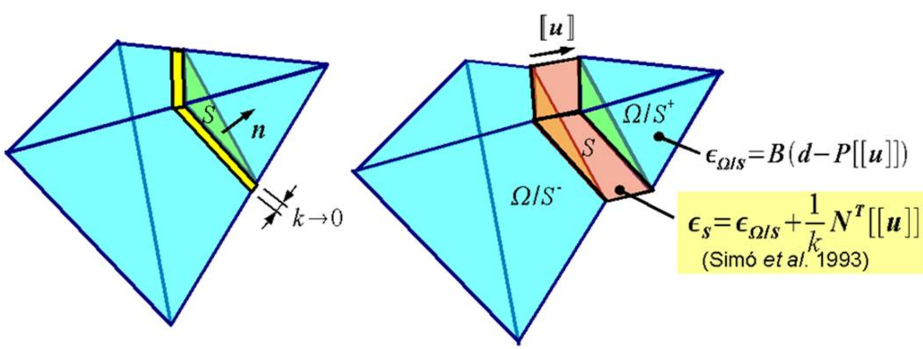

$\sigma_{\Omega/S} = \Sigma(\epsilon_{\Omega/S}) = \Sigma(B\,d - B\,P[\![u]\!])$	(continuum const. law)
$\sigma_S = \Sigma(\epsilon_S) = \Sigma(B\,d - B\,P[\![u]\!] + \frac{1}{k} N^T [\![u]\!])$	(continuum const. law)
$[\![t]\!] = N[\sigma_{\Omega/S} - \sigma_s] = 0$	(traction continuity)

Hydraulic Problem

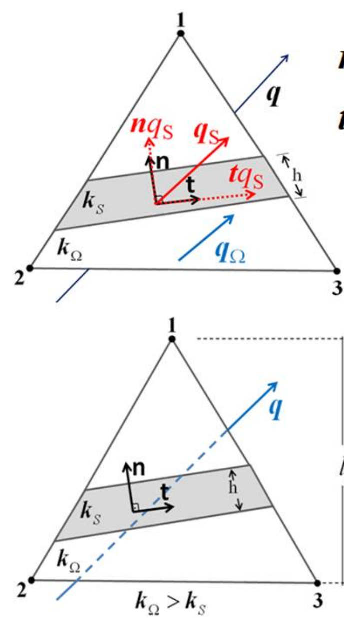

$$\boldsymbol{n} \cdot \boldsymbol{q}_s = 0 \qquad q_s = -K_s \nabla p$$

$$\boldsymbol{t} \cdot \boldsymbol{q}_s = q_s \qquad \text{with } K_s = \frac{k_s}{\mu}$$

$$\boldsymbol{q}_\Omega = -\boldsymbol{K}_\Omega \nabla p$$

$$\boldsymbol{q}_S = -\frac{h}{l_e} K_s \boldsymbol{t} \otimes \boldsymbol{t} \nabla p$$

$$\boldsymbol{q} = -\boldsymbol{K}_{ef} \nabla p$$

$$\boldsymbol{K}_{ef} = \left(\boldsymbol{K}_\Omega + \frac{h}{l_e} K_s \boldsymbol{t} \otimes \boldsymbol{t} \right)$$

Strong Discontinuity Approach

Finite element with high aspect ratio

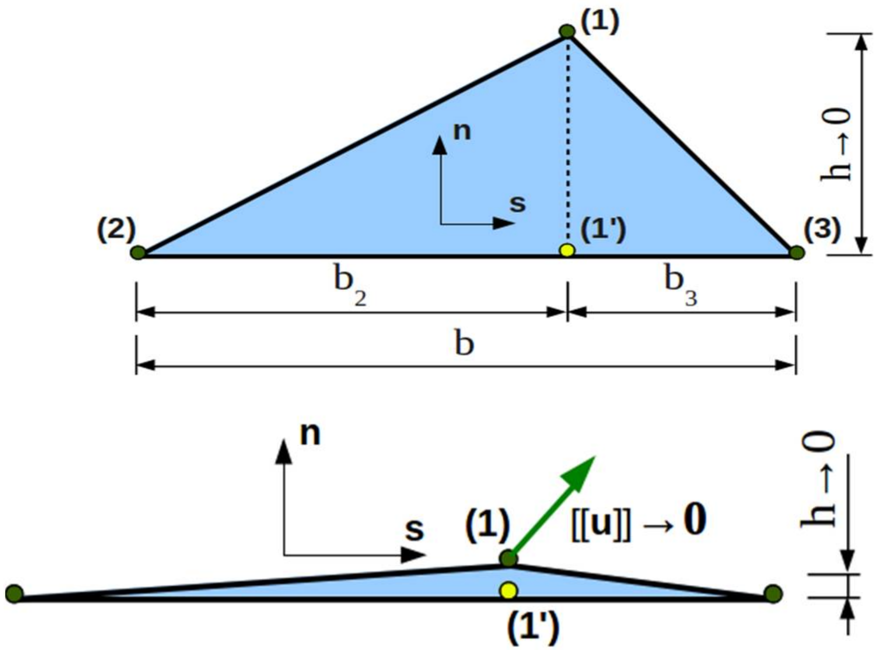

$$\epsilon = \tilde{\epsilon} + \underbrace{\frac{1}{h}(\mathbf{n} \otimes [[\mathbf{u}]])^s}_{\hat{\epsilon}}$$

Weak/strong discontinuity kinematics

Same kinematics !!!

MANZOLI *et al*, 2012

Computers and Structures 94–95 (2012) 70–82

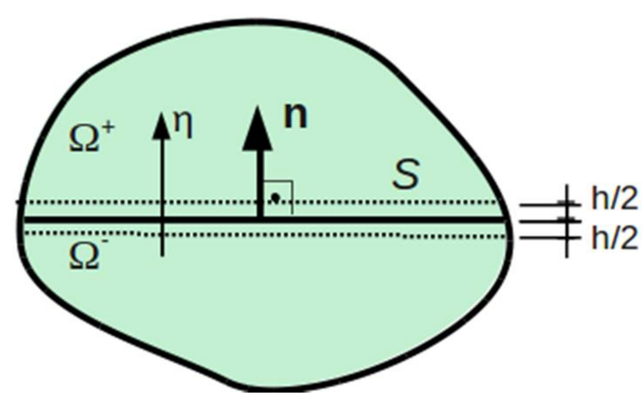

$$\epsilon = \bar{\epsilon} + \frac{\mu_s(\eta)}{h}([[\mathbf{u}]] \otimes \mathbf{n})^s$$

Interface Elements

Initial Finite Element mesh

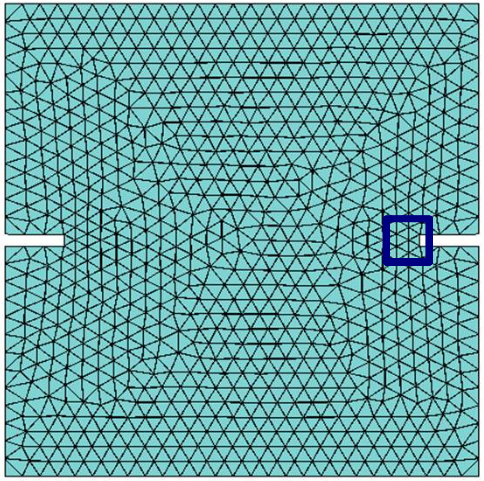

Interface finite elements are inserted throughout the mesh or in the most requested area of the mesh. Depending on the boundary conditions of the problem and stress states resulting, the elements will be opening by a preferential path, forming a fracture and relaxing the stress in other candidate elements at the same time.

Interface Elements

Initial Finite Element mesh

Interface Finite Elements

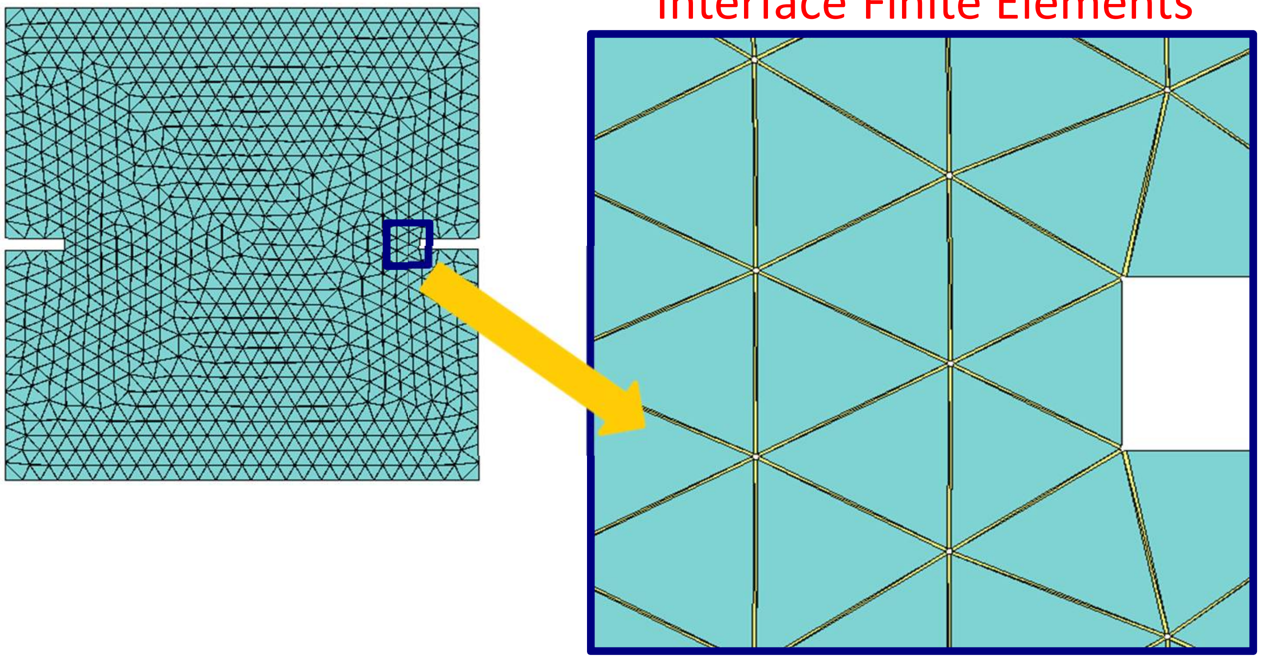

Interface finite elements are inserted throughout the mesh or in the most requested area of the mesh. Depending on the boundary conditions of the problem and stress states resulting, the elements will be opening by a preferential path, forming a fracture and relaxing the stress in other candidate elements at the same time.

Interface Elements

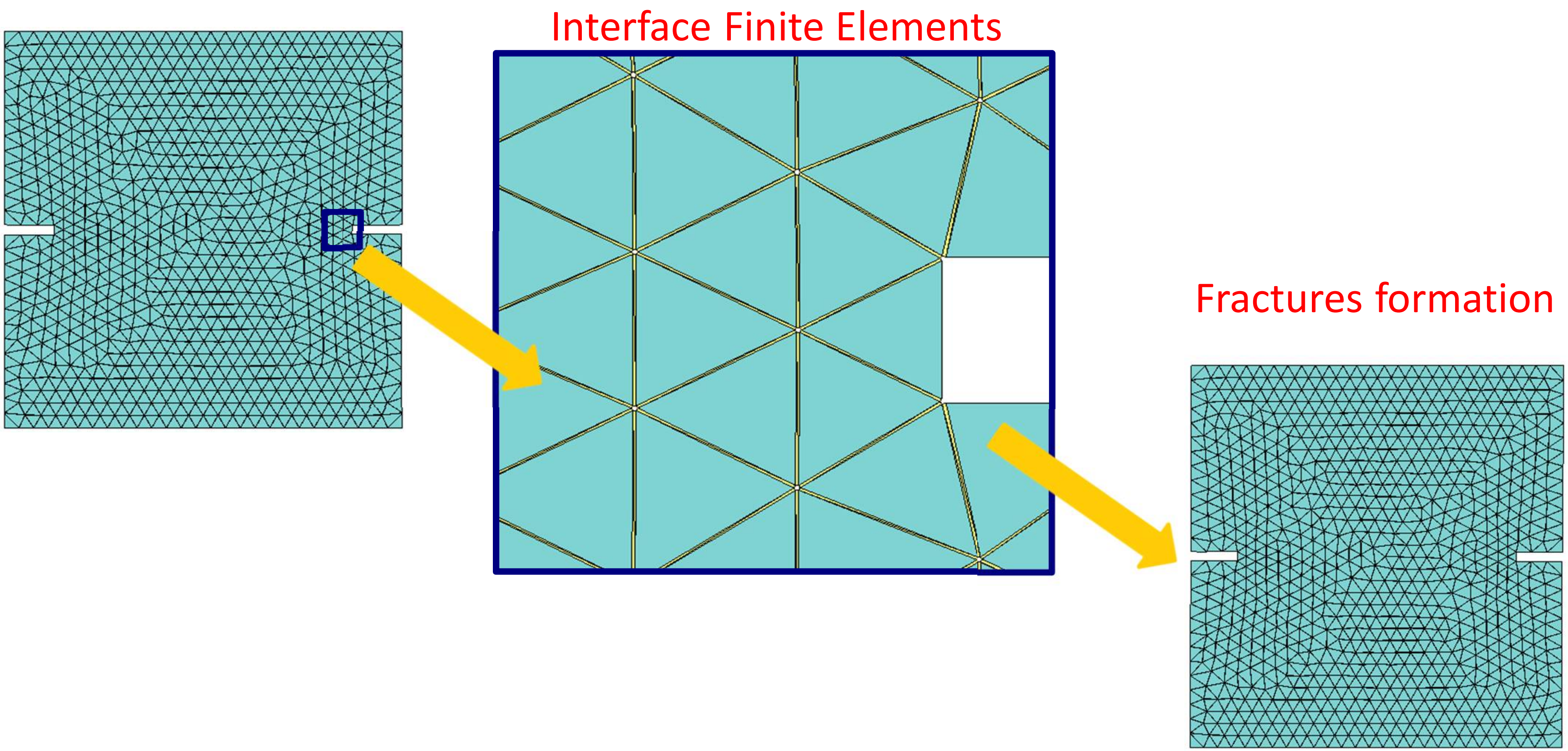

CONSTITUTIVE MODEL

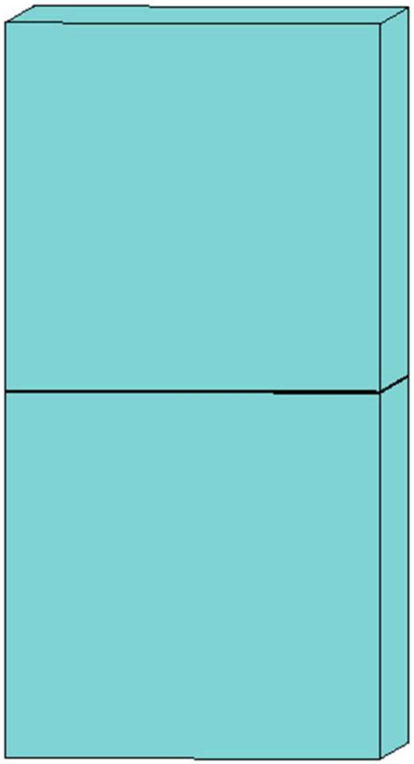

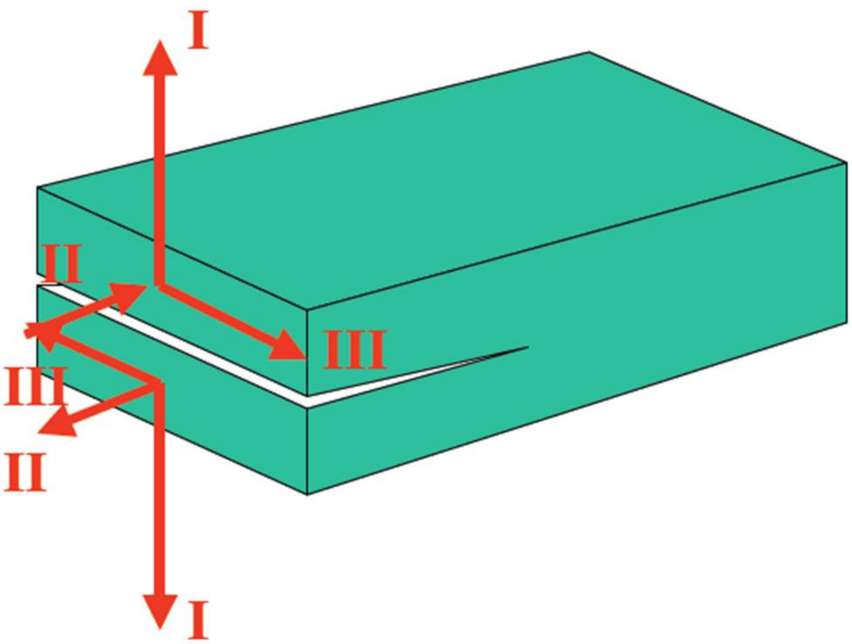

Tensile damage model (mode I)

TENSILE DAMAGE MODEL

Constitutive relation

$$\boldsymbol{\sigma} = (1-d)\bar{\boldsymbol{\sigma}}$$
$$\bar{\boldsymbol{\sigma}} = \mathbf{C} : \boldsymbol{\varepsilon}$$

Damage criterion

$$\bar{\phi} = -\bar{\sigma}_n - r \leqslant 0$$

Evolution law for the strain-type variable

$$r_t = \max_{s\in[0,t]}[-\bar{\sigma}_{n(s)}, r$$

Damage evolution

$$d_{(r)} = 1 - \frac{q_{(r)}}{r}$$

Softening law

$$q_{(r)} = f_t e^{\frac{f_t^2}{G_f E} h(1-r/f_t)}$$

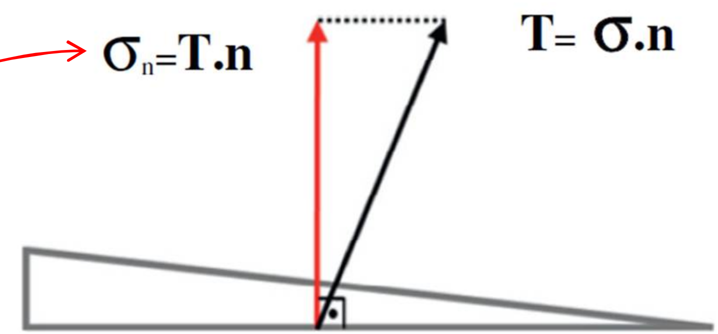

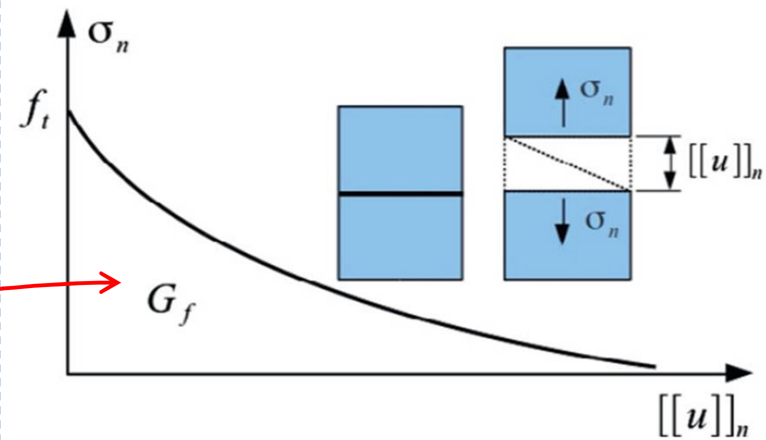

NUMERICAL SIMULATION OF THE LEAK-OFF TEST

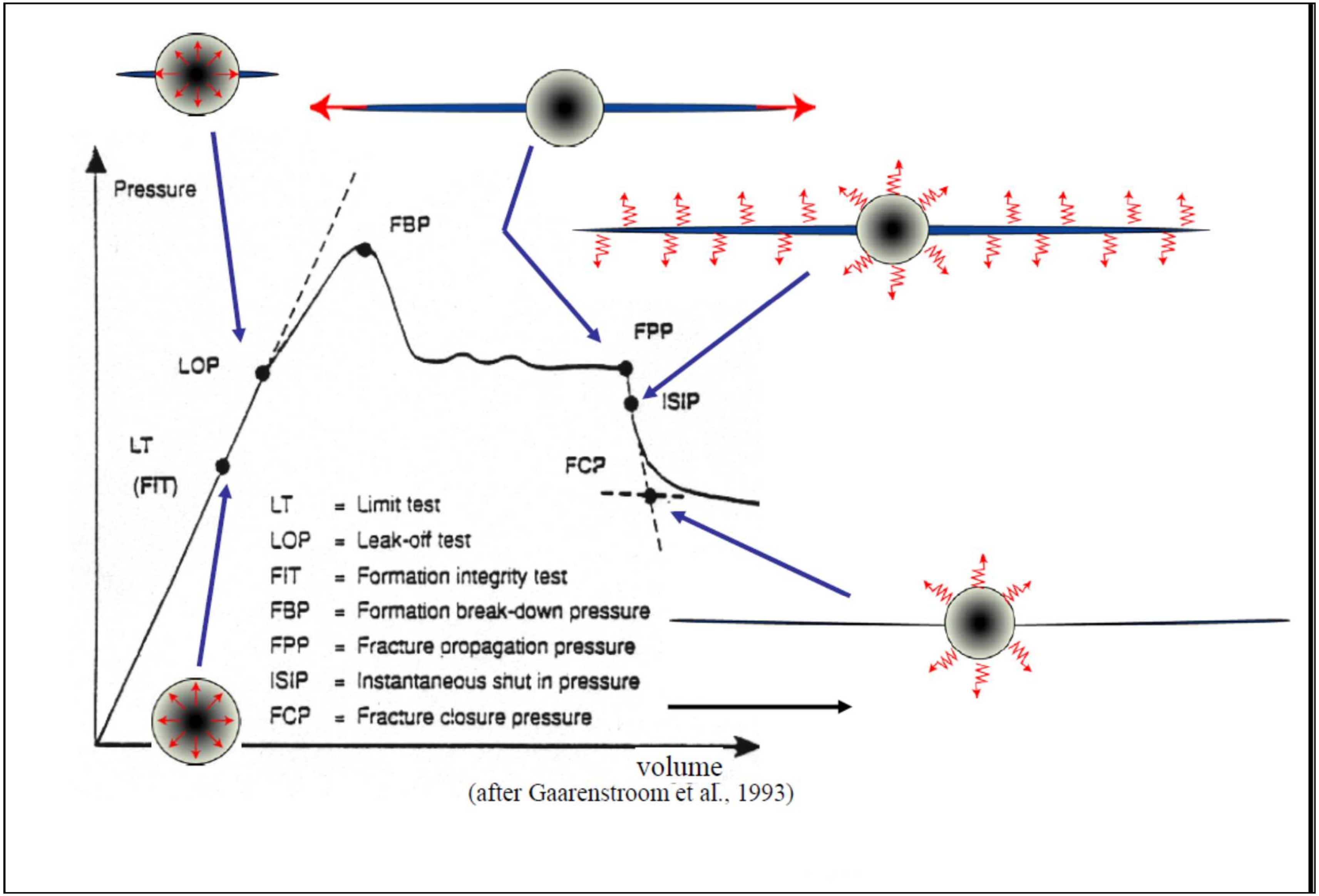

EXAMPLE 1

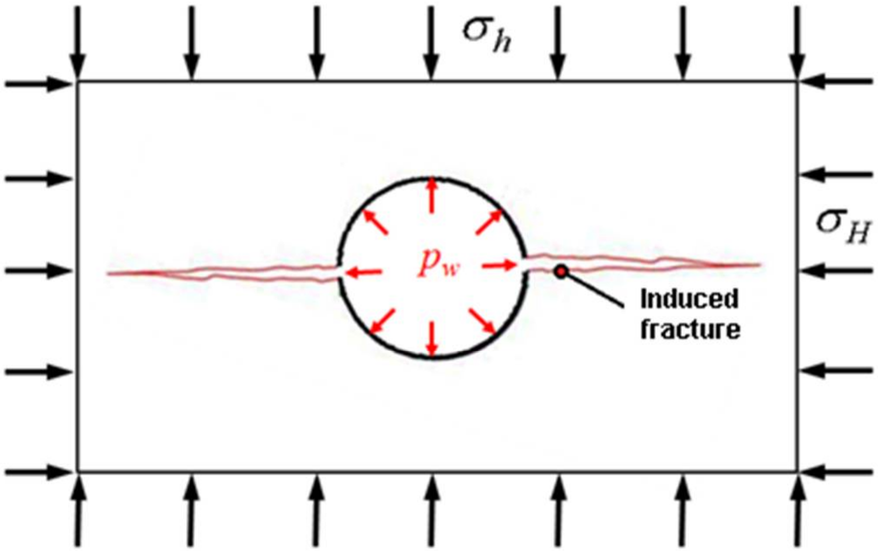

$$\Delta p_b = 3\sigma'_h - \sigma'_H + f_t$$

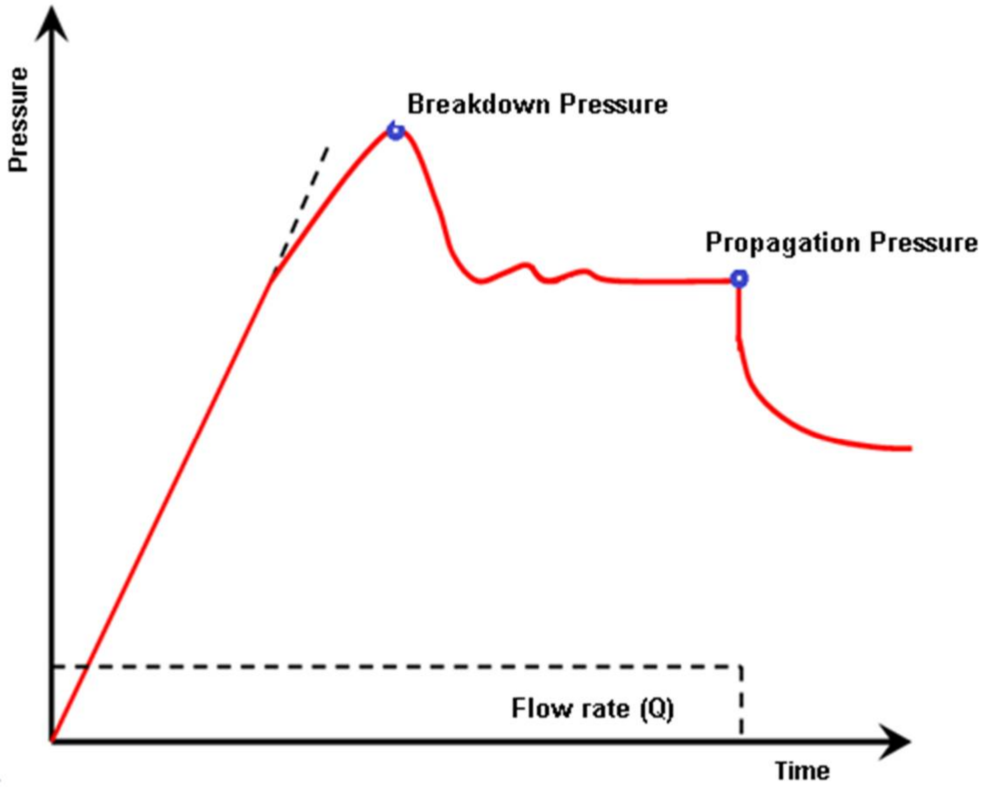

EXAMPLE 1

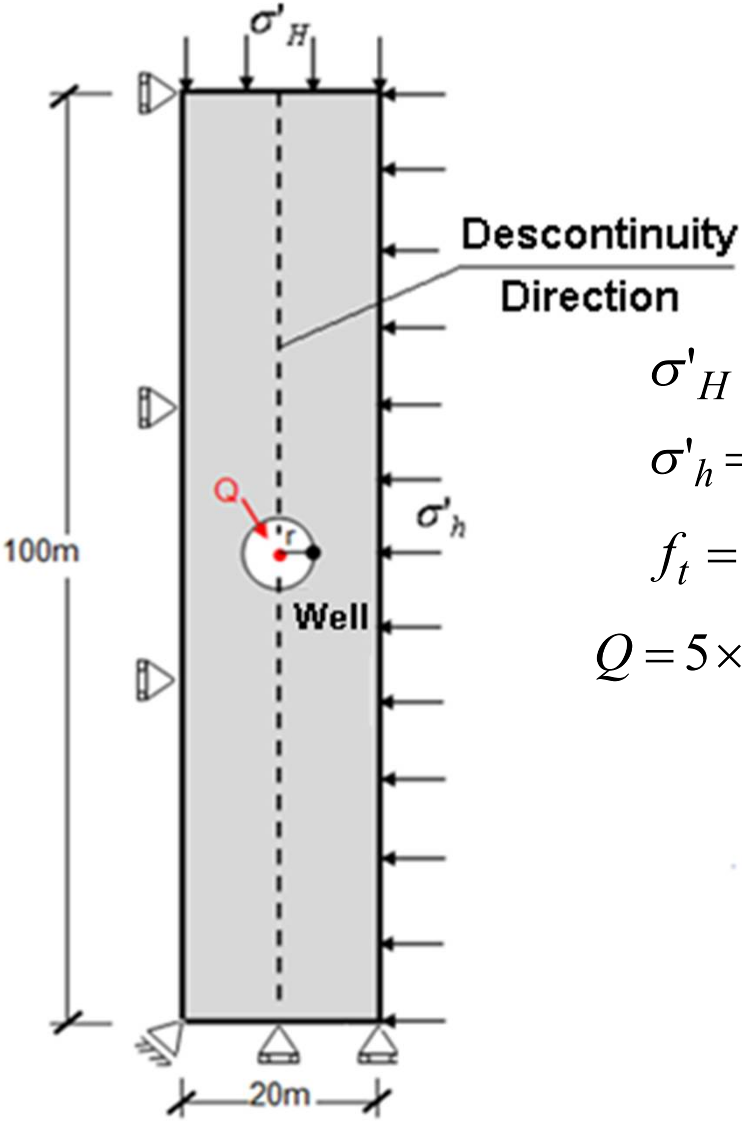

$$\sigma'_H = 5\,MPa$$

$$\sigma'_h = 3\,MPa$$

$$f_t = 1\,MPa$$

$$Q = 5 \times 10^{-6}\,kg/s$$

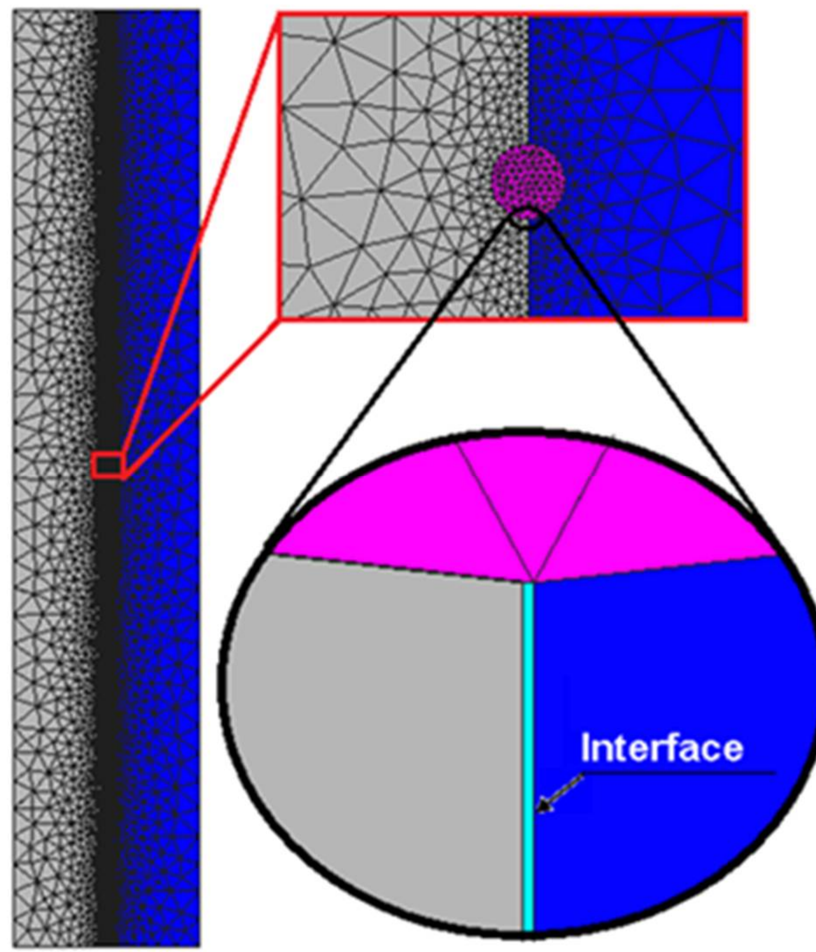

EXAMPLE 1

$$\Delta p_b = 3\sigma'_h - \sigma'_H + f_t$$

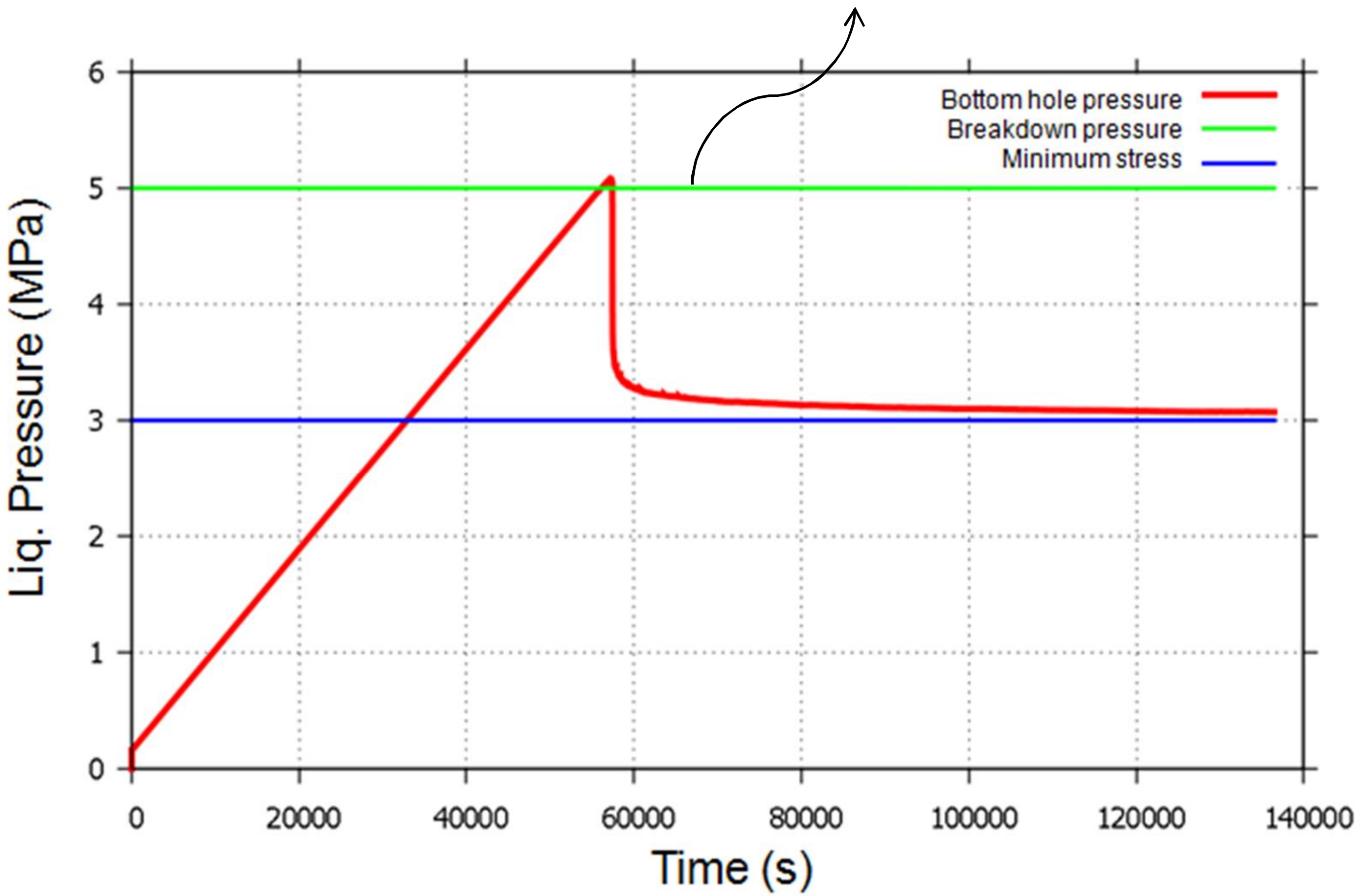

EXAMPLE 1

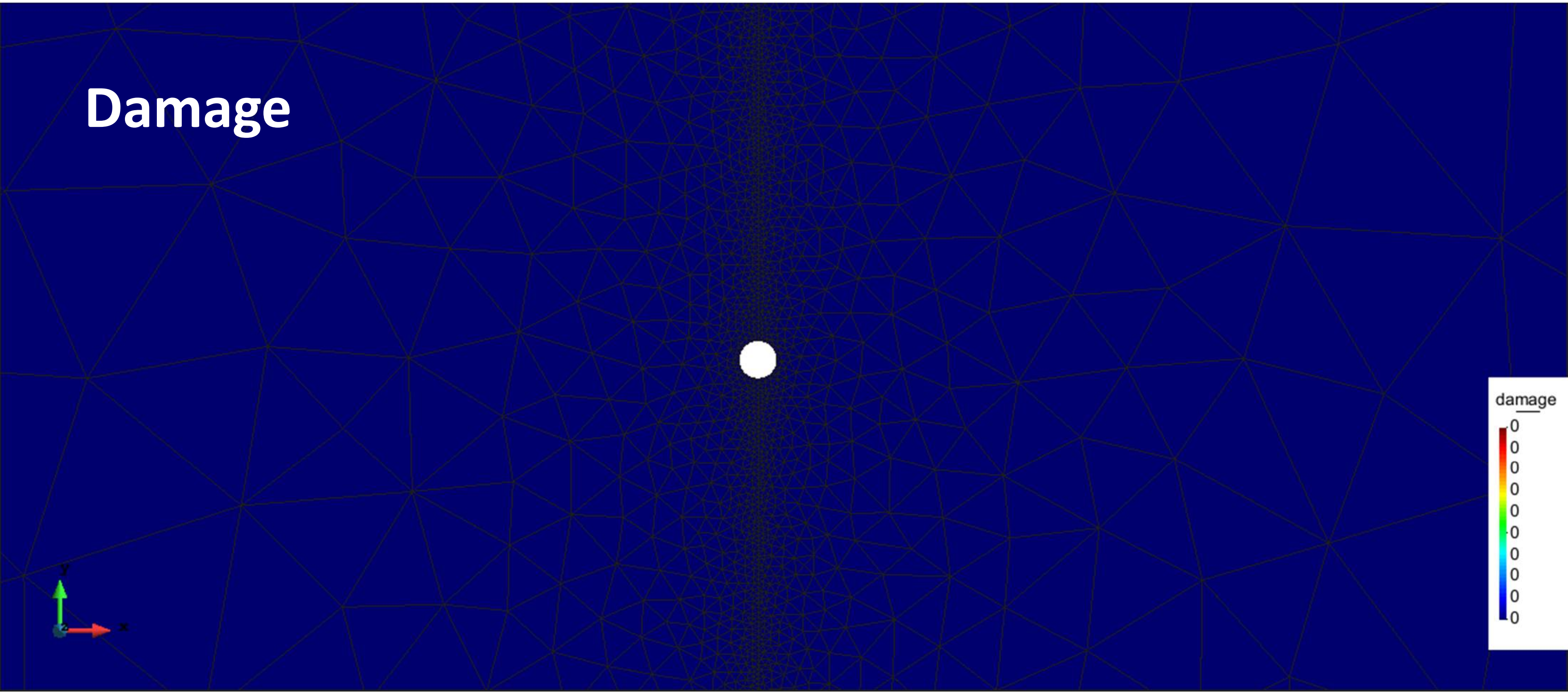

EXAMPLE 1

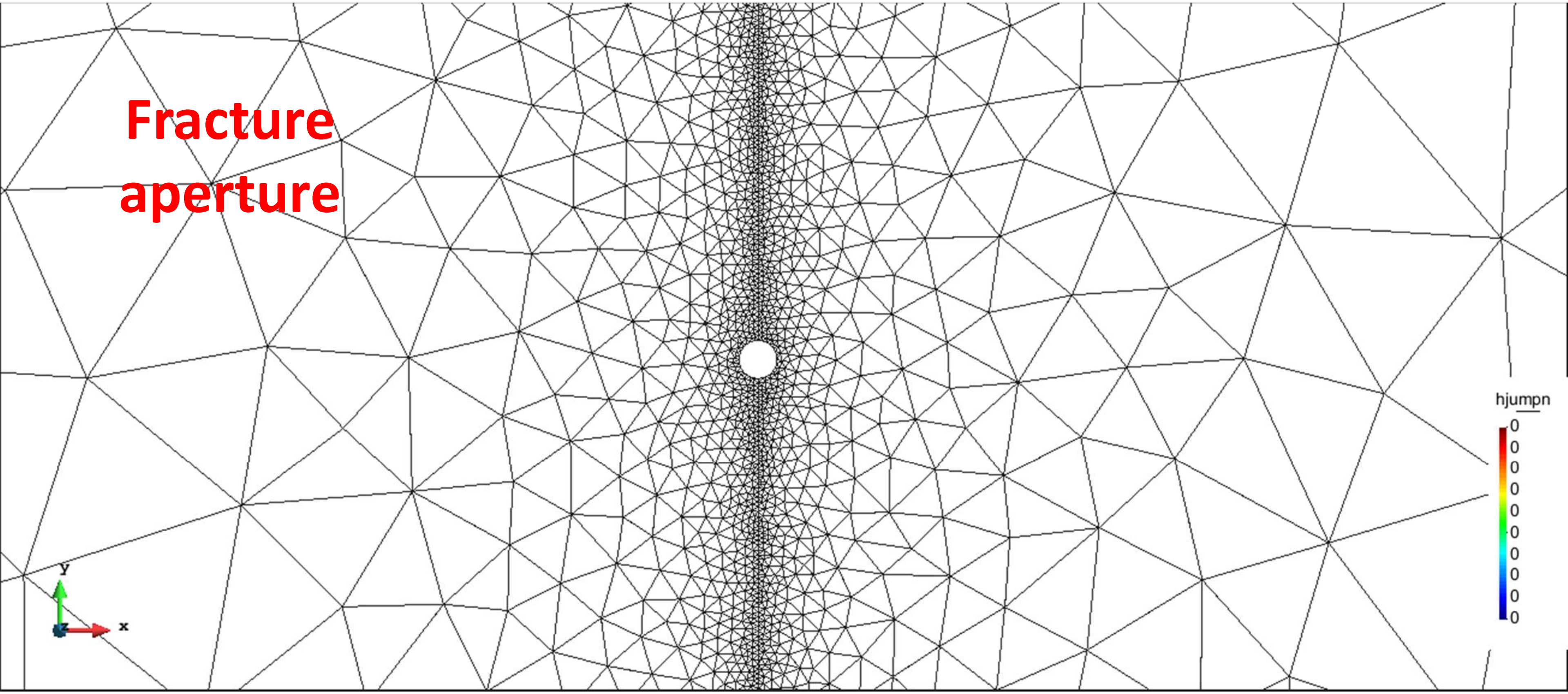

EXAMPLE 2

► **Hydro Mechanical application – Leakoff test**

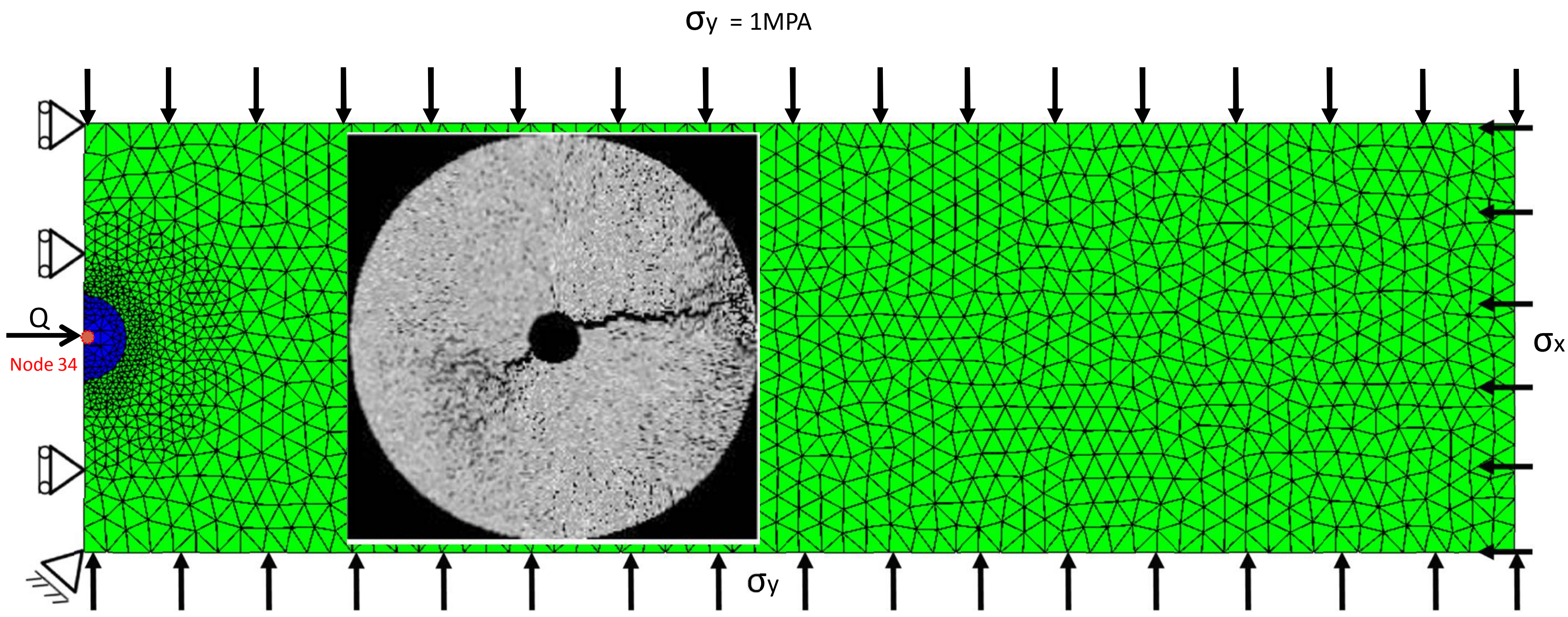

$Q=6x10^{-5}kg/s$
σv=1MPa
σx=2MPa

tensile strength of fracture material : (σy)=5 MPa

EXAMPLE 2

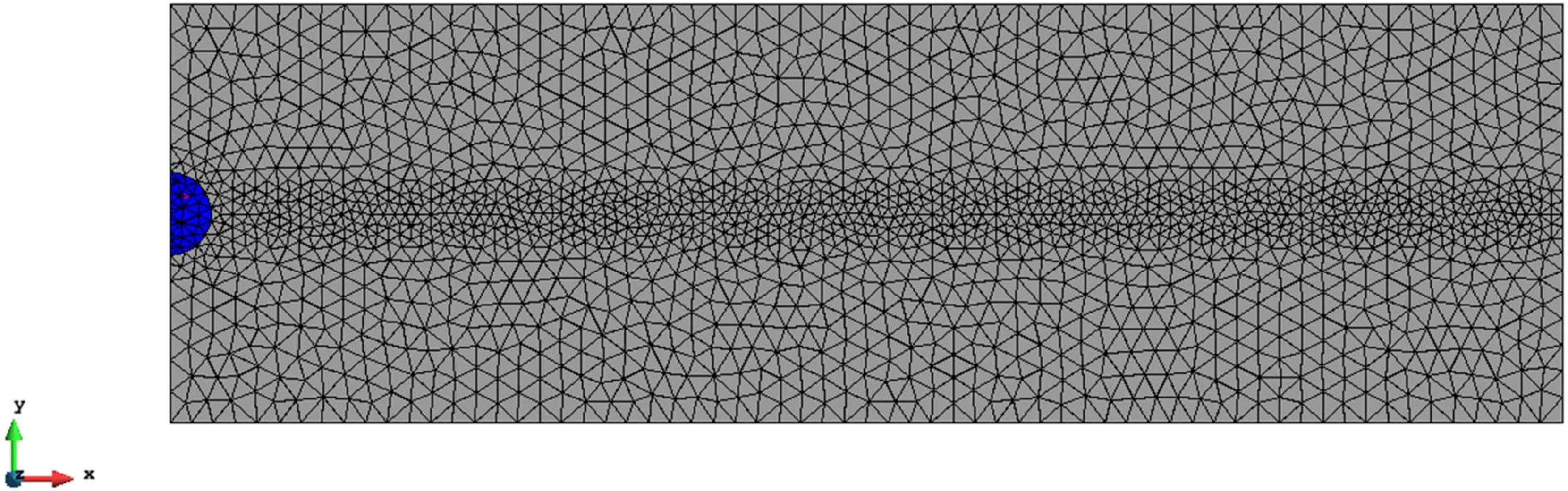
y
x

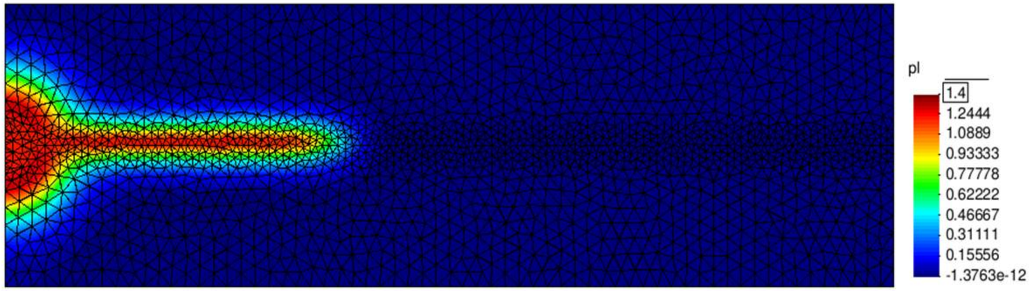
pl
1.4
1.2444
1.0889
0.93333
0.77778
0.62222
0.46667
0.31111
0.15556
-1.3763e-12

EXAMPLE 2

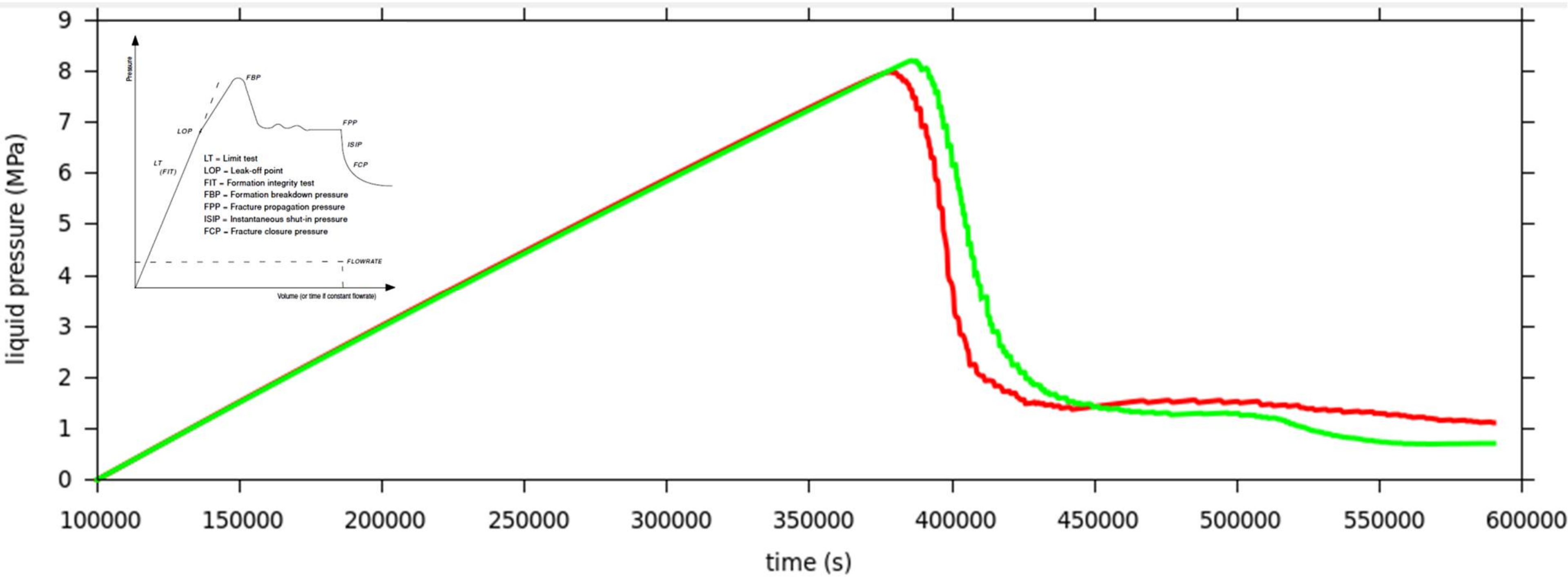

	Strong Discontinuity Approach	Interface Finite Element
Nodes	1595	10256
Elements	2993	20162
CPU time (s)	1210.51	6289.43

NATURAL FRACTURES

Geomechanics of Fracturated Reservoirs

Much more complex behavior of fractures...

Improvement of constitutive of interface elements

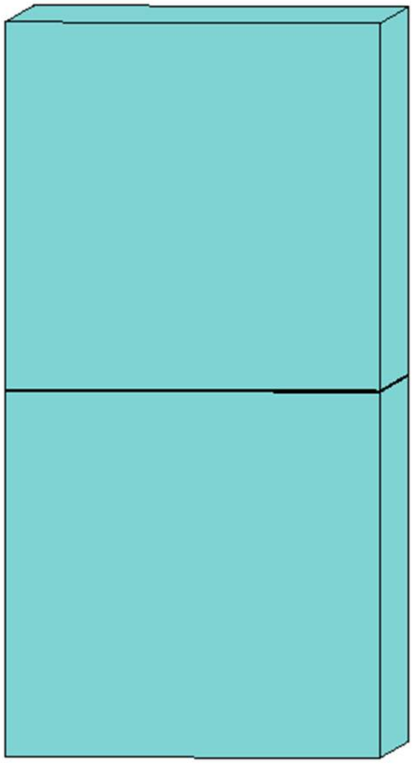

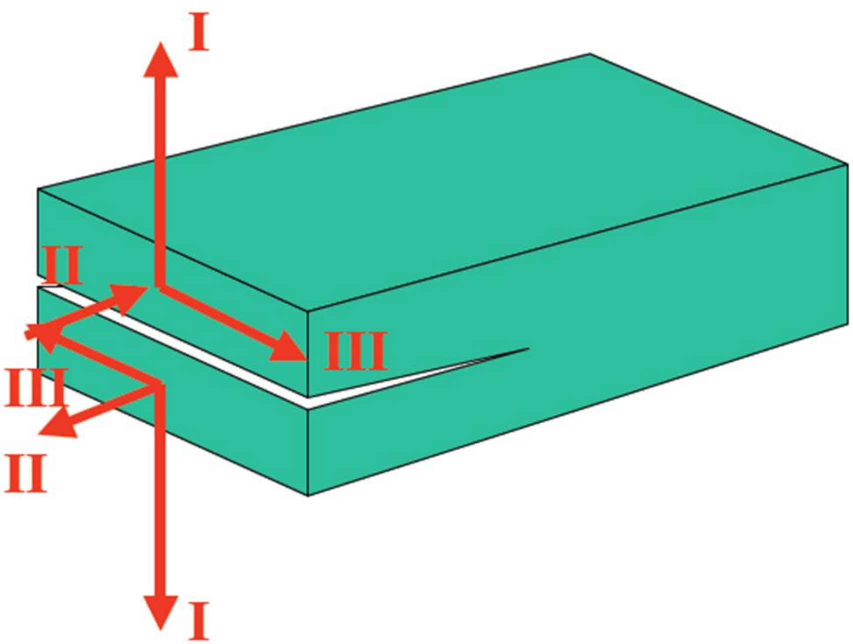

Up to now: isotropic tensile damage model (mode I)

Improvements: shear modes (II and III) and inelastic effects due to dilatancy and compression

UFPE

NATURAL FRACTURES

- Coupled hydro-mechanical analysis of hydraulic fracturing considering influence of rock and natural fracture properties, in-situ stresses and operational conditions on the induced fracture trajectory.

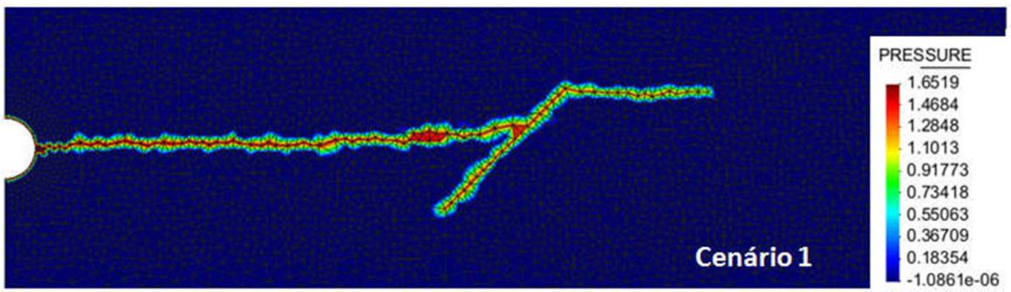

interaction between natural and induced fractures

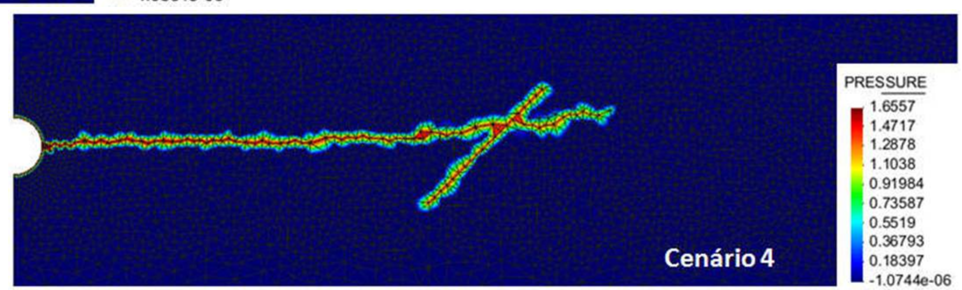

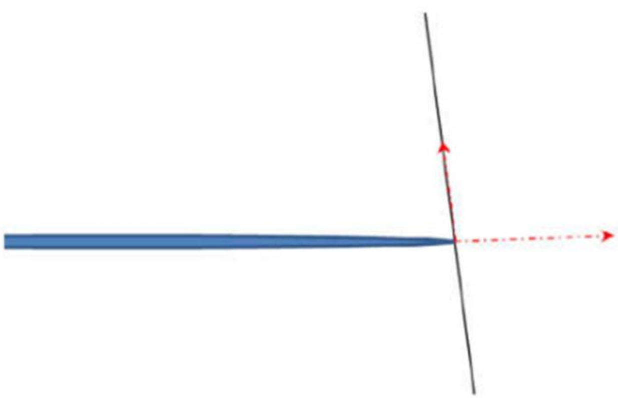

NATURAL FRACTURES

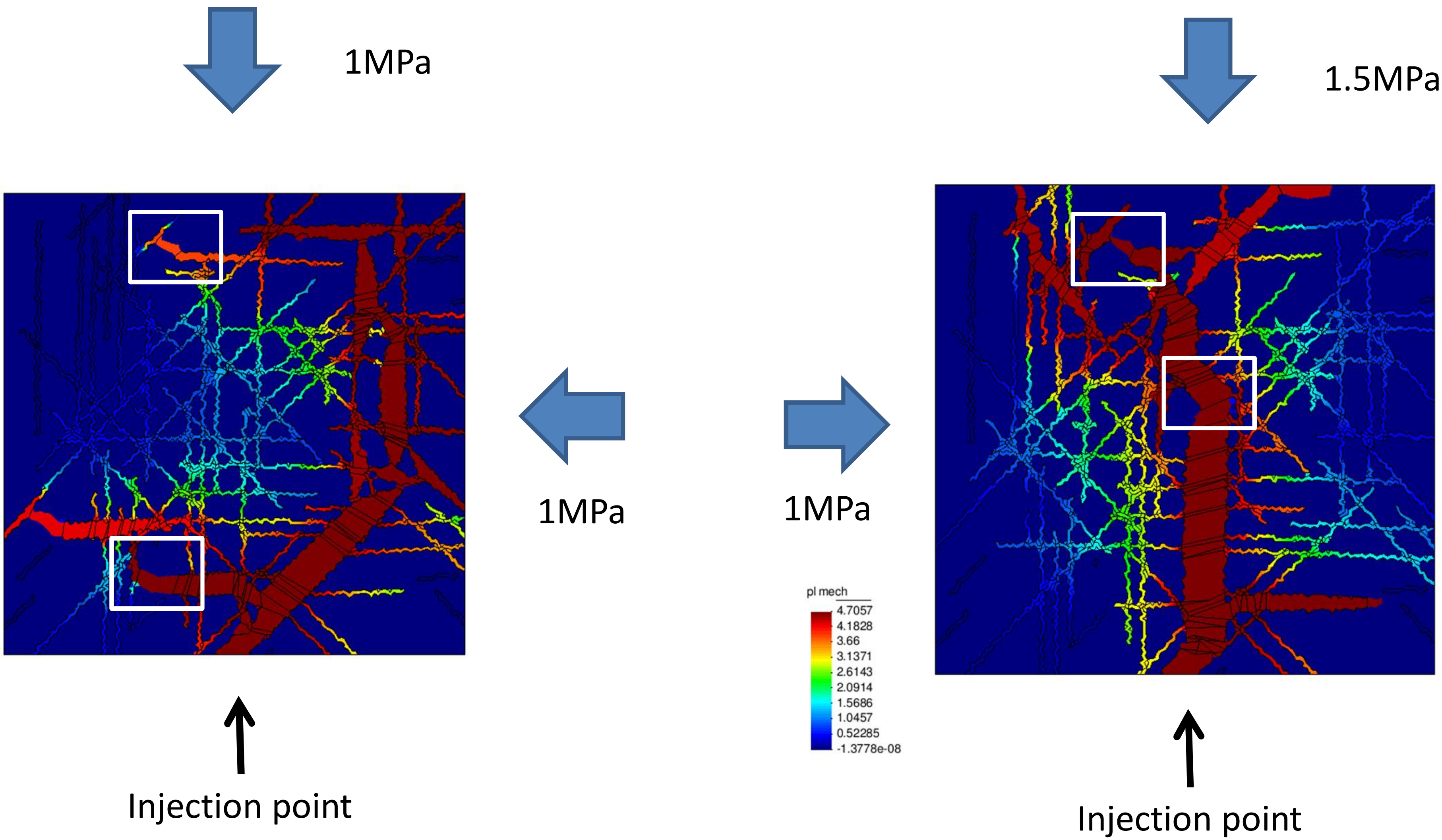

BREAKOUTS

- Este método baseia-se no mapeamento por perfil de imagem ou caliper de regiões do poço onde ocorrem rupturas por cisalhamento da parede.
- A direção dos *breakouts* é ortogonal à direção da maior tensão horizontal.

L. C. Pereira (MSc, 2007)

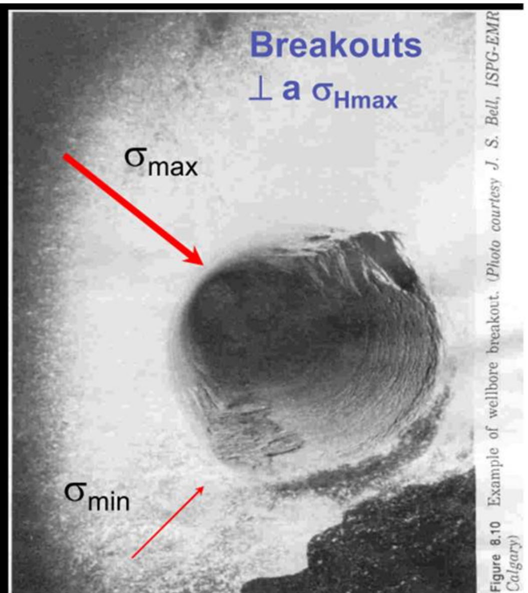

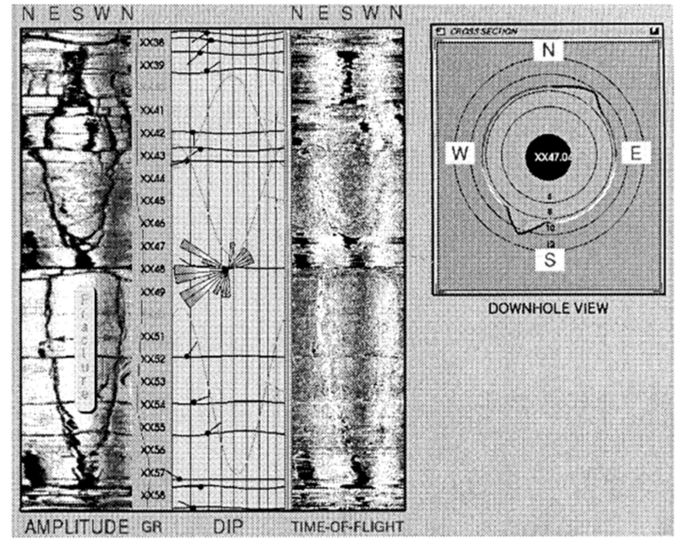

Fig. 5. Ultrasonic imaging log showing natural fractures with a cross-section showing borehole breakout in a NE–SW direction.

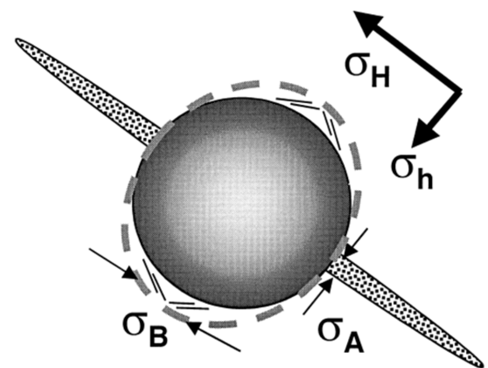

Fig. 4. Directions of borehole breakout and fractures in relation to the orientation of the horizontal stress field.

A breakout is the evidence of wall yield (the formation strength at the borehole wall is exceeded). A breakout is not considered to be a borehole failure since the borehole remains useful. Borehole breakout can be measured using four- or six-arm caliper tools. The preferred tool, however, is the ultrasonic imaging tool, which makes up to 200-caliper measurements at every depth level.

M.Y. Soliman*, Paul Boonen Journal of Petroleum Science and Engineering 25 (2000) 187–204

BREAKOUTS

R. Sousa (MSc, 2004)

Geomechanics problem: elasto-plasticity

- Mohr-Coulomb

$$F(\boldsymbol{\sigma},\boldsymbol{\kappa}) = J - \left(\frac{c'}{\tan\varphi'} + p'\right) g(\theta) = 0$$

$$g(\theta) = \frac{\operatorname{sen}\varphi'}{\cos(\theta) + \dfrac{\operatorname{sen}(\theta)\operatorname{sen}\varphi'}{\sqrt{3}}}$$

- Drucker-Prager

$$F(\boldsymbol{\sigma},\mathbf{k}) = J - \left(\frac{c'}{\tan\varphi'} + p'\right) M_{JP} = 0$$

$$M_{JP}^{\theta=-30^\circ} = \frac{2\sqrt{3}\operatorname{sen}\varphi'}{3 - \operatorname{sen}\varphi'}$$

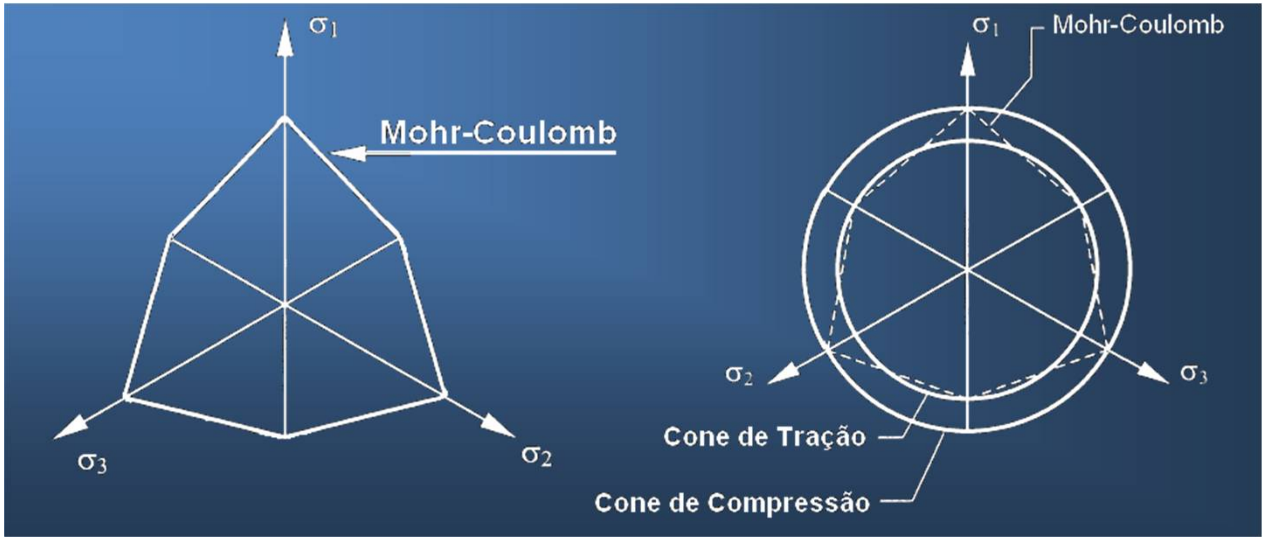

BREAKOUTS

Hardening/Softening Law

R. Sousa (MSc, 2004)

- Linear Hardening
- Perfect Plasticity
- Linear Softening

Brittle rock

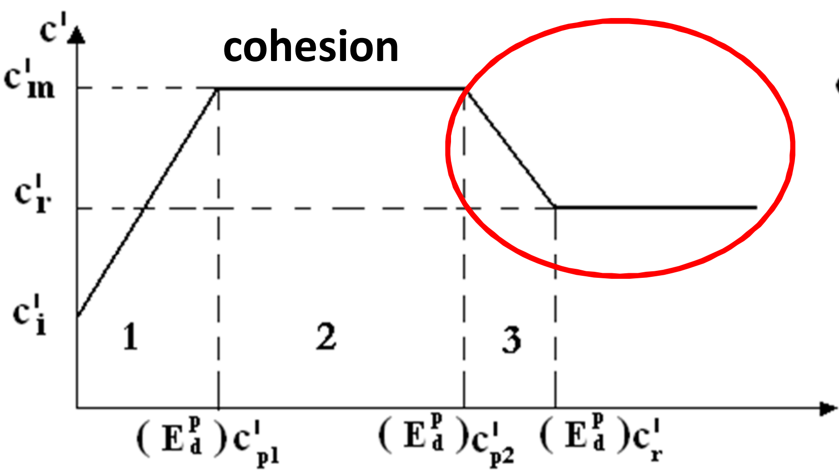

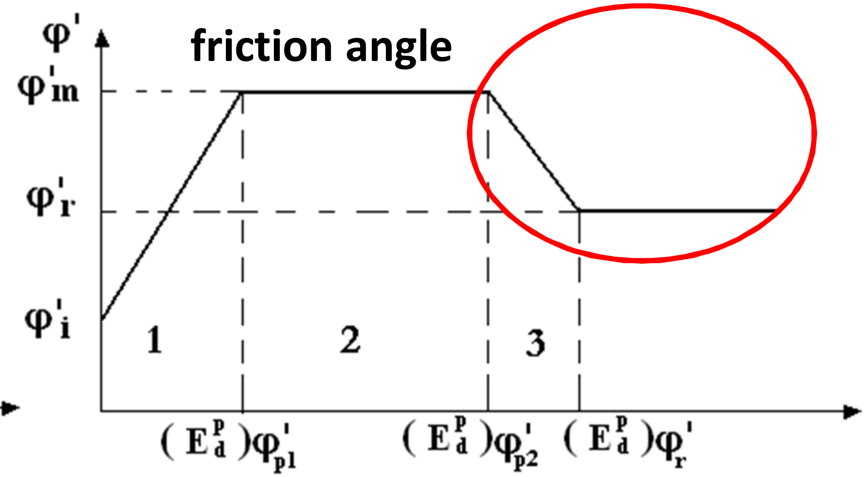

BREAKOUTS

SIMULATION

R. Sousa (MSc, 2004)

Engineering Problem

- Horizontal well perforation
  - Anisotropic and bidimensional boundary conditions
  - Adopted a finite element excavation method (Brown e Booker, 1985) on 2D analysis

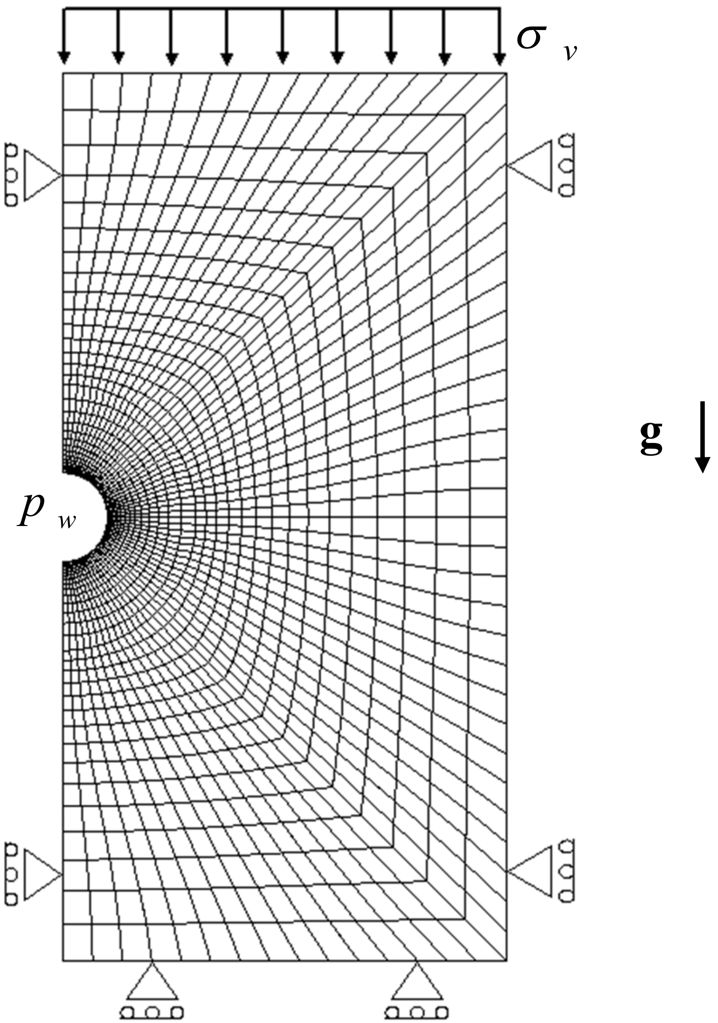

K<1:

Vertical stress > Horizontal stress

BREAKOUTS

R. Sousa (MSc, 2004)

Shear Plastic Strains

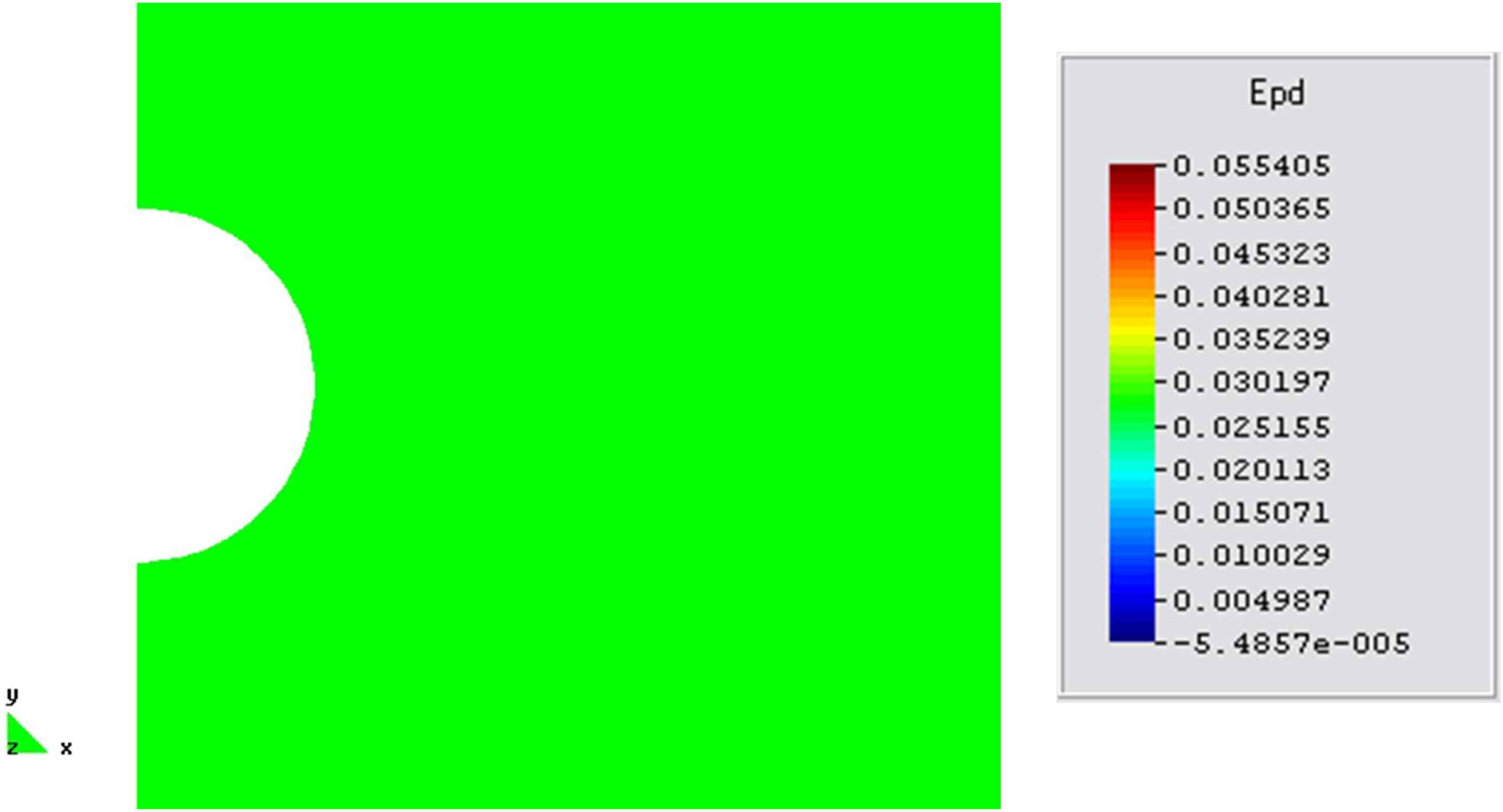

BREAKOUTS

R. Sousa (MSc, 2004)

Breakout

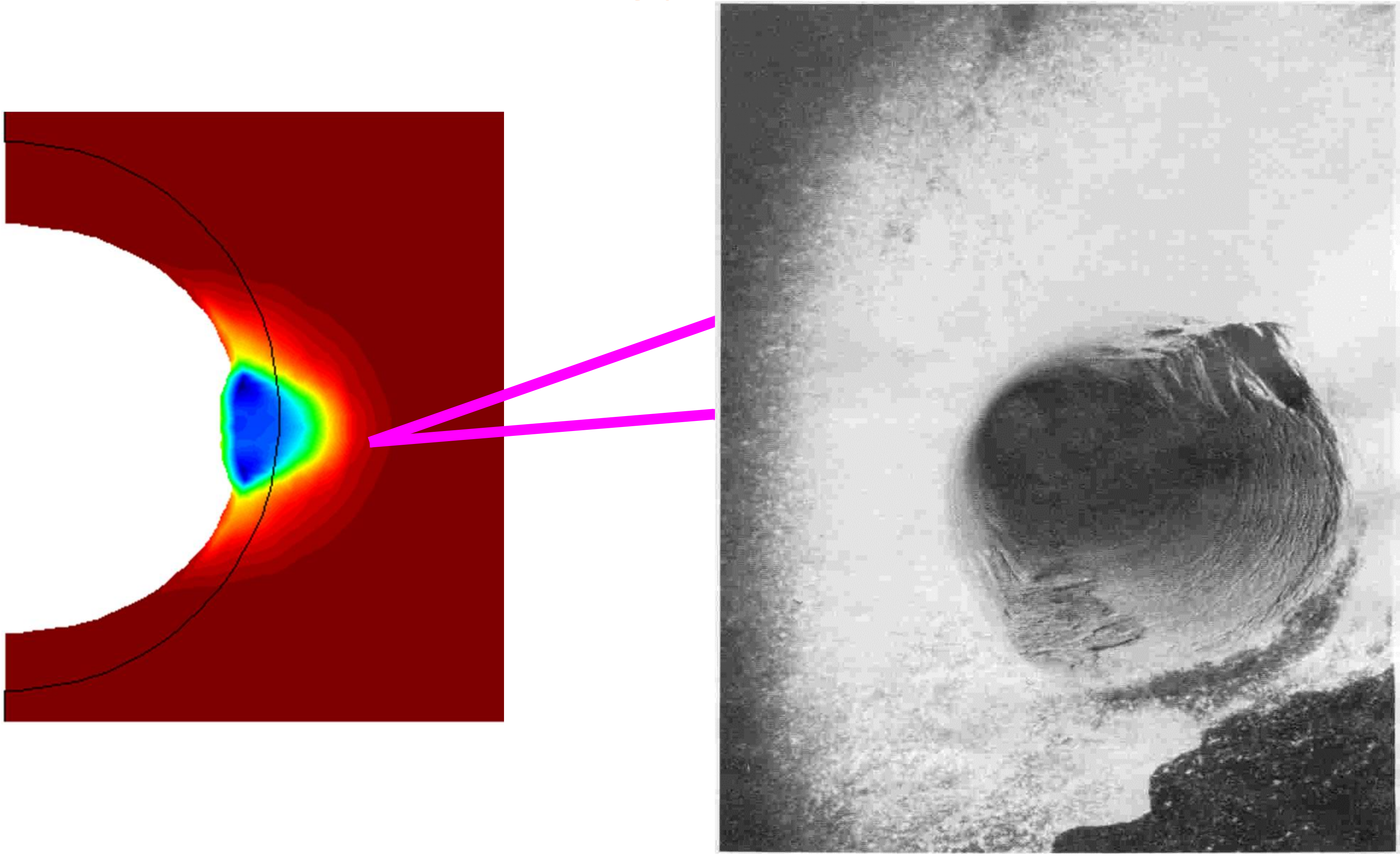

Figure 8.10 Example of wellbore breakout. *(Photo courtesy J. S. Bell, ISPG-EMR Calgary)*

BREAKOUTS

R. Sousa (MSc, 2004)

Results for Mohr-Coulomb Model with *softening*

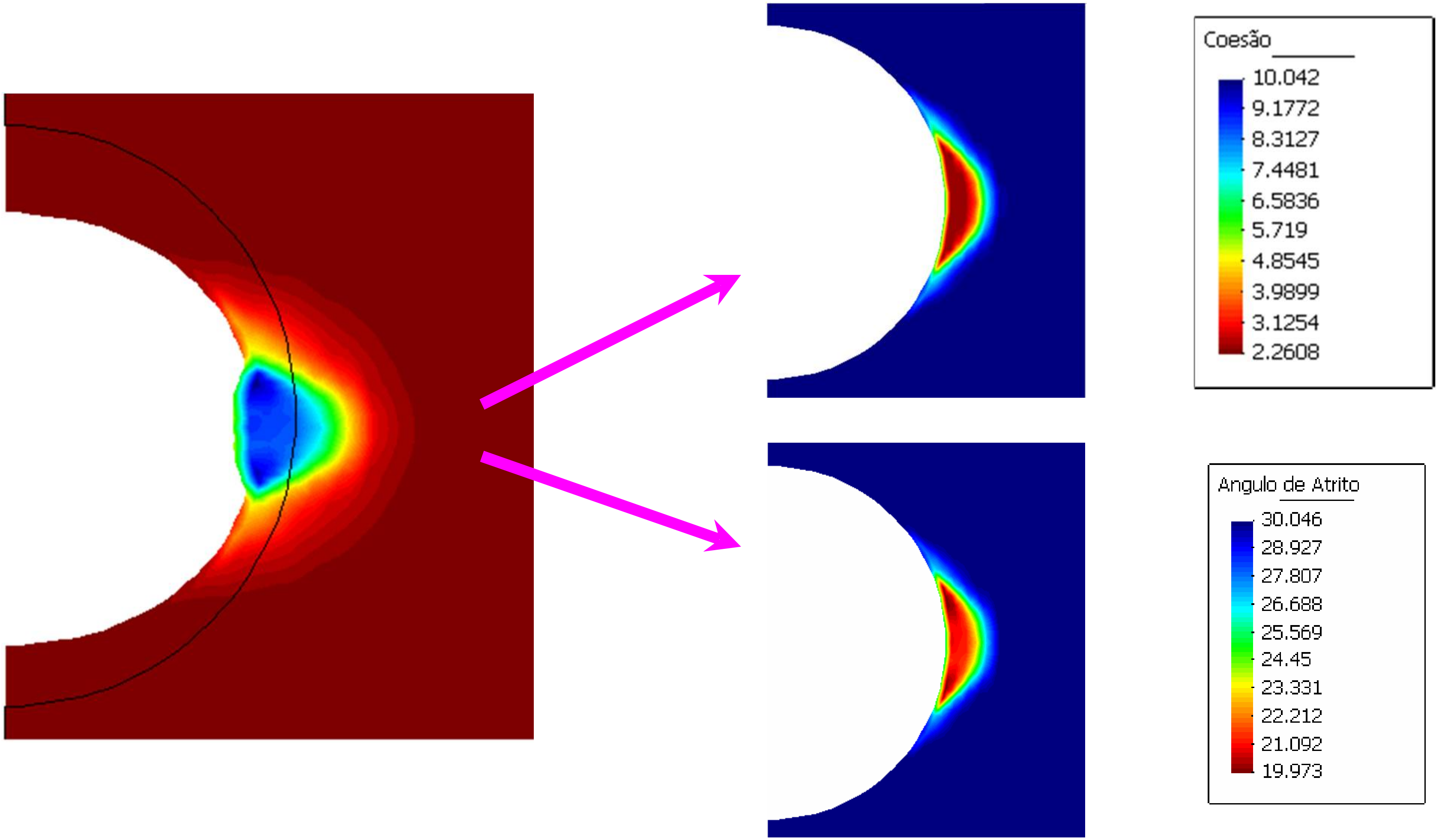

BREAKOUTS

R. Sousa (MSc, 2004)

Total Vertical Stress Redistribution

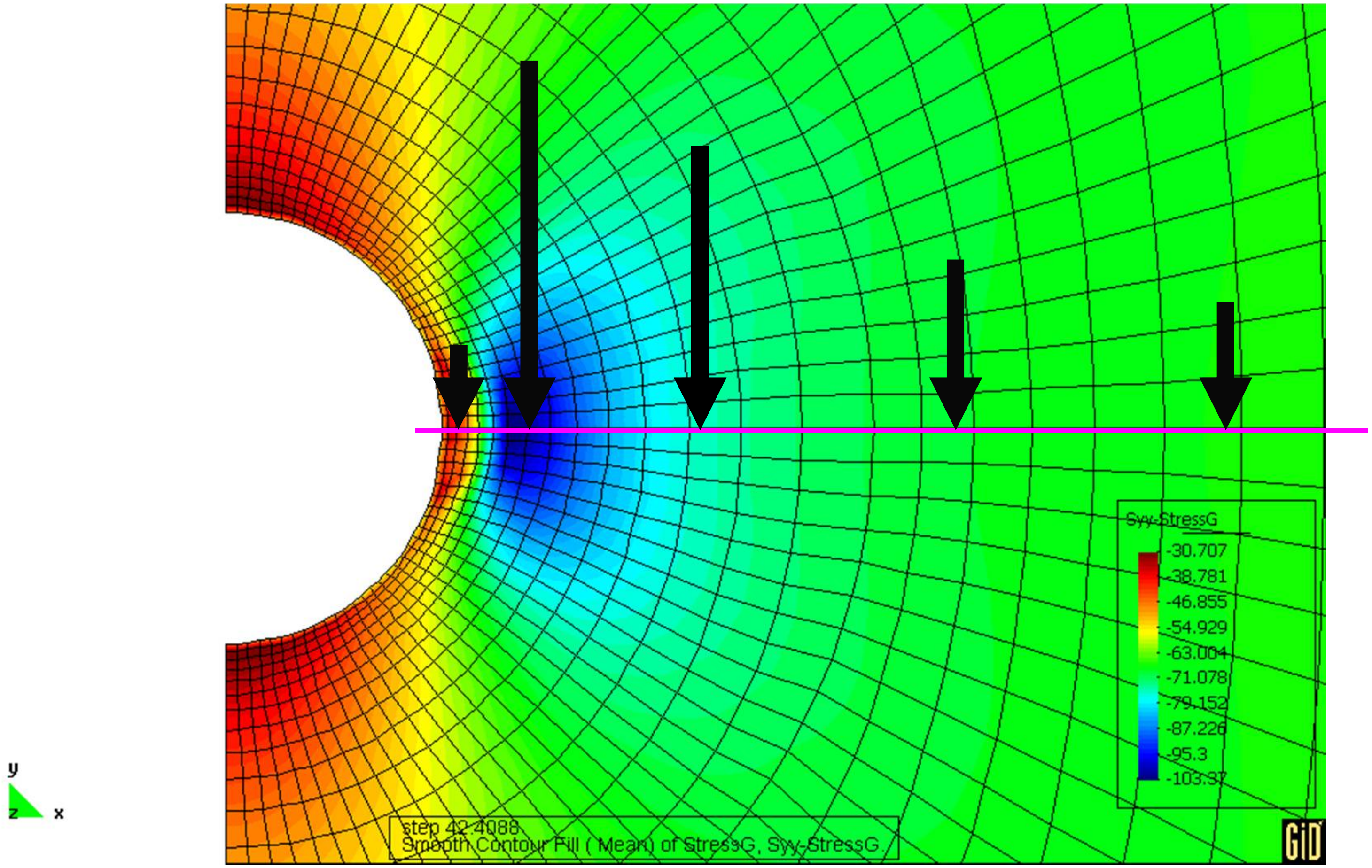

R. Sousa (MSc, 2004)

Impact on permeability and pressure distributions

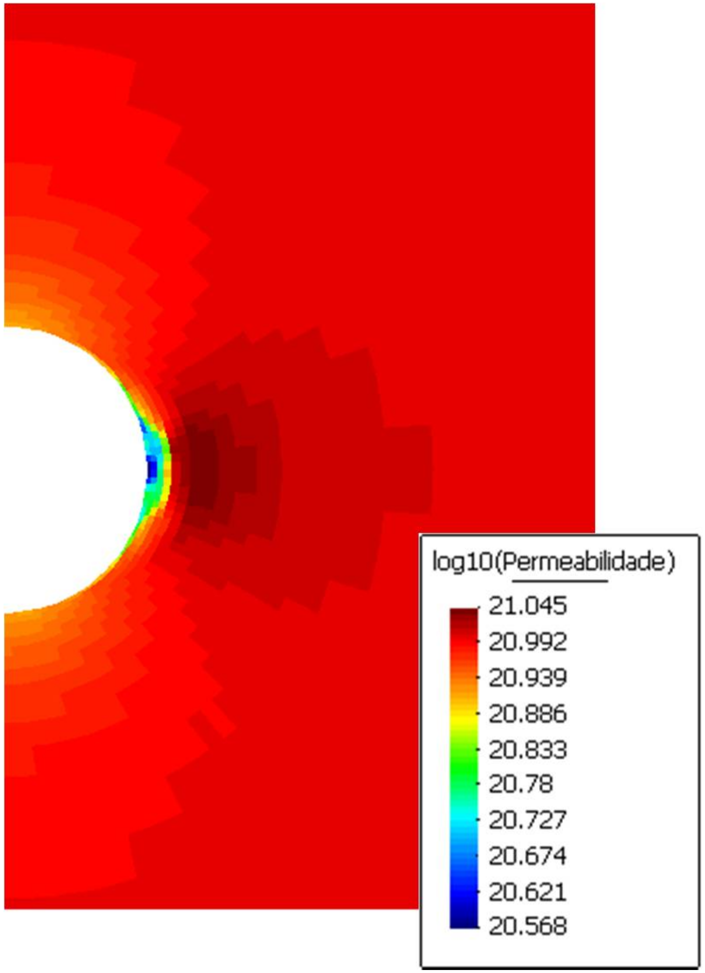

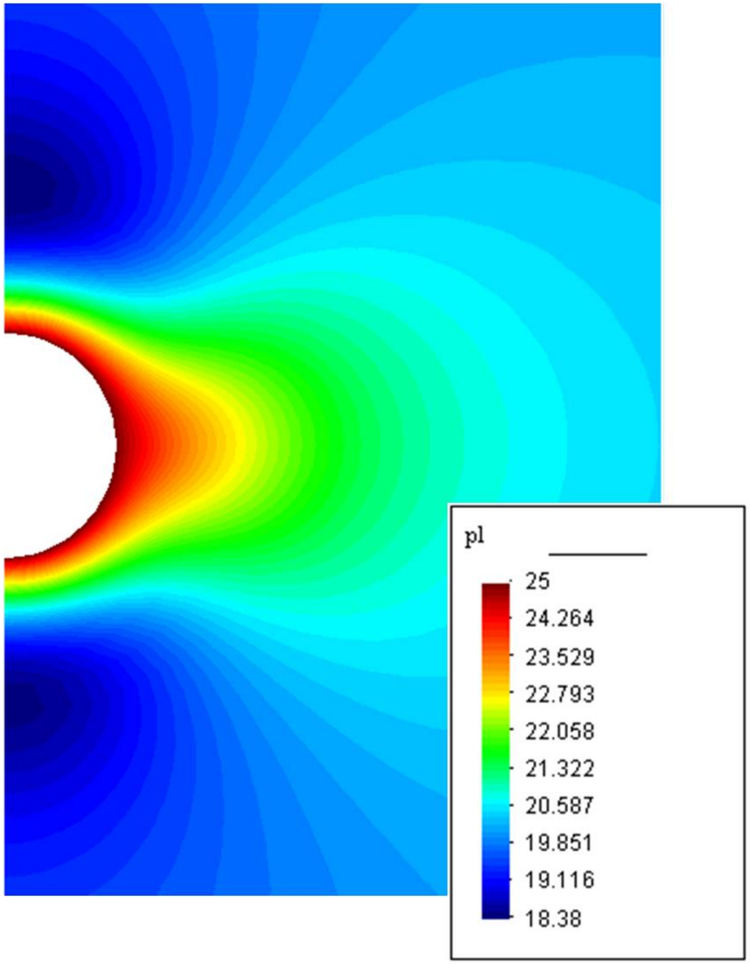

INPUTS OF A GEOMECHANICAL MODEL (SUMMARY)

In situ stress field:

Vertical stress → Density profile

$$\sigma_V = \mathbf{g}\int_{\mathbf{0}}^{\mathbf{Z}} \boldsymbol{\rho}(z).\,dz$$

Pore pressure → Direct measurement (RTF, TRF); Water hydrostatics

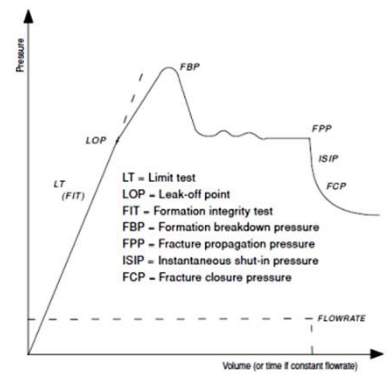

Minimum horizontal stress:
-magnitude
-direction

→ Hydraulic fracturing (LOT, XLOT)
→ Image profile

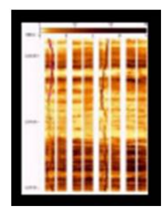

$$K_0 = \frac{\sigma'_h}{\sigma'_v}$$

Maximum horizontal stress:
-magnitude
-direction

→ Retro-analysis

f(σ’, esp.)

→ Image profile

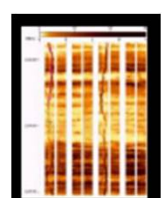

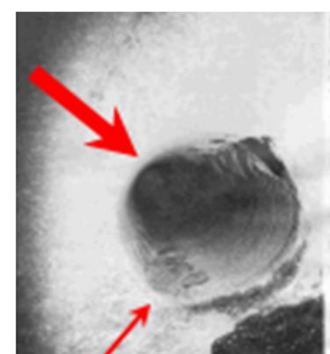

L. C. Pereira
(MSc, 2007)

INPUTS OF A GEOMECHANICAL MODEL (SUMMARY)

Rock parameters:

Deformability and strength parameters:

Elastic Modulus (E) and Poisson's ratio (ν):

Sonic profile + Elasticity theory → Equation: E and ν = f(V_p and V_s)

Cohesion (c):

Samples or sonic profile + UCS correlation = f(Δtc)

Friction angle (ϕ):

Literature → = 30° (sandstone)
= 20° (shale)

L. Cabral (MSc, 2007)

RESERVOIR COMPACTION

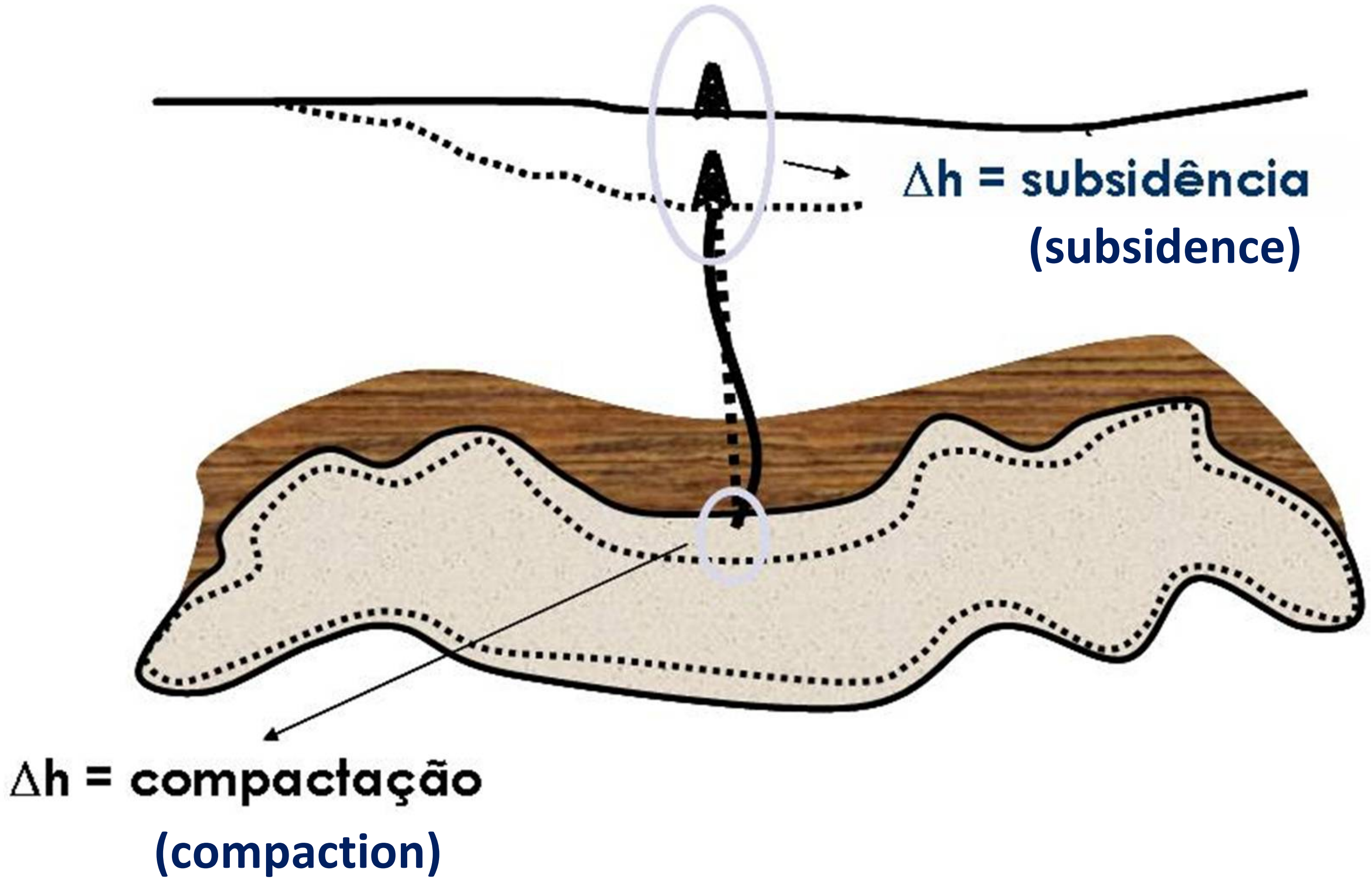

RESERVOIR COMPACTION

Valhall Field - North Sea
(SPE 83957, 2003)

- ➔ 1982 - beginning of production
- ➔ 1985 - first signs of subsidence
- ➔ 2003 - start of injection
- ➔ 2003 - accumulated subsidence of 4.9m at a rate of 25cm / year
- ➔ compaction account for 50% of total recovery

- ➔ carbonate reservoir with high porosity (between 42 and 50%)

L. C. Pereira (MSc, 2007)

RESERVOIR COMPACTION

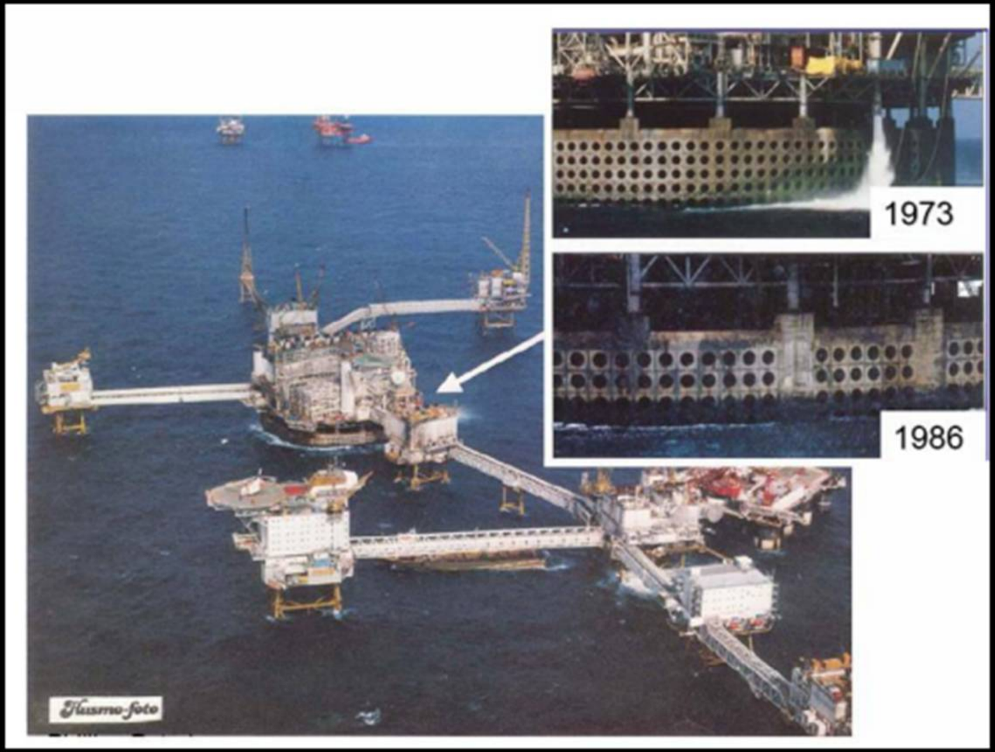

Ekofisk Field - North Sea (SPE 56426, 1999)

- 1971 - beginning of production
- 1984- first signs of subsidence
- 1987 - start of injection

Compaction causes:

- Reservoir depletion
- Waterweakening: incompatibility between carbonate rock and injected water

L. C. Pereira (MSc, 2007)

Water induced reservoir compaction

Ekofisk oilfield

1973

1984

Ekofisk 2/4 tank

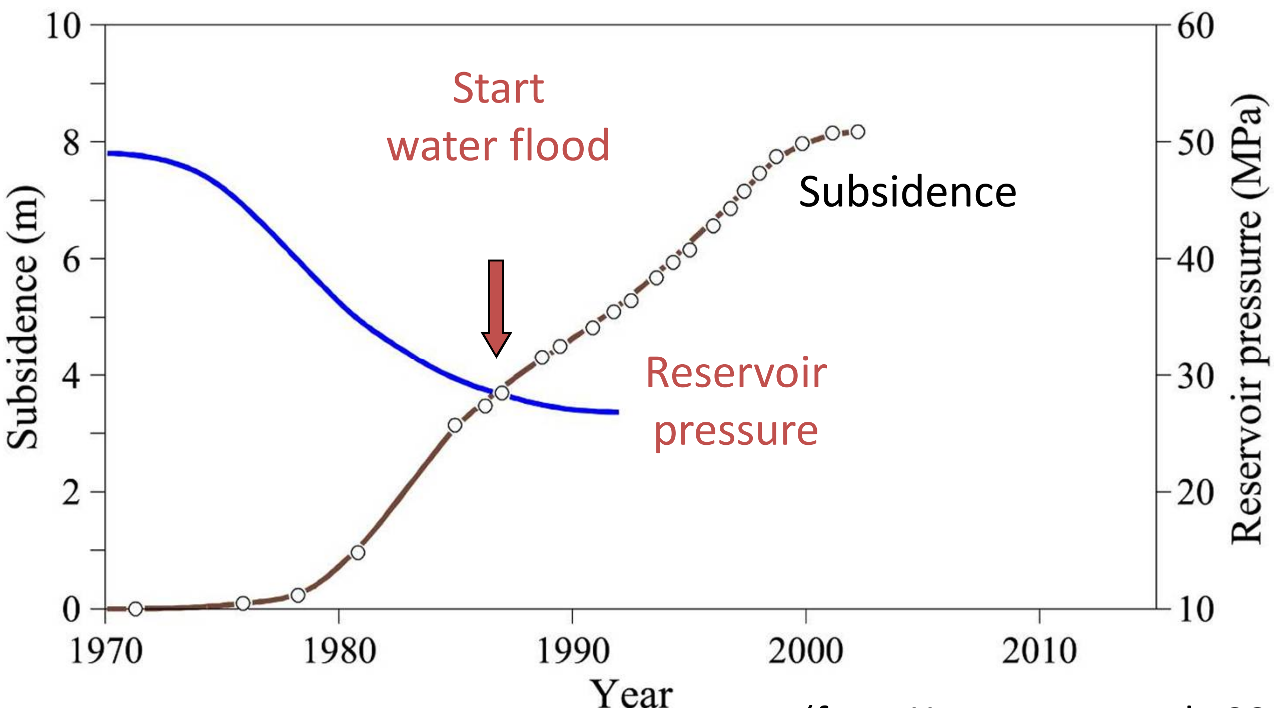

(from Hermansen et al., 2000)

Water induced reservoir compaction

Primary recovery: compaction explained by the *effective stress principle*

OK!

Secondary recovery: based on the *effective stresses concept,* the resorvoir should expand with injection!!

?

Start water flood

Possible explanation: *water weakening* mechanism (compaction under injection)

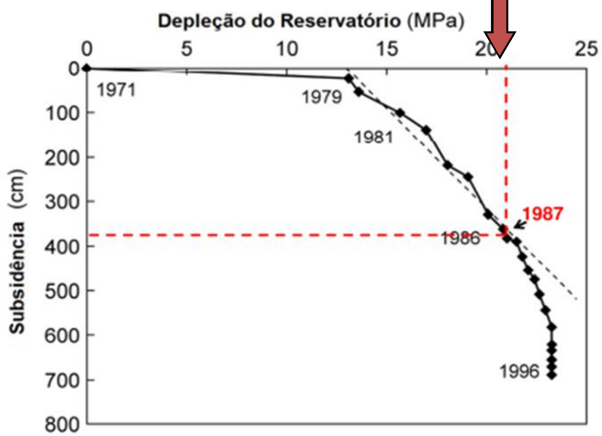

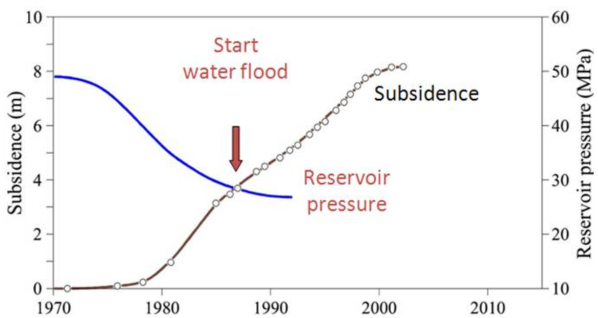

1973

1984

Ekofisk 2/4 tank

(from Hermansen et al., 2000)

Water induced reservoir compaction

Capillary pressure as a new state variable for the rock stress-strain behavior

Water weakening

Destruction of Intergranular links

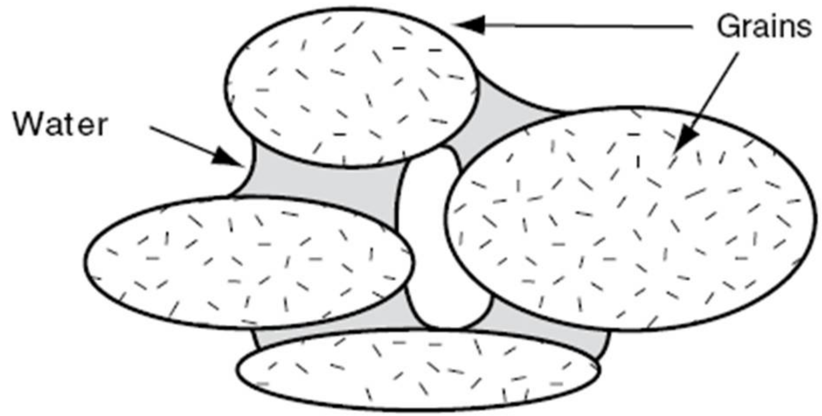

Figure 5

Chalk grains hold together by capillary forces.

Oil & Gas Science and Technology – Rev. IFP, Vol. 54 (1999), No. 6,

Mechanical Properties of Chalk with Emphasis on Chalk-Fluid Interactions and Micromechanical Aspects

R. Risnes[1] and O. Flaageng[1]

Water induced reservoir compaction

Experimental pressure solution compaction of chalk in aqueous solutions

Part 1. Deformation behavior and chemistry

ROLAND HELLMANN[1*], PETER J.N. RENDERS[1**], JEAN-PIERRE GRATIER[1], AND ROBERT GUIGUET[1]

[1] Crustal Fluids and Dynamics Group, LGIT, CNRS UMR C5559, Observatoire de Grenoble, Université J. Fourier, BP 53X, 38041 Grenoble Cedex 9, FRANCE
**present address: 211 Beekman St., Saratoga Springs, N.Y., 12866, U.S.A.

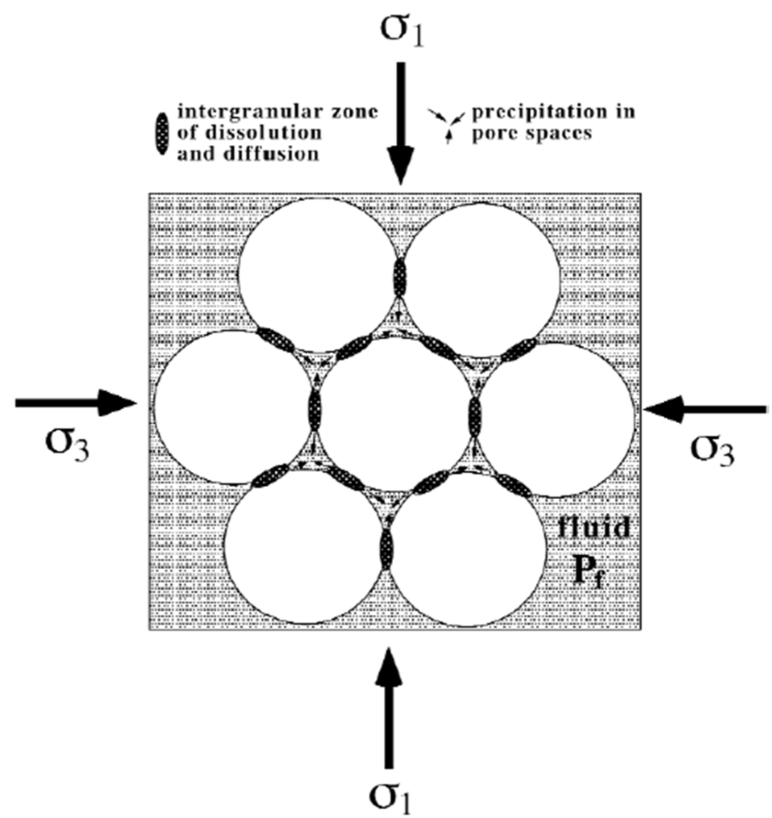

Water weakening

Destruction of Intergranular links

Chemo-mechanical Mechanism (ex: mineral dissolution)

Water induced reservoir compaction

Water weakening

Destruction of Intergranular links

Capillary pressure as a new state variable for the rock stress-strain behavior

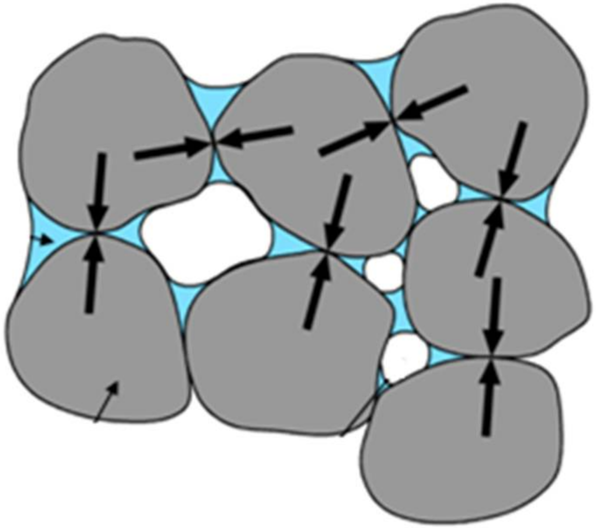

Mineral dissolution and precipitation as chemo-mechanical mechanism

Water induced reservoir compaction

Experimental pressure solution compaction of chalk in aqueous solutions

Part 1. Deformation behavior and chemistry

ROLAND HELLMANN[1*], PETER J.N. RENDERS[1**], JEAN-PIERRE GRATIER[1], AND ROBERT GUIGUET[1]

[1] Crustal Fluids and Dynamics Group, LGIT, CNRS UMR C5559, Observatoire de Grenoble,
Université J. Fourier, BP 53X, 38041 Grenoble Cedex 9, FRANCE

Water-Rock Interactions, Ore Deposits, and Environmental Geochemistry: A Tribute to David A. Crerar

Editors: Roland Hellmann and Scott A. Wood

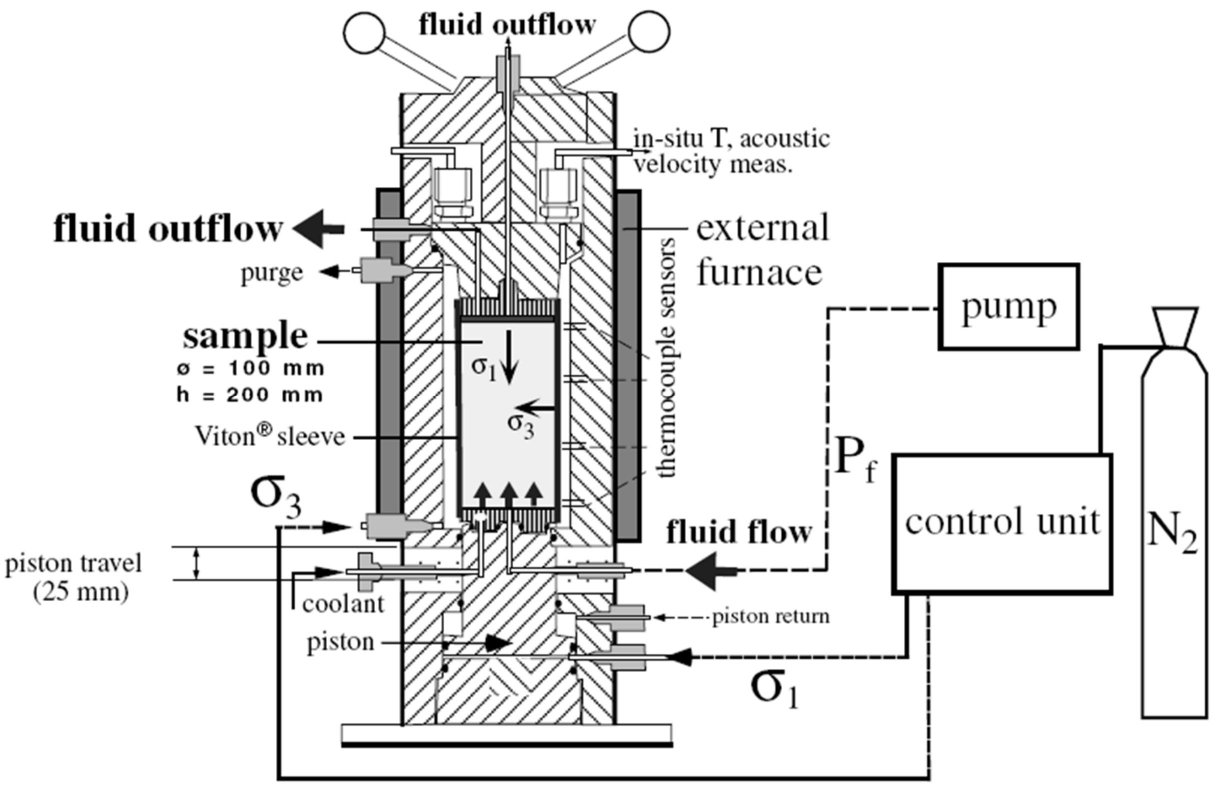

Chemical Mechanism

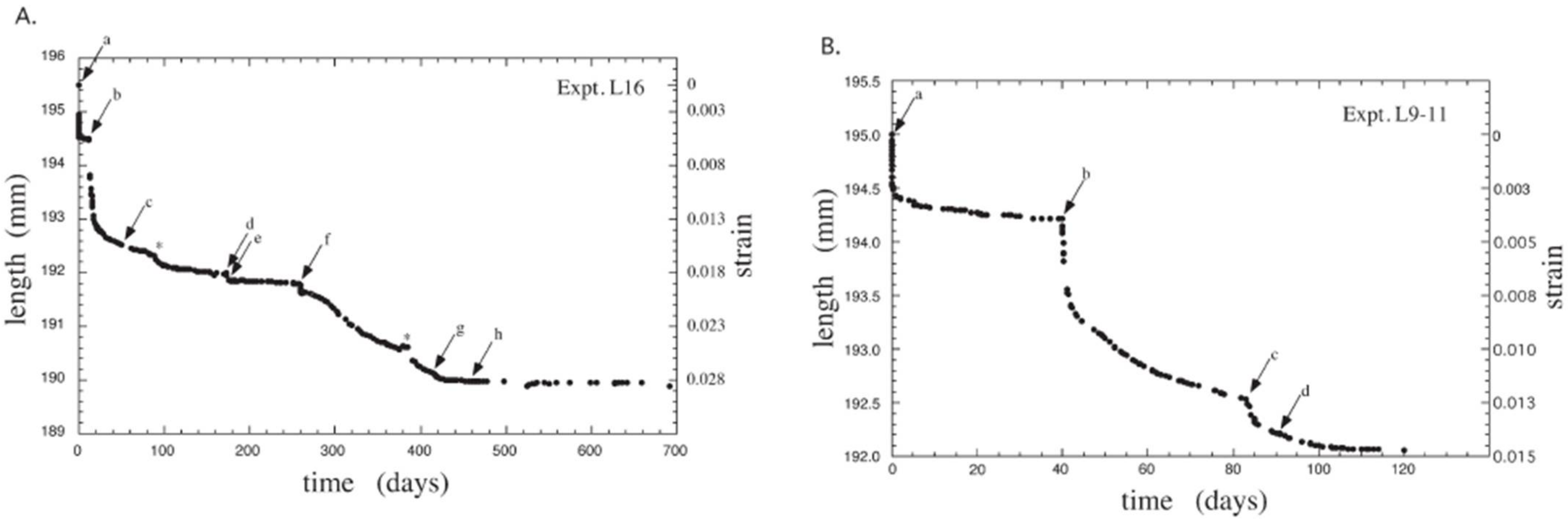

Fig. 5. Deformation curves for experiments L16 and L9-11 (note that strain (ε) increases in negative direction along ordinate axis). Changes in various strain rate-influencing parameters during the course of each experiment served to perturb local "steady-state" deformation behavior. (A) L16 parameter changes a: start of dry deformation, $\sigma_1 = 6.0$, $\sigma_3 = 4.0$ MPa, 25 °C b: injection H_2O, $v = 0.5 \rightarrow 0.1$ ml min^{-1}, T = 25 → 50 °C c: $v = 0$ over t = 50-172 days; *instability, gas bottle change d: injection saline solution over t = 179-189 days, v = variable e: $v = 0$ over t = 189-259 days f: T = 50 → 77 °C, $v = 0$ over t = 259-417 days; * instability, gas bottle change, $\sigma_1 = 7.0$, $\sigma_3 = 4.0$ MPa g: $v = 0.1$ ml min^{-1} over t = 417-461 days h: injection propanol, $v = 0.1 \rightarrow 0$ ml min^{-1}. (B) L9-11 parameter changes a: dry deformation: 0 - 0.08 days, followed by start of fluid-assisted deformation, injection H_2O, $v = 0.5 \rightarrow 0.2$ ml min^{-1}, $\sigma_1 = 4.9$, $\sigma_3 = 4.0$ MPa b: $\sigma_1 = 7.0$, $\sigma_3 = 4.0$ MPa, $v = 0.2 \rightarrow 0.1$ ml min^{-1} c: T = 25 → 50 °C d: injection of saline solution, $v = 0.1$ ml min^{-1}.

RESERVOIR COMPACTION

Environmental damages in regional scale:

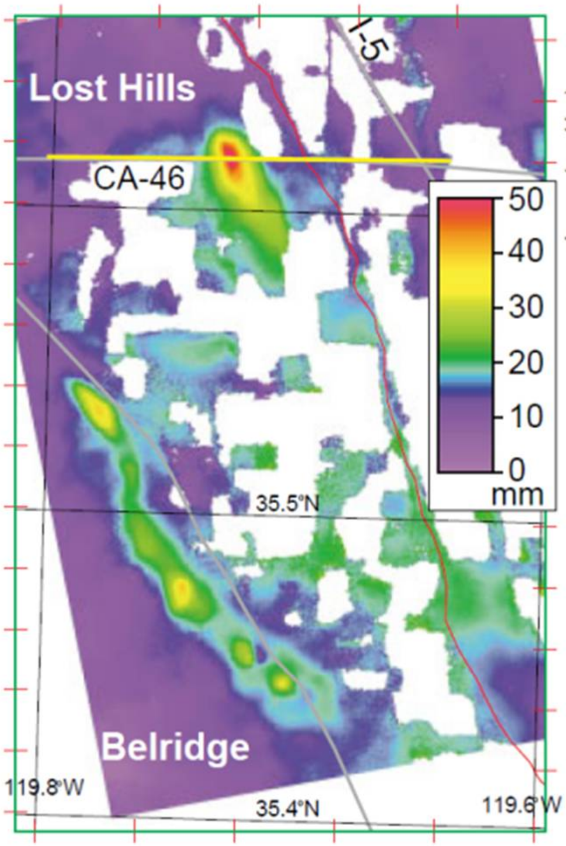

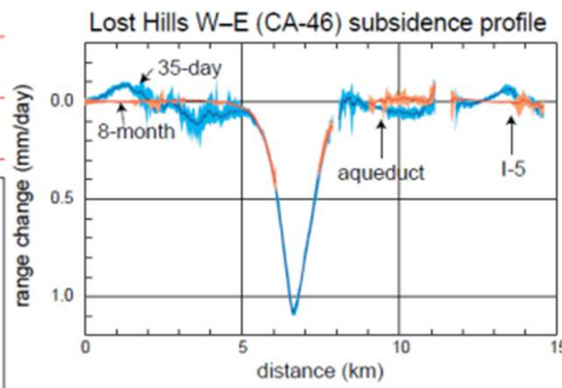

TROUGH SUBSIDENCE

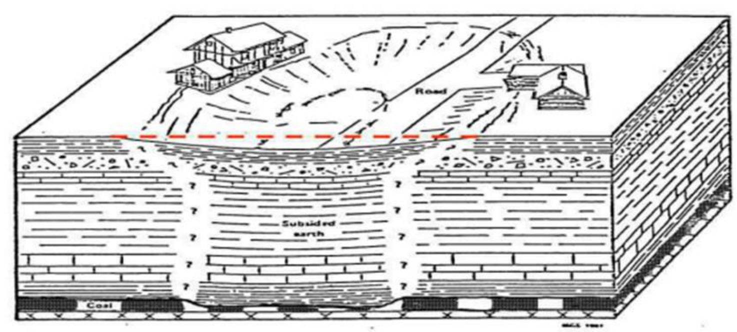

Figura 5.1: *Medição por satélite da subsidência em campo de petróleo na região Lost Hills-Califórnia. Seguindo a linha leste-oeste (CA-46), nota-se uma taxa de subsidência média de mais de 1 mm/dia - E.J.Fielding, R.G. Blom & R.M.Goldstein - JPL - Nasa - Califórnia*

RESERVOIR COMPACTION

Environmental damages in regional scale:

Sign warning motorists of subsidence hazard was erected after an earth fissure damaged Snyder Hill Road in Pima County, Arizona, 1981.

RESERVOIR COMPACTION

Cap rock integrity during depletion:

Fault regimes induced by reservoir compaction:
NF – Normal faults
RF – Reverse faults
The upper part of the reservoir tends to move downwards while the lower part moves upwards

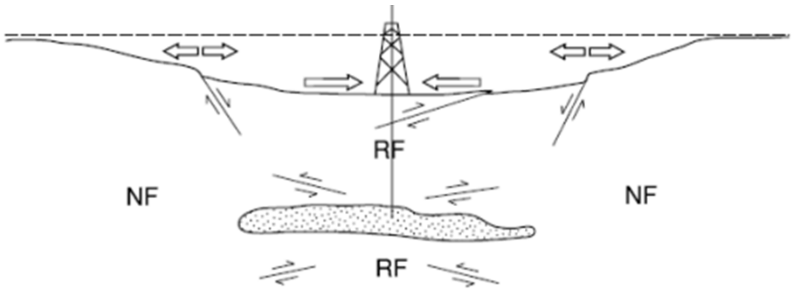

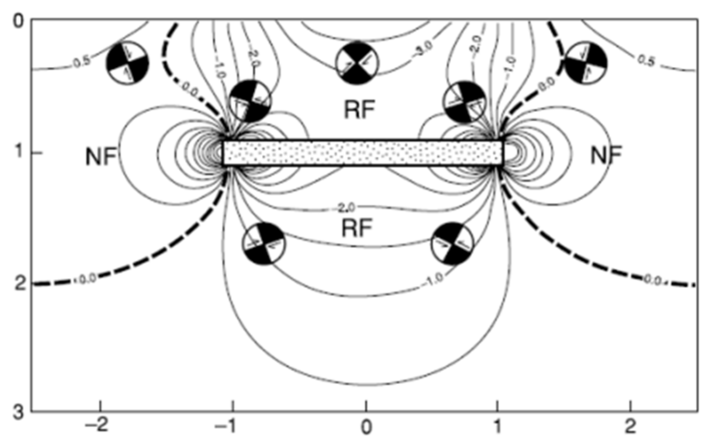

Figura 5.6: *Diagrama mostrando a deformação que ocorre na vizinhança de um reservatório que está sendo depletado (Segall-1990)(Zoback, M. D., 2007)*

RESERVOIR COMPACTION

and other consequences…

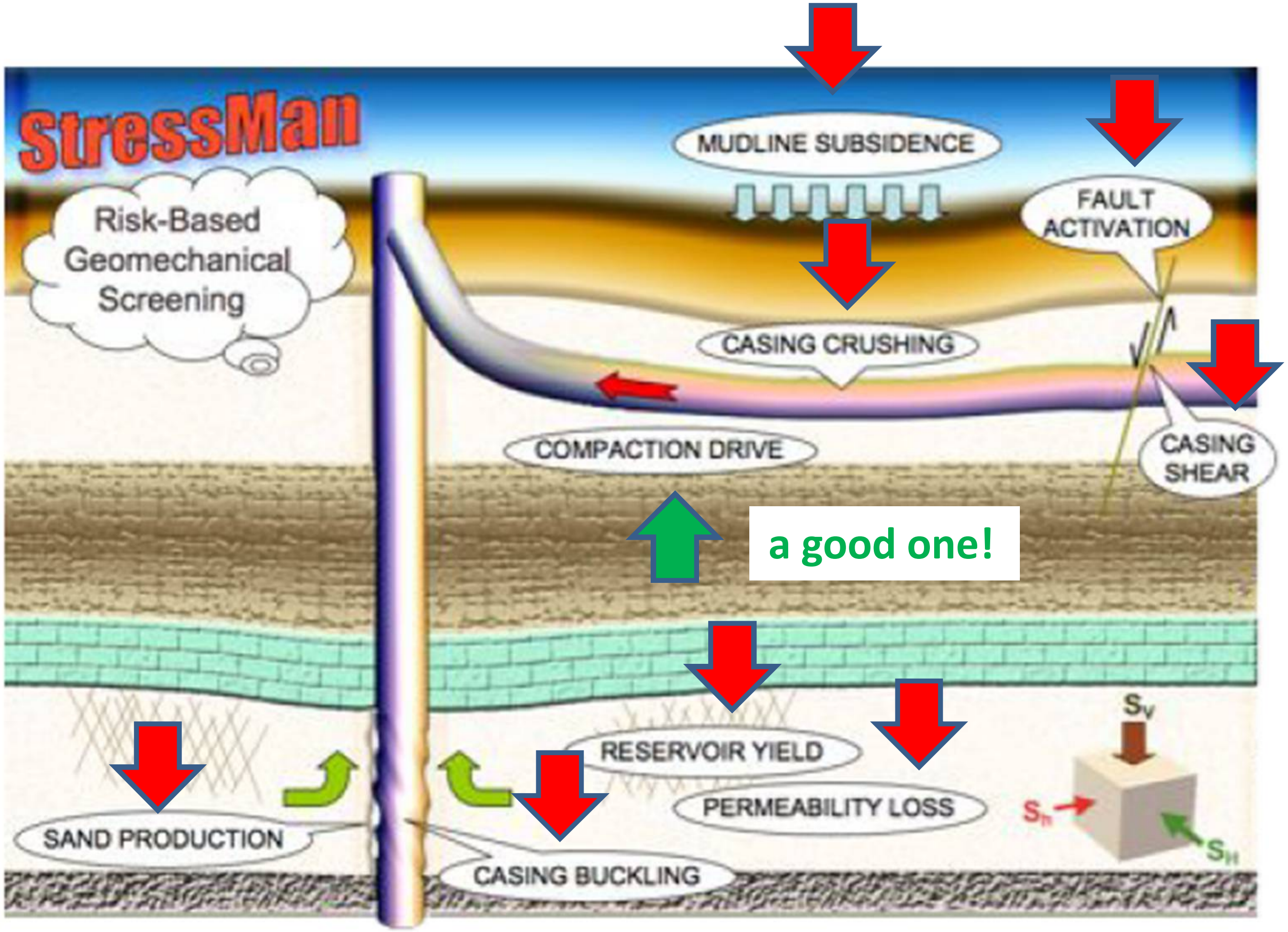

RESERVOIR COMPACTION

Hydraulic problem: two phase flow equations for deformable porous media

$$\frac{\partial(\phi s_\alpha \rho_\alpha)}{\partial t} + \nabla\left(\rho_\alpha q_\alpha + \boxed{\phi s_\alpha \rho_\alpha \dot{\mathbf{u}}}\right) = 0 \qquad \alpha = w, o$$

$$q_\alpha = -\frac{k k_{r\alpha}}{\mu_\alpha}\left(\nabla p_\alpha - \rho_\alpha \tilde{g}\right)$$

where: $s_w + s_o = 1$ $\quad p_c = p_o - p_w$ $\quad \lambda_\alpha = k_{r\alpha} / \mu_\alpha$

ϕ	porosity
s_α	fluid saturation
ρ_α	fluid density
q_α	Darcy flow
μ_α	phase viscosity
$\dot{\mathbf{u}}$	Solid velocity
$\mathbf{k}$	permeability tensor
$k_{r\alpha}$	fluid relative permeability
λ_α	fluid mobility
p_α	Fluid pressure
p_c	capillary pressure
$\tilde{g}$	gravity

RESERVOIR COMPACTION

UFPE

Mechanical problem for geomaterials:

- Equilibrium Equation:

$$\nabla \cdot \boldsymbol{\sigma} + \mathbf{b} = \mathbf{0}$$

- Principle of Effective Stresses:

$$\boldsymbol{\sigma} = \boldsymbol{\sigma}' + \alpha \cdot p_f \cdot \mathbf{I}$$

- Stress-strain relationship:

$$\mathbf{d}\boldsymbol{\sigma}' = \mathbf{D} \cdot \mathbf{d}\boldsymbol{\varepsilon}$$

Specific for each geomaterial

HM FORMULATION

HYDRO-MECHANICAL COUPLINGS:

- Rock porosity:

$$\frac{\partial}{\partial t}\left[(1-\phi)\rho_s\right]+\nabla\left[(1-\phi)\rho_s\,.\dot{\mathbf{u}}\right]=0$$

(mass conservation of solids)

(material derivative)

$$\frac{d\bullet}{dt}=\frac{\partial\bullet}{\partial t}+\dot{\mathbf{u}}\cdot\nabla\bullet$$

$$\frac{d\phi}{dt}=\frac{(1-\phi)}{\rho_s}\frac{d\rho_s}{dt}+(1-\phi)\frac{d\varepsilon_v}{dt}$$

(changes of porosity as

a function of volumetric strains)

- Rock permeability:

$$\mathbf{k}=\mathbf{k}_{\mathbf{i}}\exp\left[b(\phi-\phi_i)\right]$$

Other: Kozeny-Carman

$$\mathbf{k}=\mathbf{k}_o\frac{\phi^3}{(1-\phi)^2}\frac{(1-\phi_o)^2}{\phi_o^{\ 3}}$$

ϕ_o : reference porosity

$\mathbf{k}_o$: intrinsic permeability for matrix ϕ_o

RESERVOIR COMPACTION

HYDRAULIC

- **Water and oil flow: Darcy's law**

$$q_w = -K_w(\nabla P_w - \rho_w g)$$
$$q_o = -K_o(\nabla P_o - \rho_o g)$$

- **Water and oil flow driven by pressure gradients**
- **Permeability tensor**

$$K_\alpha = k\, k_{r\alpha} / \mu_\alpha$$

k : intrinsic permeability tensor

$k_{r\alpha}$: relative permeability

μ_α: dynamic viscosity

$$\mathbf{k} = \mathbf{k_i} \exp\left[b(\phi - \phi_i)\right]$$

$$\frac{\partial(\phi s_\alpha \rho_\alpha)}{\partial t} + \nabla\left(\rho_\alpha q_\alpha + \phi s_\alpha \rho_\alpha \dot{\mathbf{u}}\right) = 0$$

MECHANICAL:

$$\nabla \boldsymbol{\sigma} + \mathbf{b} = 0$$
$$\boldsymbol{\sigma} = \boldsymbol{\sigma}' + S_w \cdot P_w + S_o \cdot P_o$$
$$\boldsymbol{\sigma}' = \mathbf{D} \cdot \boldsymbol{\varepsilon}$$
$$\varepsilon_v = Tr(\boldsymbol{\varepsilon}) = \nabla \mathbf{u}$$

SOLID BALANCE:

$$\frac{d\phi}{dt} = \frac{(1-\phi)}{\rho_s}\frac{d\rho_s}{dt} + (1-\phi)\frac{d\varepsilon_v}{dt}$$

RESERVOIR COMPACTION

Increase of fluid flow apparent velocity

$$\mathbf{v}_{\alpha} = \frac{\mathbf{q}_{\alpha}}{\phi}$$

Porosity decrease

Volumetric strain in mass balance equations:

Compaction-driven mechanism

$$\rightarrow \frac{D}{Dt}\phi = \frac{(1-\phi)}{\rho_s}\frac{D}{Dt}\rho_s + (1-\phi)\dot{\boldsymbol{\varepsilon}}_v$$

Pressure maintenance

$$\phi\frac{D}{Dt}\rho_w + \nabla\cdot\left[-\mathbf{K}\frac{\rho_w}{\mu_w}\nabla\rho_w - \mathbf{K}\frac{\rho_w{}^2}{\mu_w}\mathbf{g}\right] + \rho_w\dot{\boldsymbol{\varepsilon}}_v = 0 \quad \text{(Eq.7)}$$

Mass balance Final Equation

SECONDARY OIL RECOVERY: WATER INJECTION

UFPE

Sensitivity analysis of reservoir compaction parameters:

***Elastic* and *Elasto-plastic (with CAP)* reservoir**

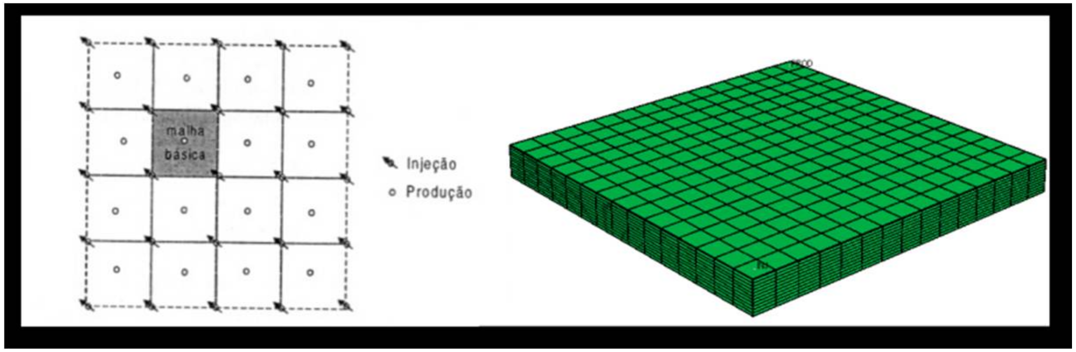

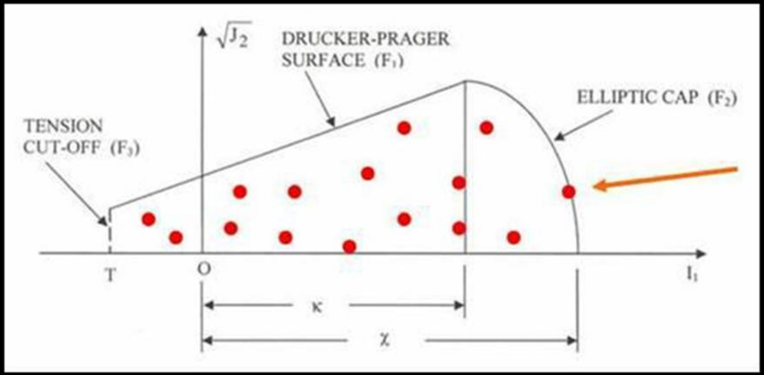

$$\sigma'_v = \sigma'_H = \sigma'_h = 3515\,psi$$

L. C. Pereira (MSc, 2007)

RESERVOIR COMPACTION

Sensitivity analysis on cummulative oil production:

Variable

Parâmetros	Intervalo		Unidade
Coeficiente de Biot	0,8	1,0	
Módulo de Elasticidade	8E+05	2E+06	psi
Ângulo de Atrito	30	40	°
Poisson	0,2	0,4	
Coesão	1000	3000	psi
Posição do "cap"	5000	10000	psi

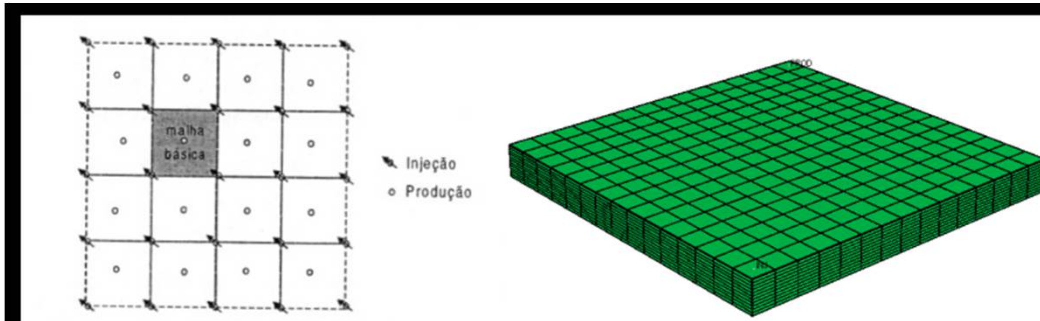

Fixed

μ_o:	14,38 *cP*
μ_w:	0,4 *cP*
ϕ:	0,2
K_x e K_y:	40 *mD*
K_z:	4 *mD*
P:	19149 *psi*

Q_{inj}:	3000 *bbl/d*
Q_{prod}:	3000 *bbl/d*
P_{min}:	1000 *psi*
t:	30 *anos*
Prod:	31/12/2008
Inj:	31/12/2013

L. C. Pereira (MSc, 2007)

RESERVOIR COMPACTION

Sensitivity analysis of reservoir compaction parameters:

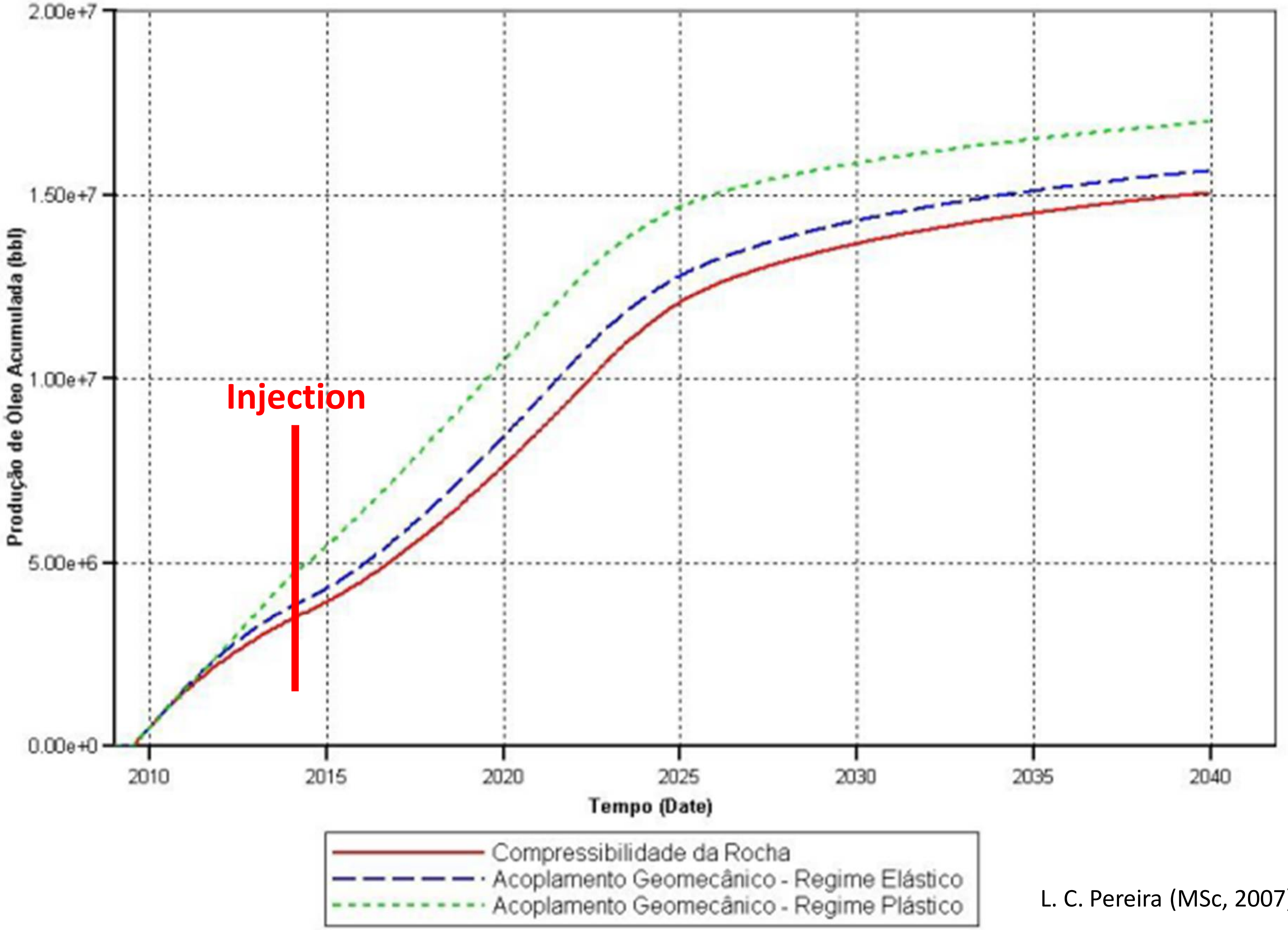

L. C. Pereira (MSc, 2007)

RESERVOIR COMPACTION

Sensitivity analysis of reservoir compaction parameters:

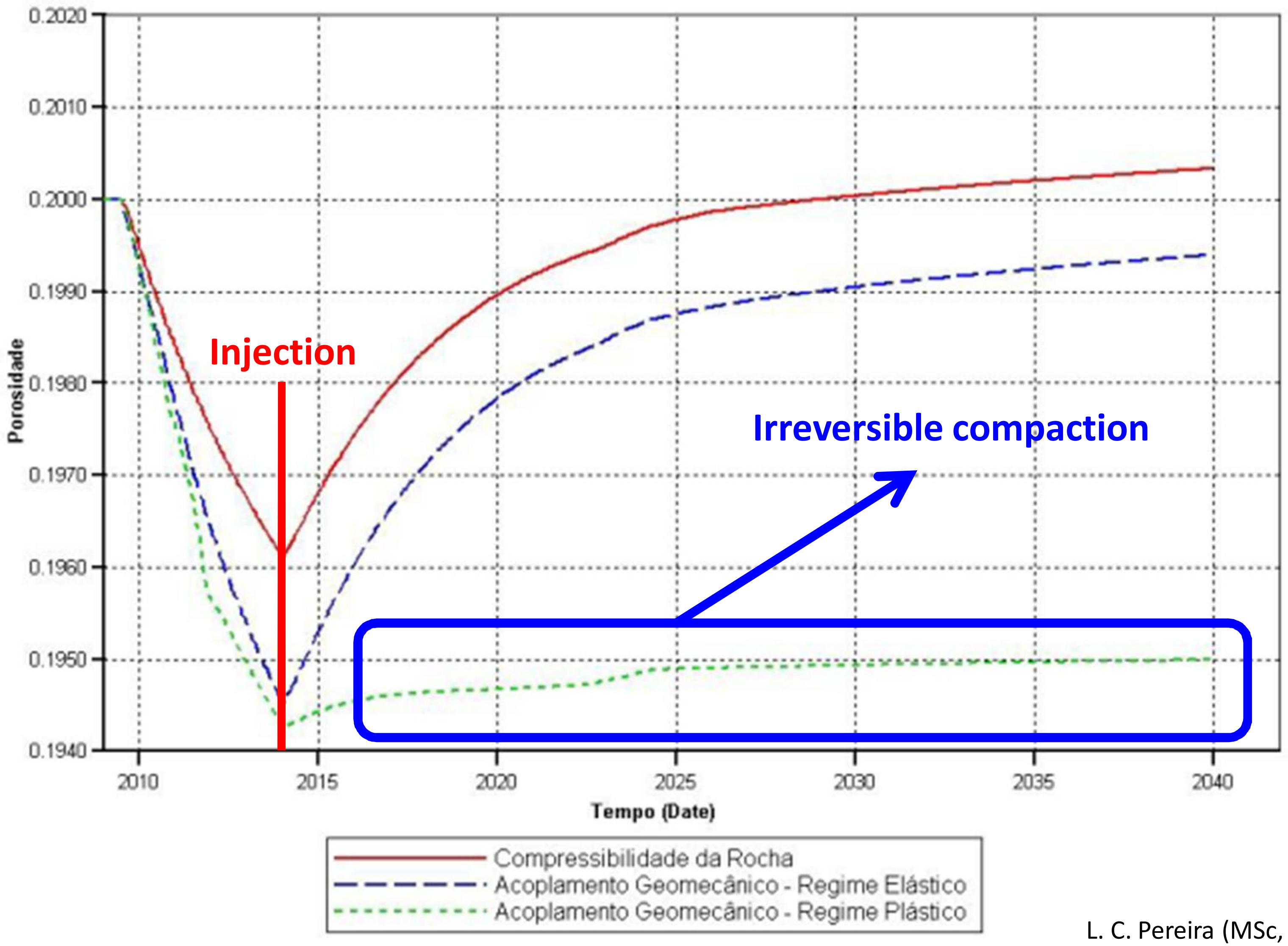

L. C. Pereira (MSc, 2007)

RESERVOIR COMPACTION

Sensitivity analysis of reservoir compaction parameters:

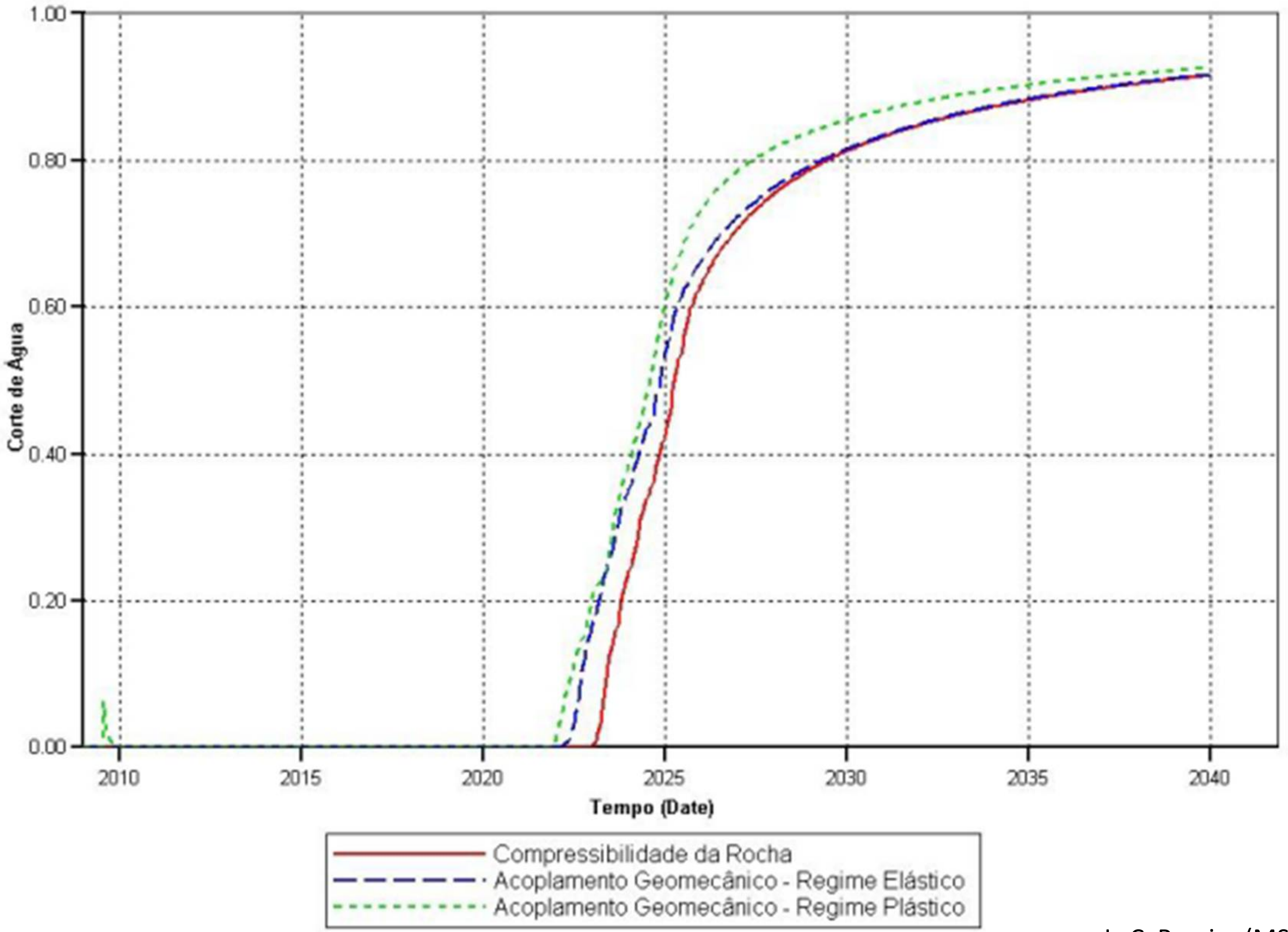

L. C. Pereira (MSc, 2007)

RESERVOIR COMPACTION

Sensitivity analysis of reservoir compaction parameters:

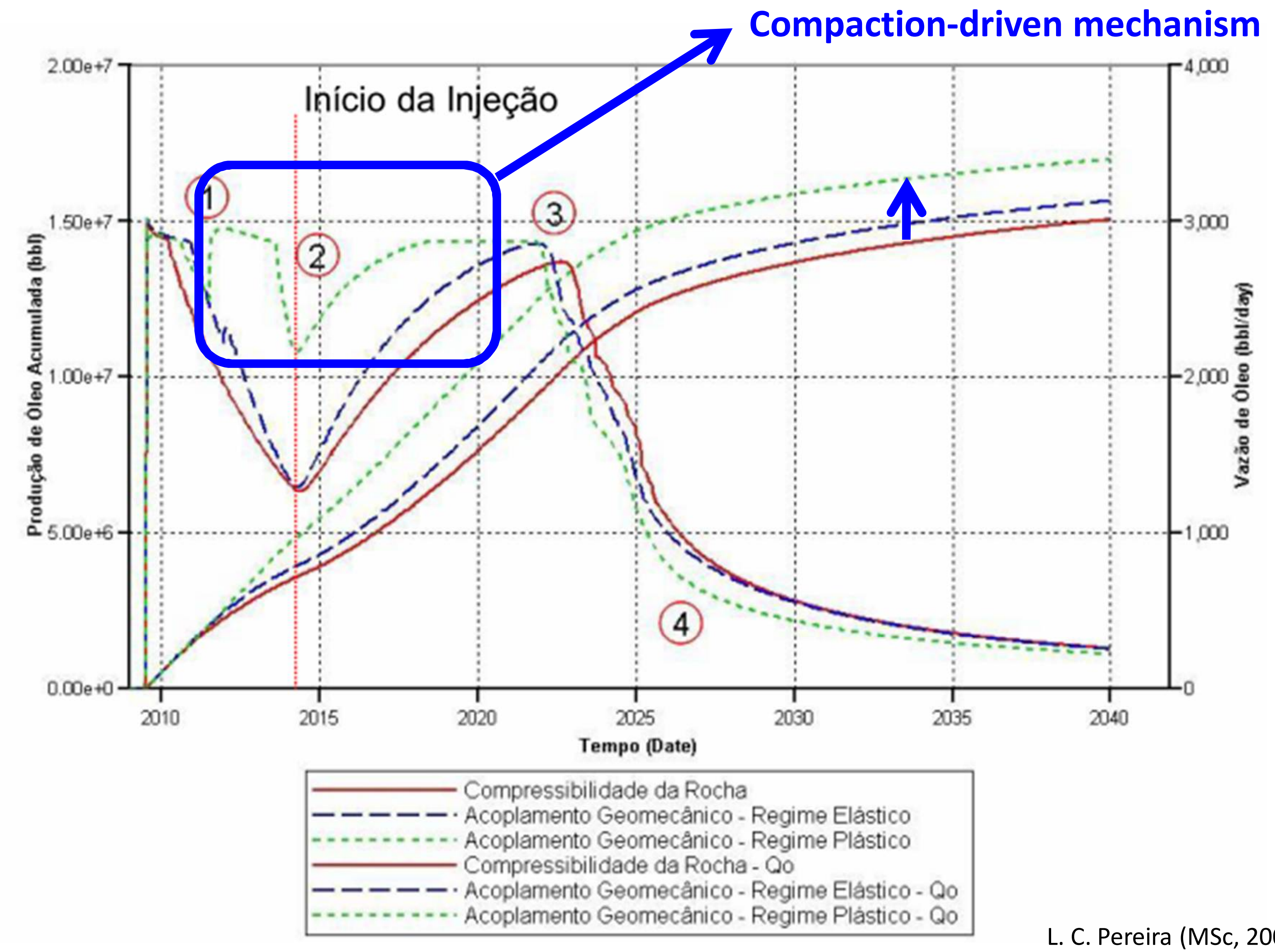

L. C. Pereira (MSc, 2007)

RESERVOIR COMPACTION

Sensitivity analysis of reservoir compaction parameters:

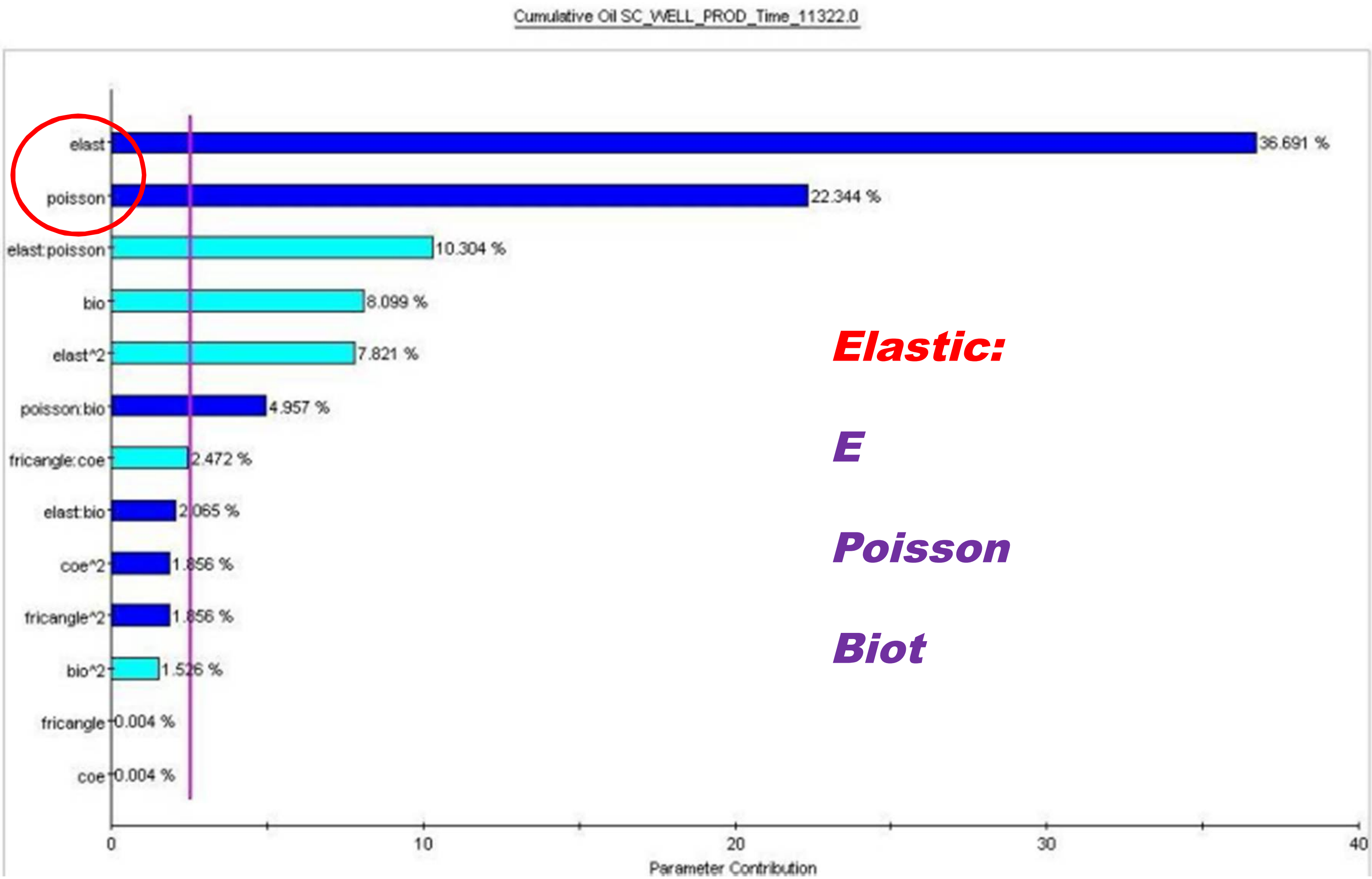

Elastic:

E

Poisson

Biot

L. C. Pereira (MSc, 2007)

Sensitivity analysis of reservoir compaction parameters:

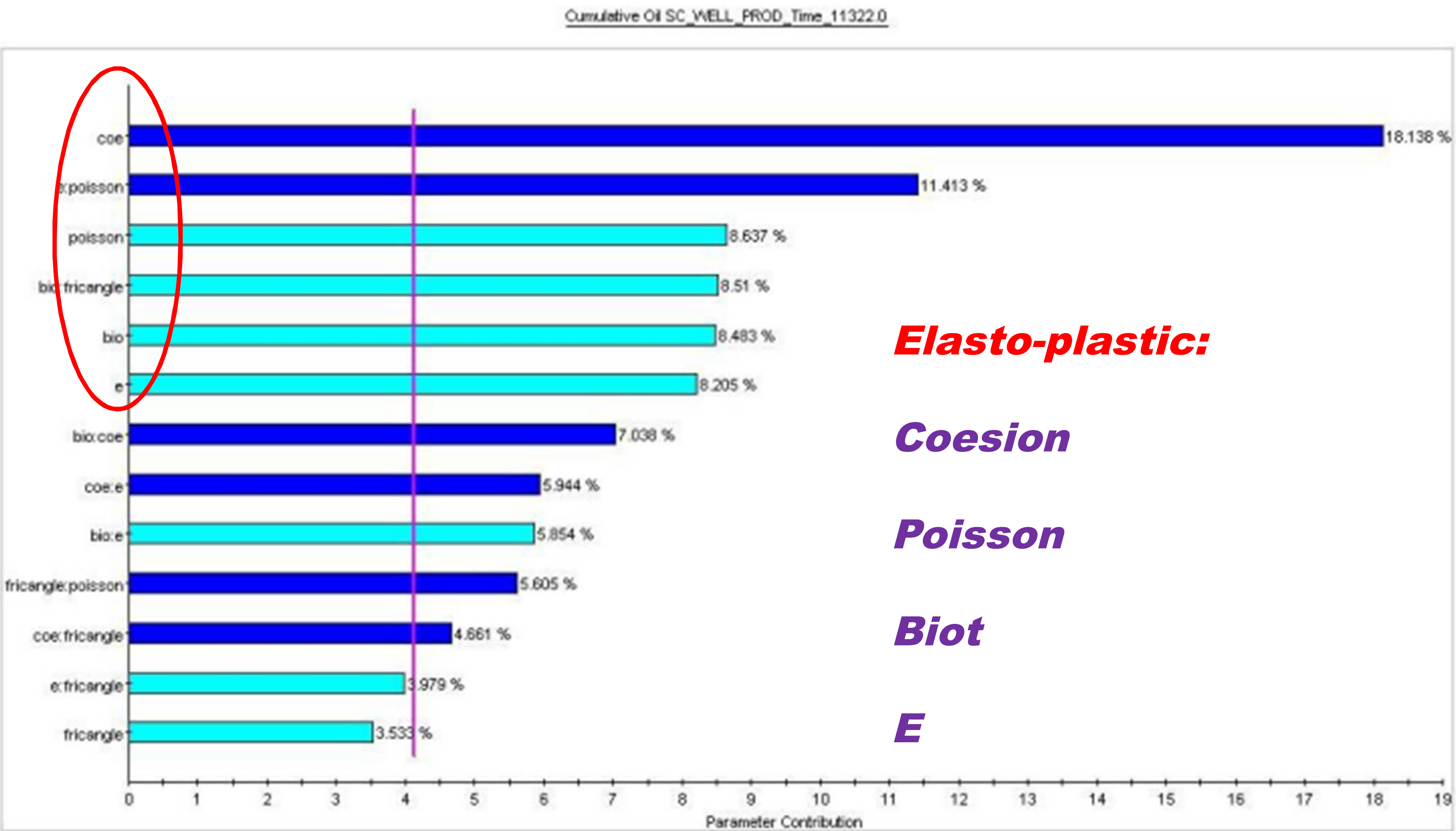

Elasto-plastic:

Coesion

Poisson

Biot

E

L. C. Pereira (MSc, 2007)

RESERVOIR COMPACTION

Real case:

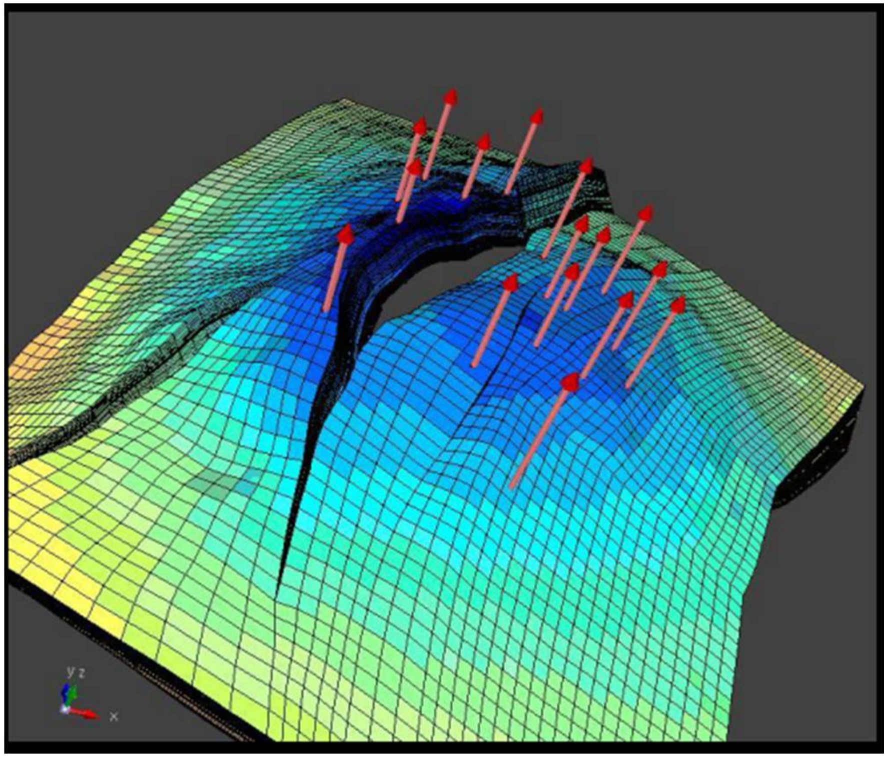

HT/HP reservoir (Pereira, 2007)

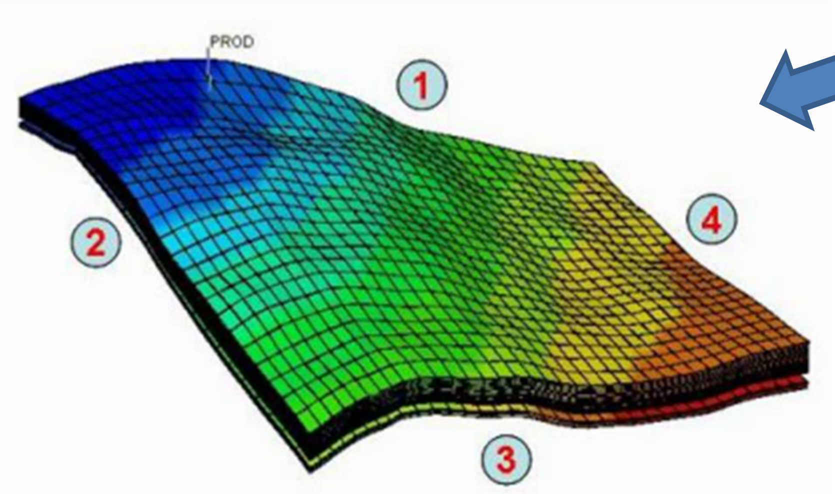

L. C. Pereira (MSc, 2007)

RESERVOIR COMPACTION

Real case:

Displacement

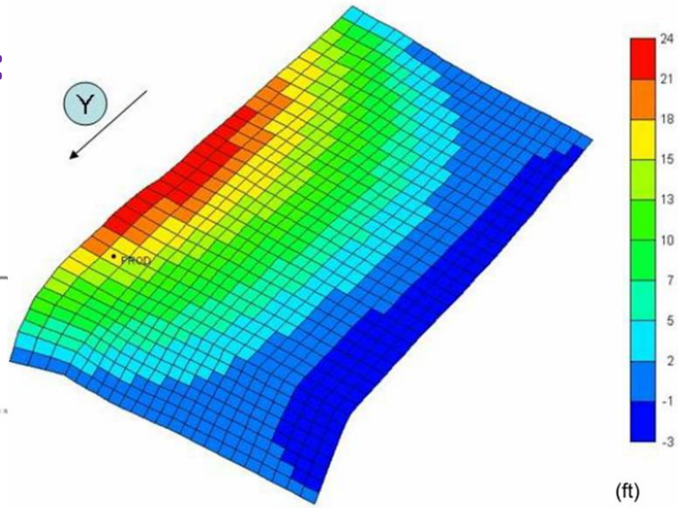

Plastic strains

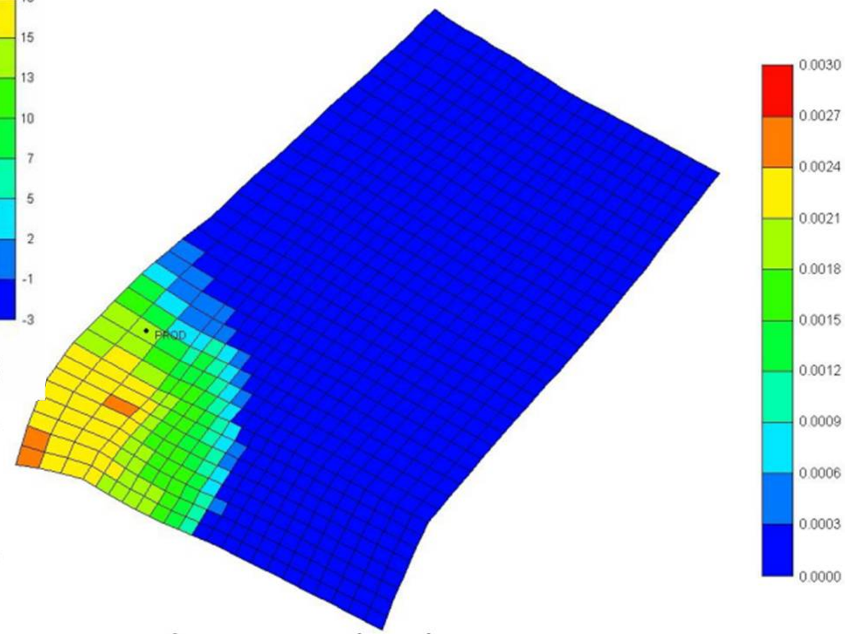

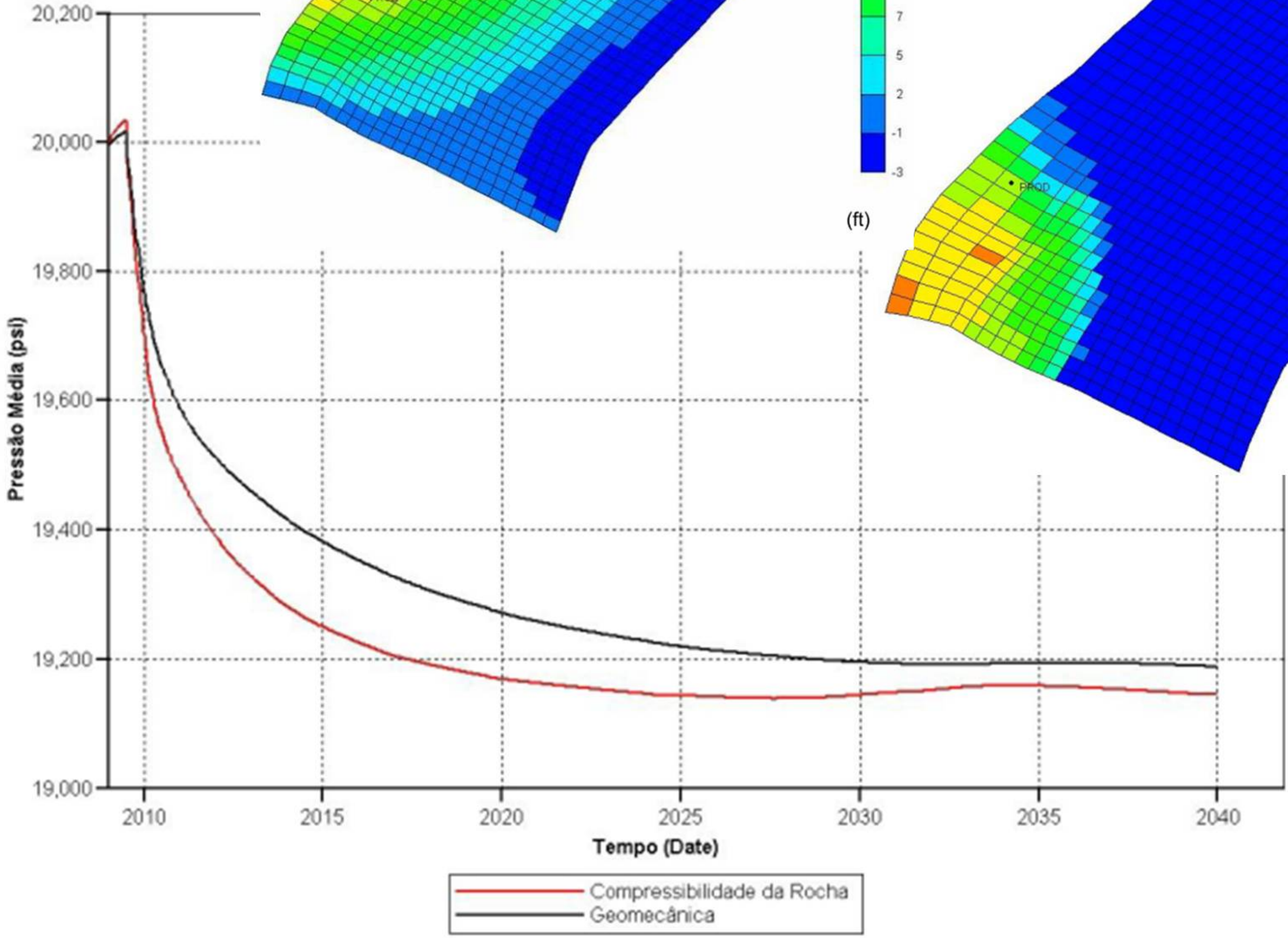

L. C. Pereira (MSc, 2007)

RESERVOIR COMPACTION

Is it correct to use in conventional reservoir simulation **Permeability** as a function of **Pressure**?? K(P)?

It depends!! More critical close to wellbores.

Points at elastic regions

Points at elasto-plastic (compaction and dilation) regions

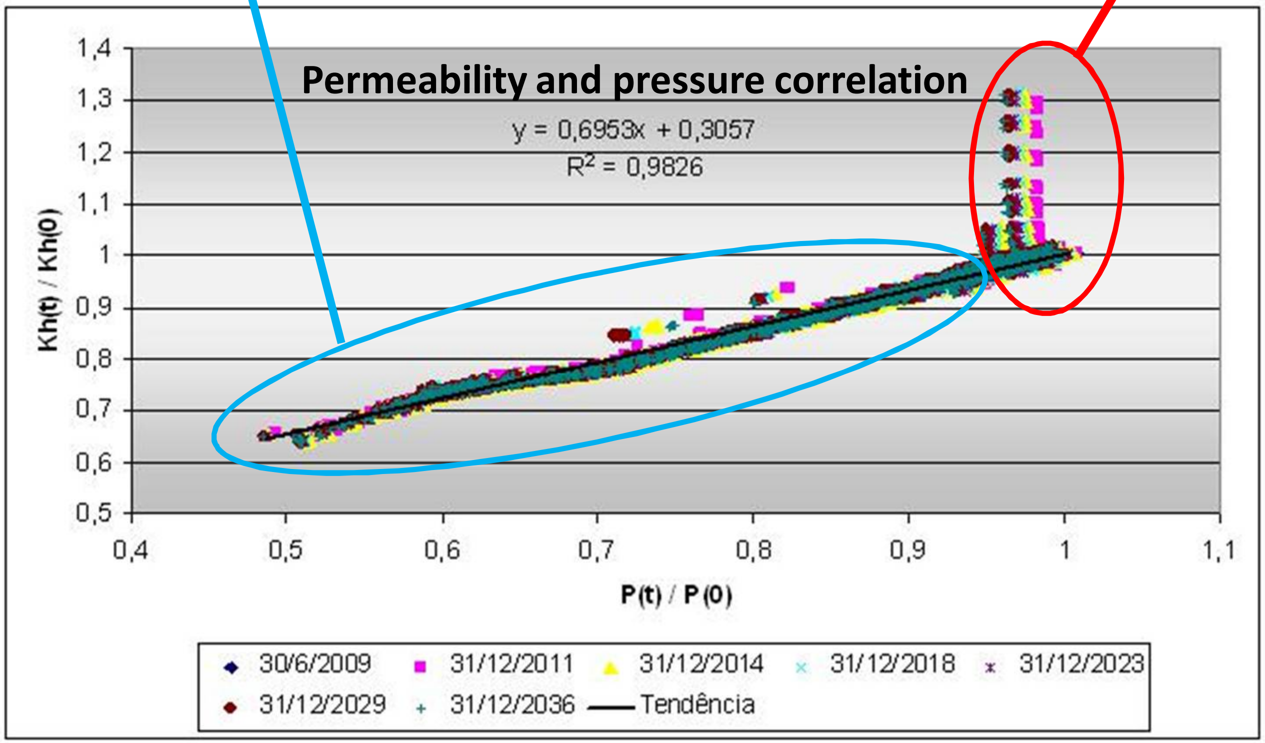

Permeability and pressure correlation in a coupled geomechanical simulation

L. C. Pereira (MSc, 2007)

FAULT REACTIVATION

Why it is important to study fault reactivation?

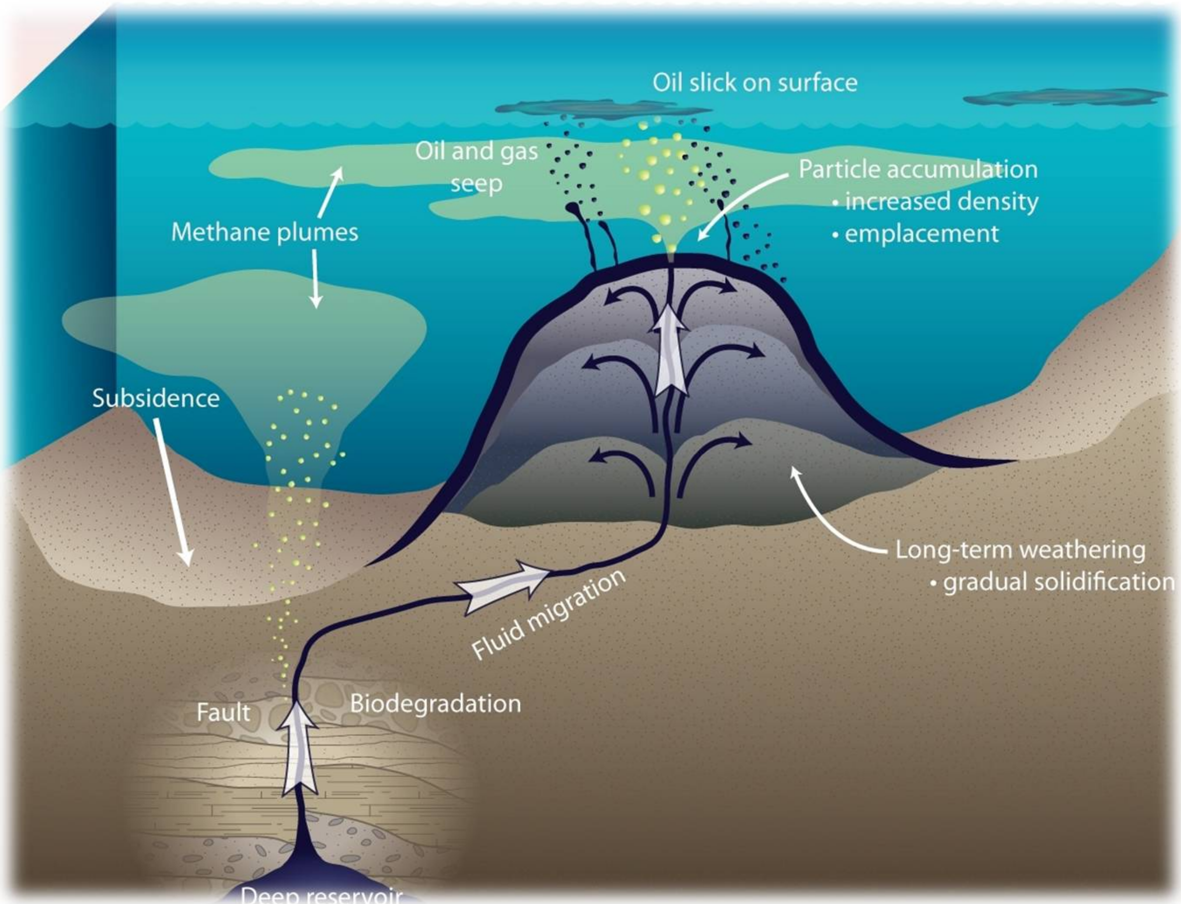

FAULT REACTIVATION

Why it is important to study fault reactivation?

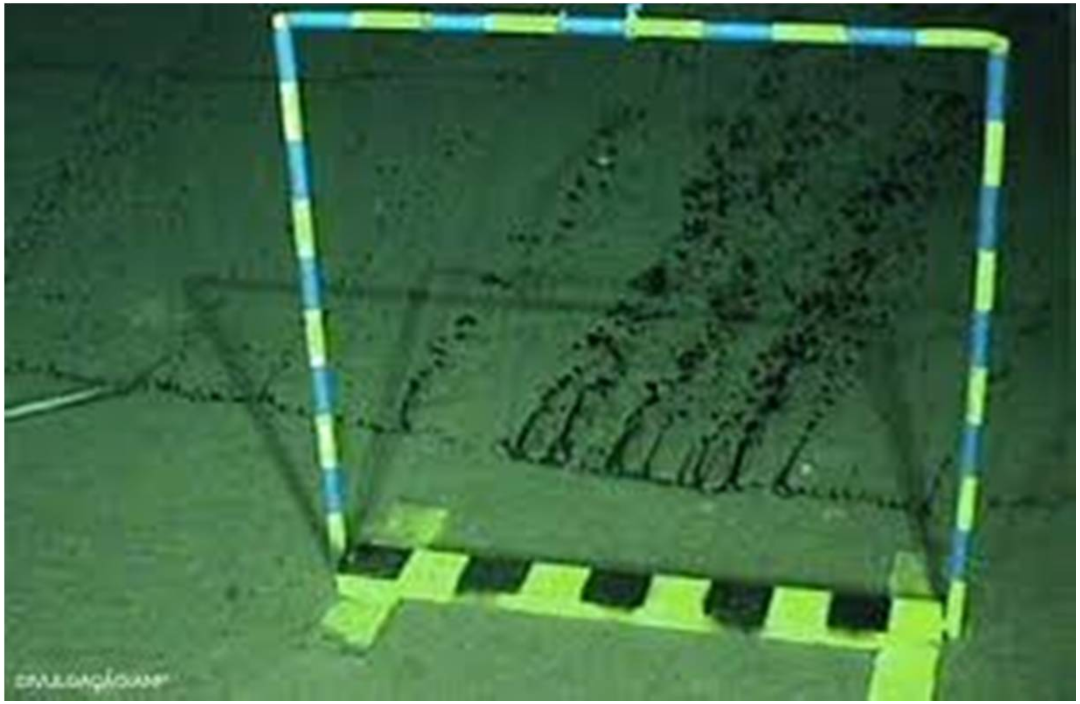

FAULT REACTIVATION

Why it is important to study fault reactivation?

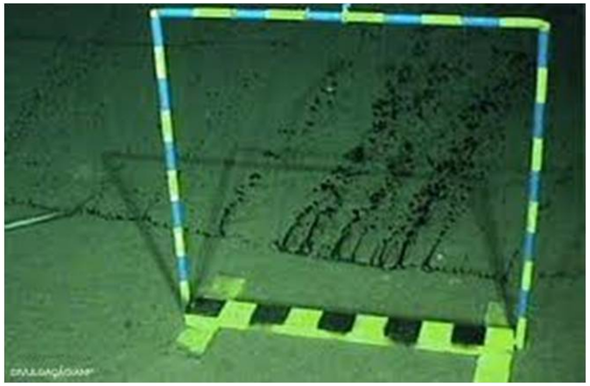

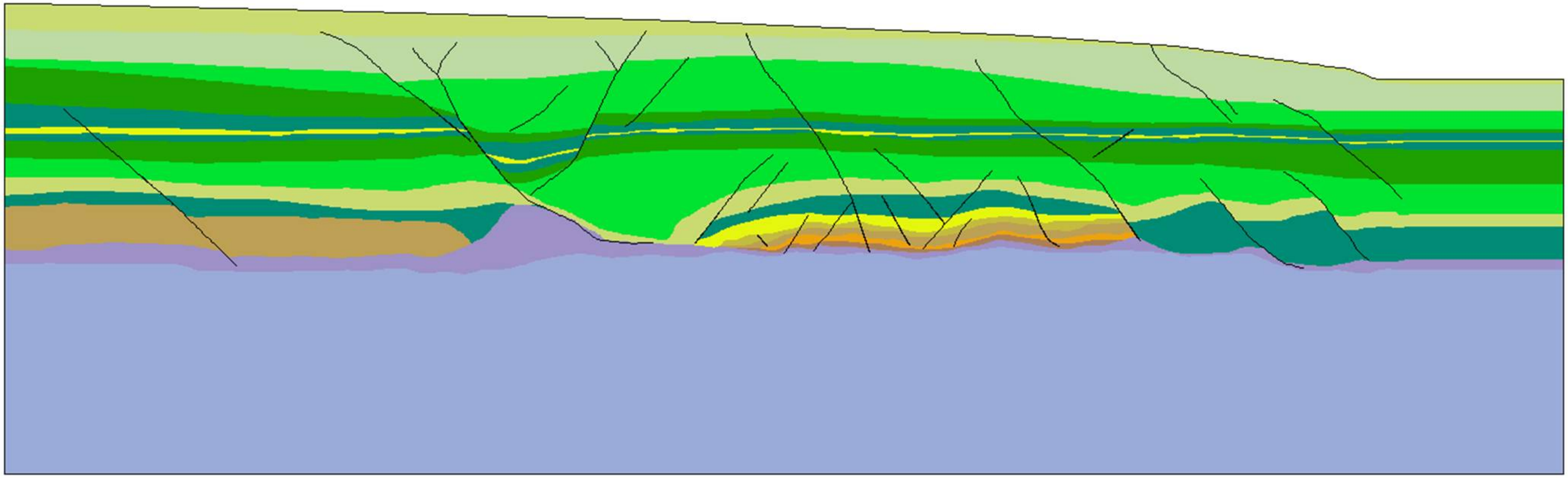

FAULT REACTIVATION

Why it is important to study fault reactivation?

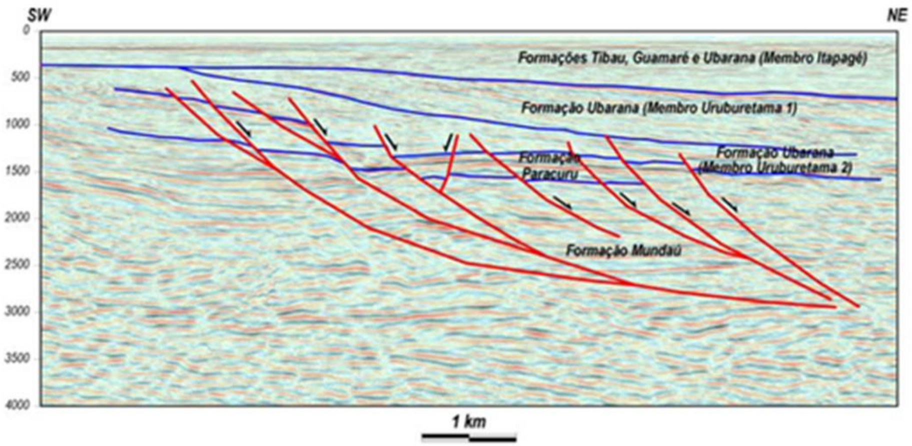

Campo de Xaréu
Sub-bacia de Mundaú
Bacia do Ceará - NE

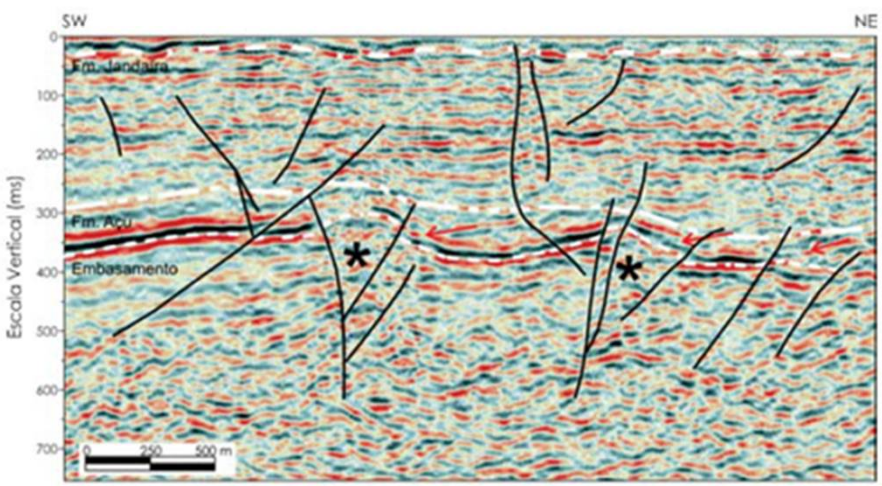

Icapuí-Ponta Grossa(CE)
Bacia Potiguar

FAULT REACTIVATION

How to represent them properly?

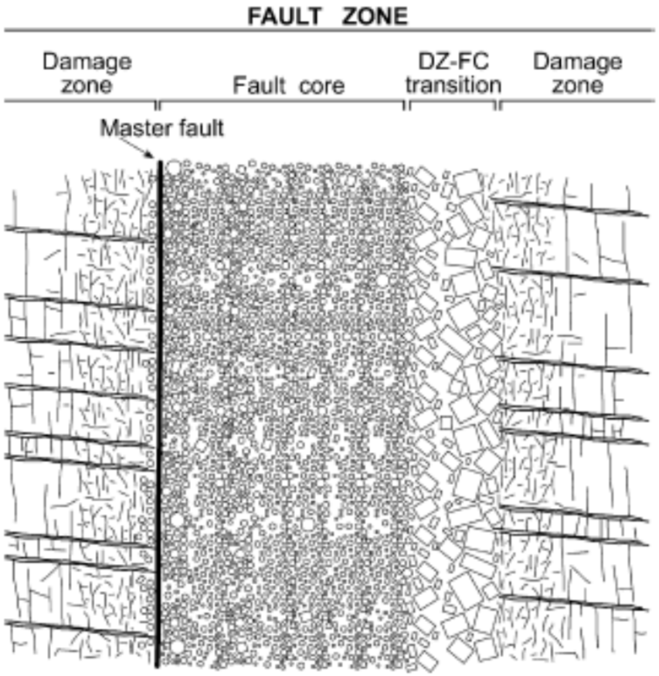

FAULT REACTIVATION

Criteria to define the maximum injection pressure:

Mohr-Coulomb

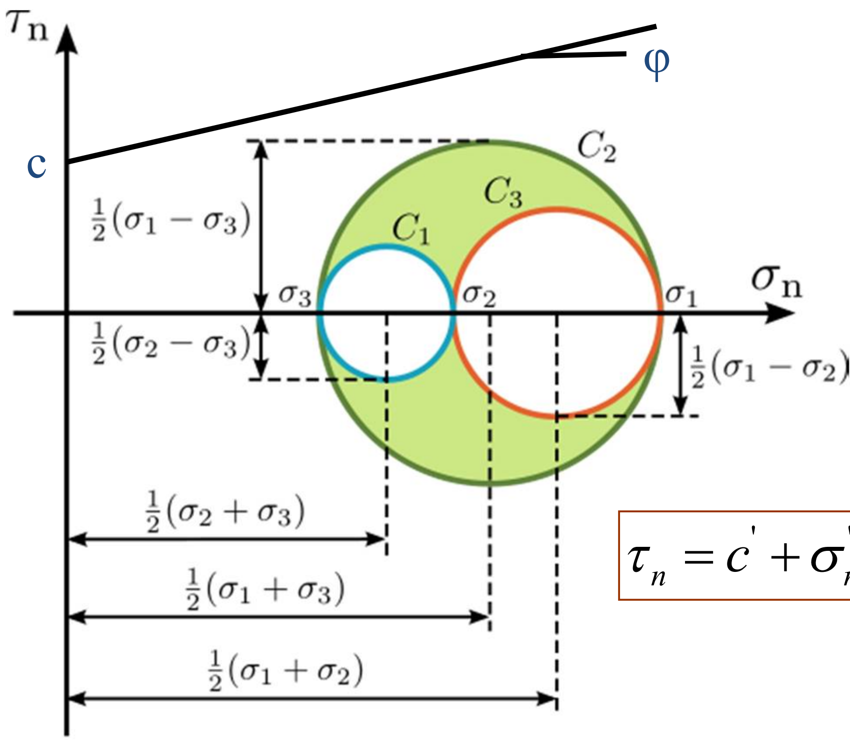

$$\tau_n = c' + \sigma_n'.\tan\varphi'$$

FAULT REACTIVATION

Criteria to define the maximum injection pressure:

Mohr-Coulomb

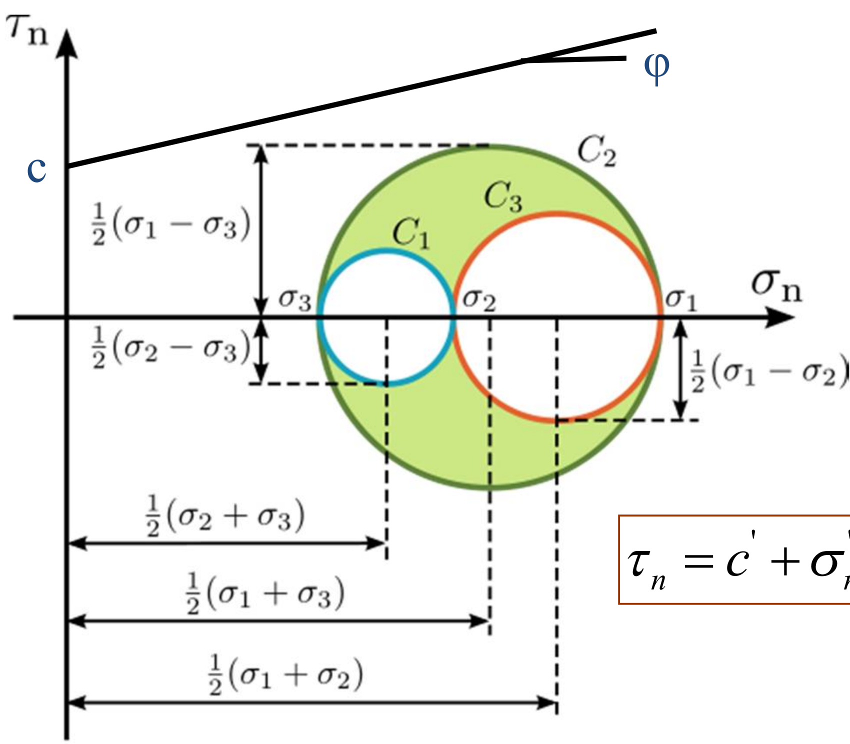

$$\tau_n = c' + \sigma_n'.\tan\varphi'$$

Total plastic work

$$W_c = \int_0^{\varepsilon_{Pf}} \sigma_Y d\varepsilon_p$$

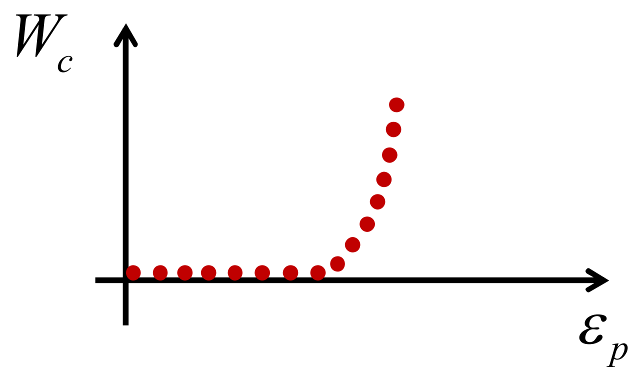

Analytical analysis or FEM analysis

only FEM analysis

Example: Fault Reactivation Problem

Oil Reservoir crossed by a fault

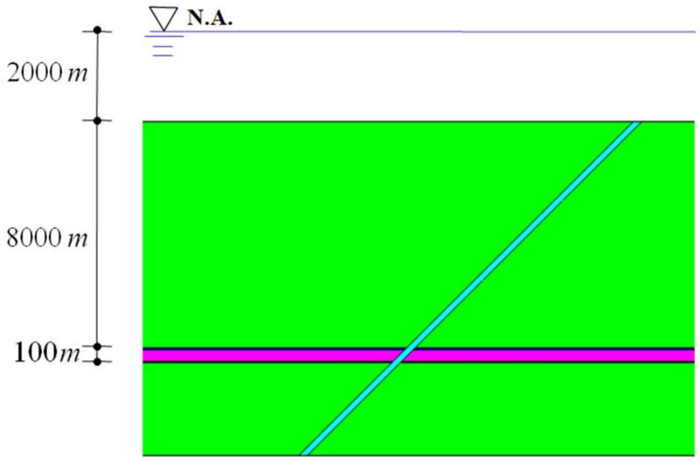

Example: Fault Reactivation Problem

Oil Reservoir crossed by a fault

In situ stresses (estimated)

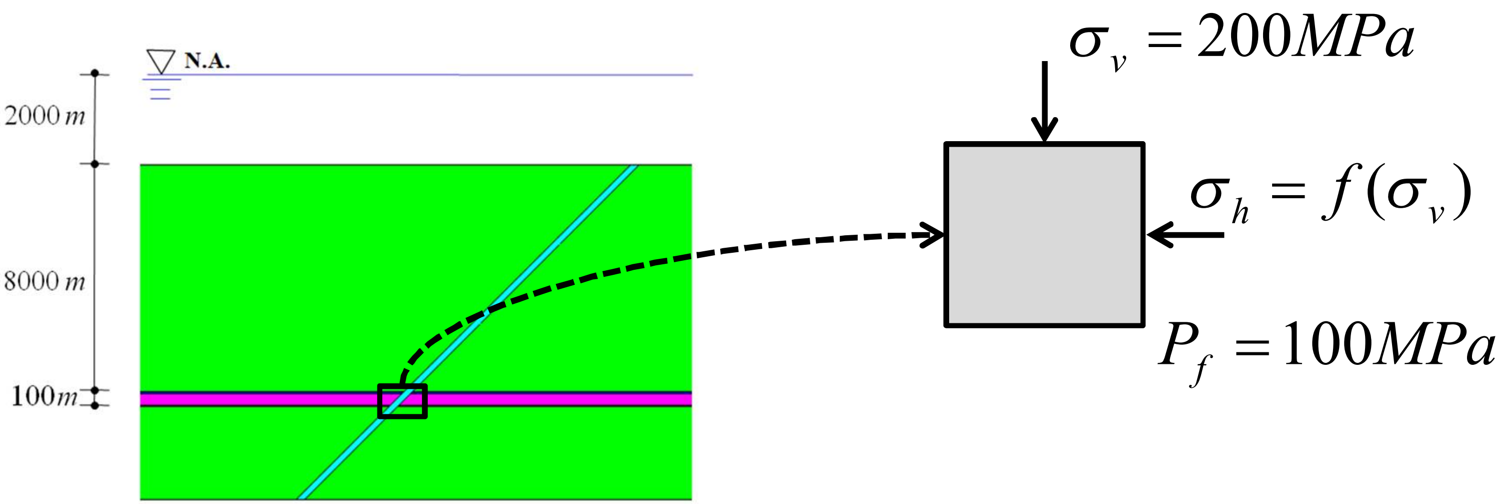

Example: Fault Reactivation Problem

Oil Reservoir crossed by a fault

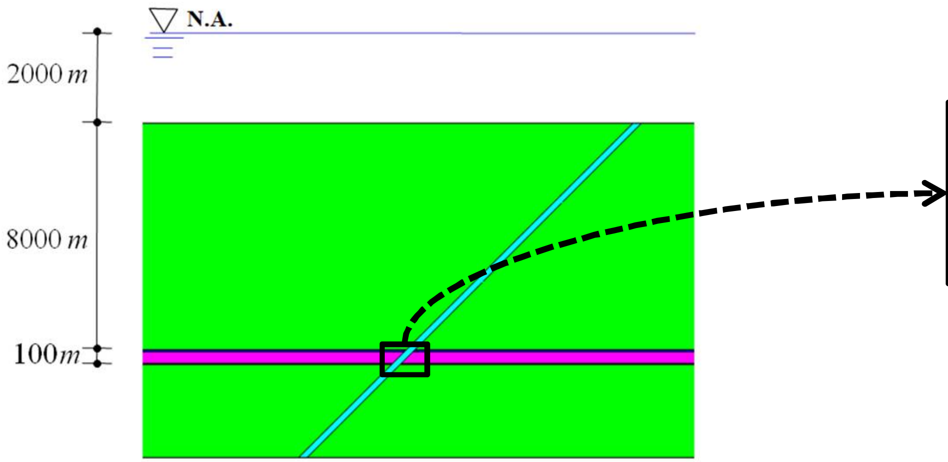

***In situ* stresses (estimated)**

$$\sigma_v = 200MPa$$

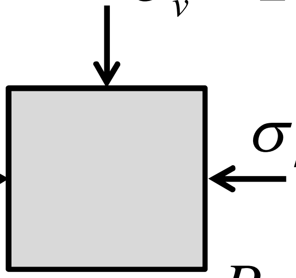

$$\sigma_h = f(\sigma_v)$$

$$P_f = 100MPa$$

Fault Properties:

Friction angle $\varphi = 18°$

Cohesion $c = 8Mpa$

Example: Fault Reactivation Problem

Oil Reservoir crossed by a fault

In situ stresses (estimated)

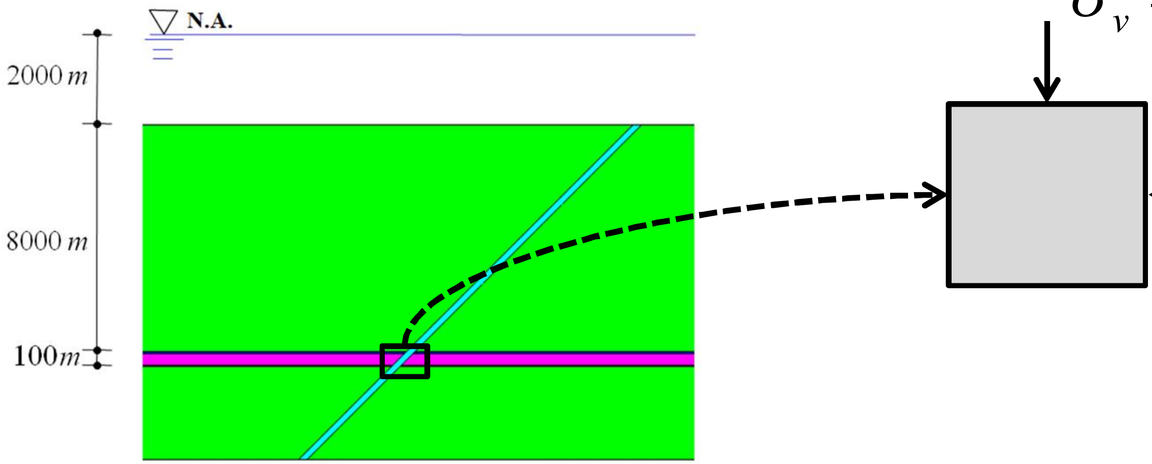

$\sigma_v = 200MPa$

$\sigma_h = f(\sigma_v)$

$P_f = 100MPa$

Fault Properties:

Friction angle $\varphi = 18°$

Cohesion $c = 8Mpa$

Horizontal stress ratio

$k_0 = 0.4$

Biot's coefficient

$\alpha_{Biot} = 0.9$

Example: Fault Reactivation Problem

Oil Reservoir crossed by a fault

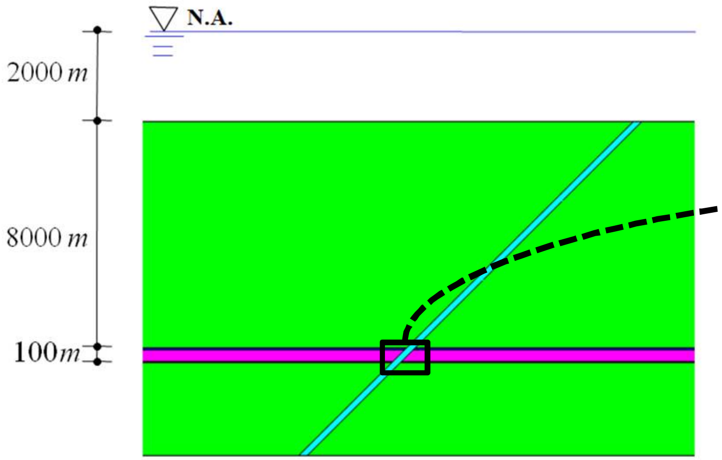

***In situ* stresses (estimated)**

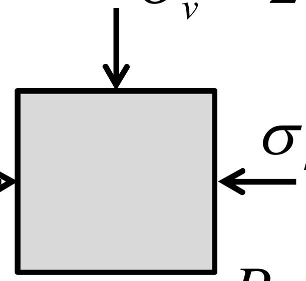

$$\sigma_v = 200MPa$$

$$\sigma_h = f(\sigma_v)$$

$$P_f = 100MPa$$

Fault Properties:

Friction angle $\varphi = 18°$

Cohesion $c = 8Mpa$

Horizontal stress ratio

$$k_0 = 0.4$$

Biot's coefficient

$$\alpha_{Biot} = 0.9$$

Principal effective stresses

$$\sigma_1 = \sigma_v$$

$$\sigma_1^{'} = \sigma_1 - \alpha_{Biot} P_f$$

$$\sigma_1^{'} = 110MPa$$

$$\sigma_3^{'} = k_0 \sigma_1^{'}$$

$$\sigma_3^{'} = 44MPa$$

Example: Fault Reactivation Problem

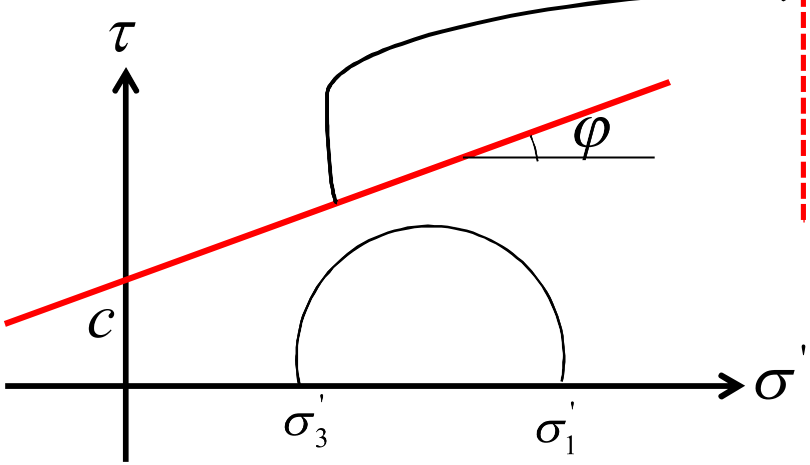

Mohr–Coulomb failure criteria

(Potts e Zdravkovic, 1999

$$F = \sigma_1^{'} - \sigma_3^{'} - 2c\cos\varphi - (\sigma_1^{'} + \sigma_3^{'})sen\varphi$$

How much can the fluid pressure be increased??

Example: Fault Reactivation Problem

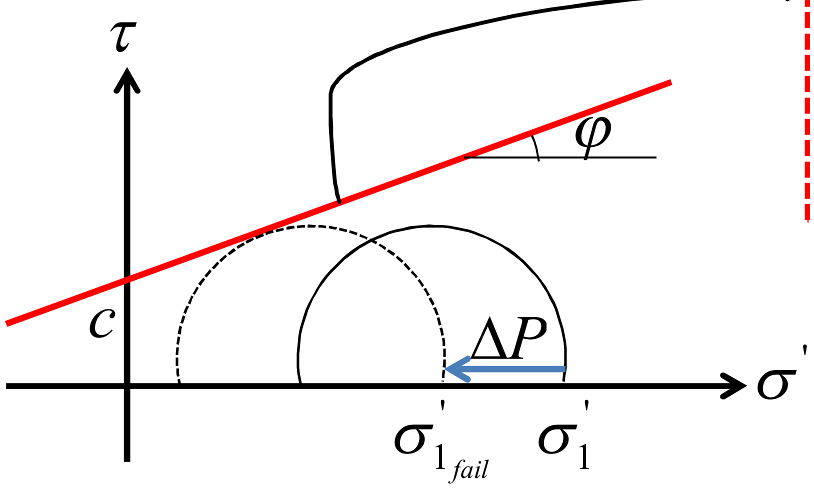

Mohr–Coulomb failure criteria
(Potts e Zdravkovic, 1999)

$$F = \sigma_1' - \sigma_3' - 2c\cos\varphi - (\sigma_1' + \sigma_3')sen\varphi$$

How much can the fluid pressure be increased??

Example: Fault Reactivation Problem

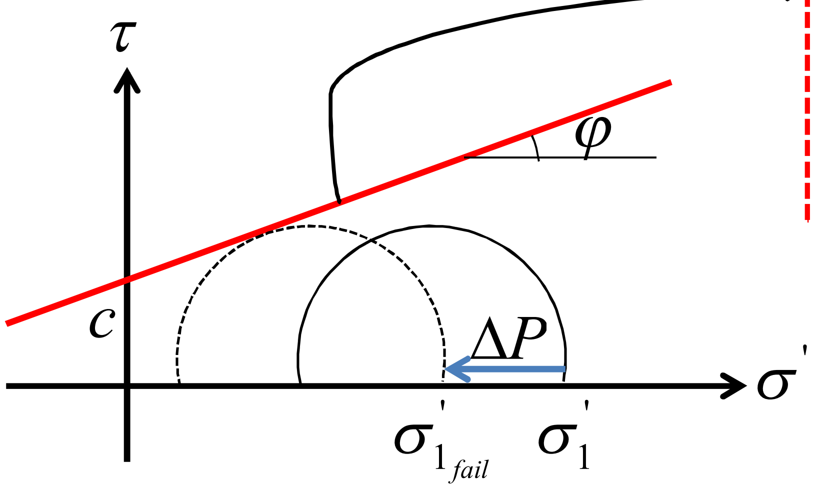

Mohr–Coulomb failure criteria
(Potts e Zdravkovic, 1999)

$$F = \sigma_1^{'} - \sigma_3^{'} - 2c\cos\varphi - (\sigma_1^{'} + \sigma_3^{'})sen\varphi$$

How much can the fluid pressure be increased??

Supposing:
$$\sigma_3^{'} = k_0 \sigma_1^{'}$$

Example: Fault Reactivation Problem

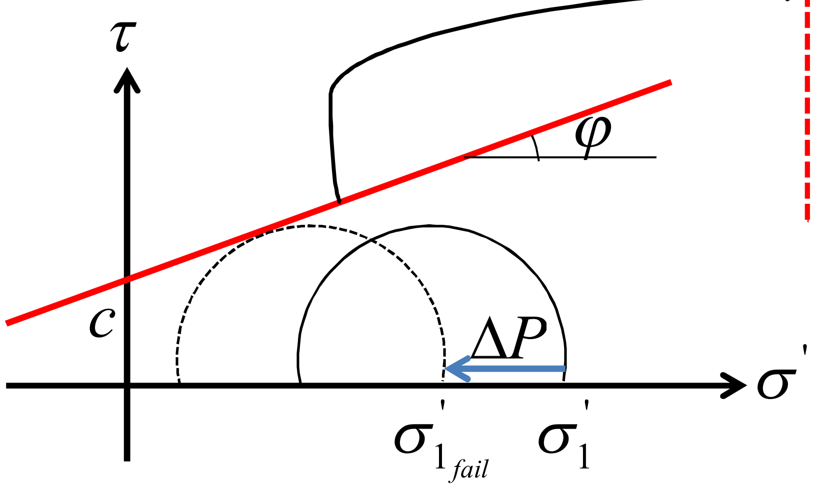

Mohr–Coulomb failure criteria
(Potts e Zdravkovic, 1999)

$$F = \sigma_1' - \sigma_3' - 2c\cos\varphi - (\sigma_1' + \sigma_3') sen\varphi$$

How much can the fluid pressure be increased??

Supposing:

$$\sigma_3' = k_0 \sigma_1'$$

From failure criteria:

$$\sigma_1' - k_0\sigma_1' - 2c\cos\varphi - (\sigma_1' + k_0\sigma_1') sen\varphi = 0$$

Example: Fault Reactivation Problem

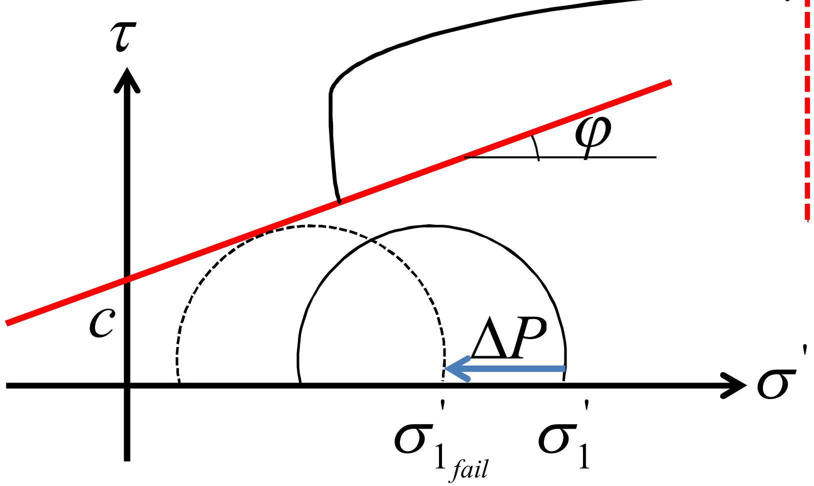

Mohr–Coulomb failure criteria
(Potts e Zdravkovic, 1999)

$$F = \sigma_1^{'} - \sigma_3^{'} - 2c\cos\varphi - (\sigma_1^{'} + \sigma_3^{'})sen\varphi$$

How much can the fluid pressure be increased??

Supposing:

$$\sigma_3^{'} = k_0\sigma_1^{'}$$

From failure criteria:

$$\sigma_1^{'} - k_0\sigma_1^{'} - 2c\cos\varphi - (\sigma_1^{'} + k_0\sigma_1^{'})sen\varphi = 0$$

From the fault propeties:

$$\left.\begin{array}{l} \varphi = 18° \\ c = 8Mpa \end{array}\right\} \sigma_{1_{fail}}^{'} = 90,9MPa$$

Example: Fault Reactivation Problem

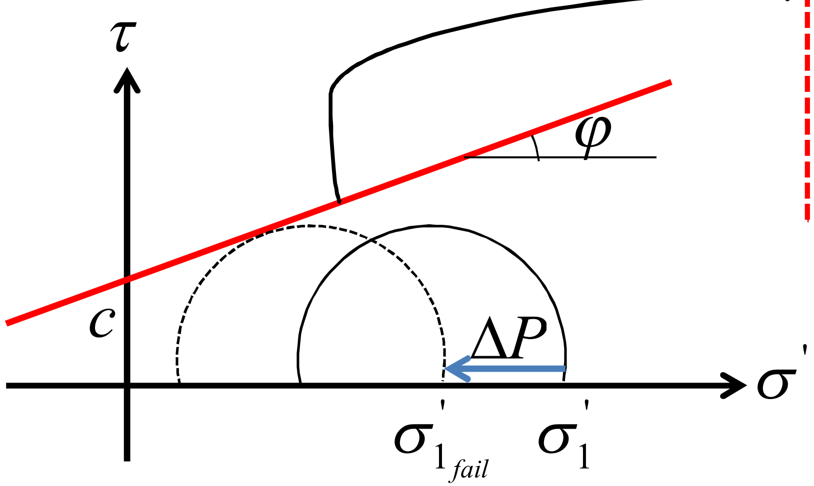

Mohr–Coulomb failure criteria
(Potts e Zdravkovic, 1999)

$$F = \sigma_1^{'} - \sigma_3^{'} - 2c\cos\varphi - (\sigma_1^{'} + \sigma_3^{'})sen\varphi$$

How much can the fluid pressure be increased??

Supposing:

$$\sigma_3^{'} = k_0 \sigma_1^{'}$$

$$\sigma_{1_{fail}}^{'} = \sigma_1 - \alpha_{Biot}(P_f + \Delta P)$$

From failure criteria:

$$\sigma_1^{'} - k_0\sigma_1^{'} - 2c\cos\varphi - (\sigma_1^{'} + k_0\sigma_1^{'})sen\varphi = 0$$

From the fault propeties:

$$\left.\begin{aligned} \varphi &= 18^\circ \\ c &= 8Mpa \end{aligned}\right\} \sigma_{1_{fail}}^{'} = 90{,}9MPa$$

Example: Fault Reactivation Problem

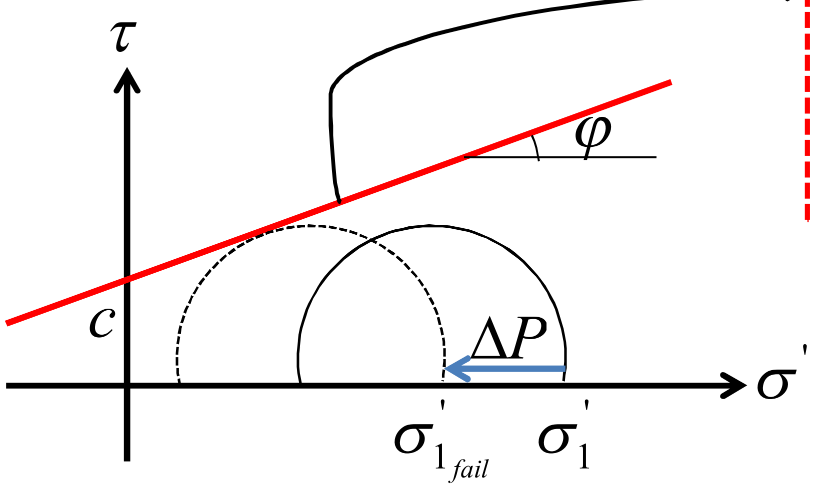

Mohr–Coulomb failure criteria
(Potts e Zdravkovic, 1999)

$$F = \sigma_1^{'} - \sigma_3^{'} - 2c\cos\varphi - (\sigma_1^{'} + \sigma_3^{'})sen\varphi$$

How much can the fluid pressure be increased??

Supposing:

$$\sigma_3^{'} = k_0\sigma_1^{'}$$

From failure criteria:

$$\sigma_1^{'} - k_0\sigma_1^{'} - 2c\cos\varphi - (\sigma_1^{'} + k_0\sigma_1^{'})sen\varphi = 0$$

From the fault propeties:

$$\left.\begin{array}{l}\varphi = 18^\circ \\ c = 8Mpa\end{array}\right\} \sigma_{1_{fail}}^{'} = 90{,}9MPa$$

$$\sigma_{1_{fail}}^{'} = \sigma_1 - \alpha_{Biot}(P_f + \Delta P)$$

remains constant

Example: Fault Reactivation Problem

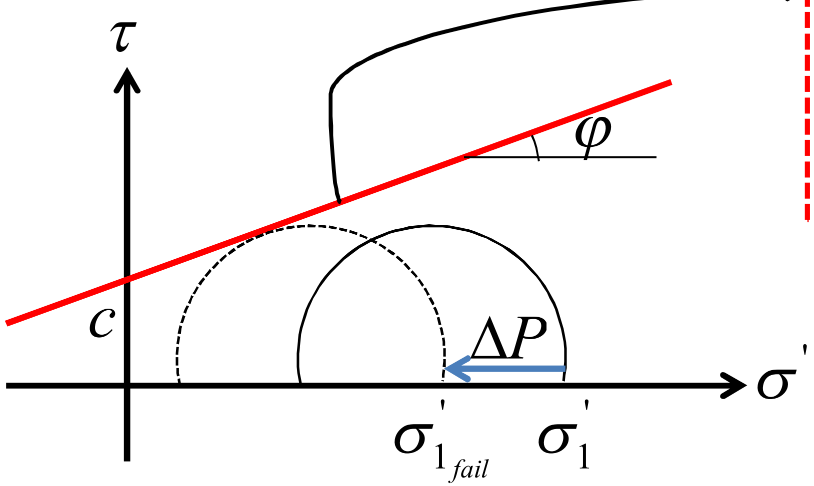

Mohr–Coulomb failure criteria
(Potts e Zdravkovic, 1999)

$$F = \sigma'_1 - \sigma'_3 - 2c\cos\varphi - (\sigma'_1 + \sigma'_3)sen\varphi$$

How much can the fluid pressure be increased??

Supposing:

$$\sigma'_3 = k_0\sigma'_1$$

From failure criteria:

$$\sigma'_1 - k_0\sigma'_1 - 2c\cos\varphi - (\sigma'_1 + k_0\sigma'_1)sen\varphi = 0$$

From the fault propeties:

$$\left.\begin{matrix}\varphi = 18^\circ \\ c = 8Mpa\end{matrix}\right\} \sigma'_{1_{fail}} = 90{,}9MPa$$

$$\sigma'_{1_{fail}} = \sigma_1 - \alpha_{Biot}(P_f + \Delta P)$$

remains constant

$$\Delta P = 21{,}2MPa$$

FAULT REACTIVATION MECHANISM

Well starting:

➔new p_f distribution

➔new effective stress state:

$$\boldsymbol{\sigma} = \boldsymbol{\sigma}' + p_f \cdot \mathbf{I}$$

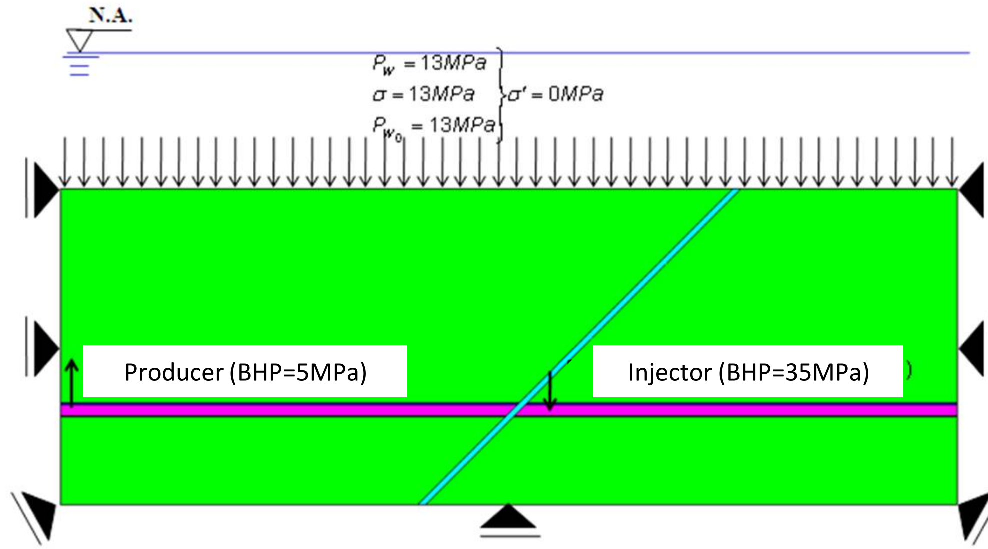

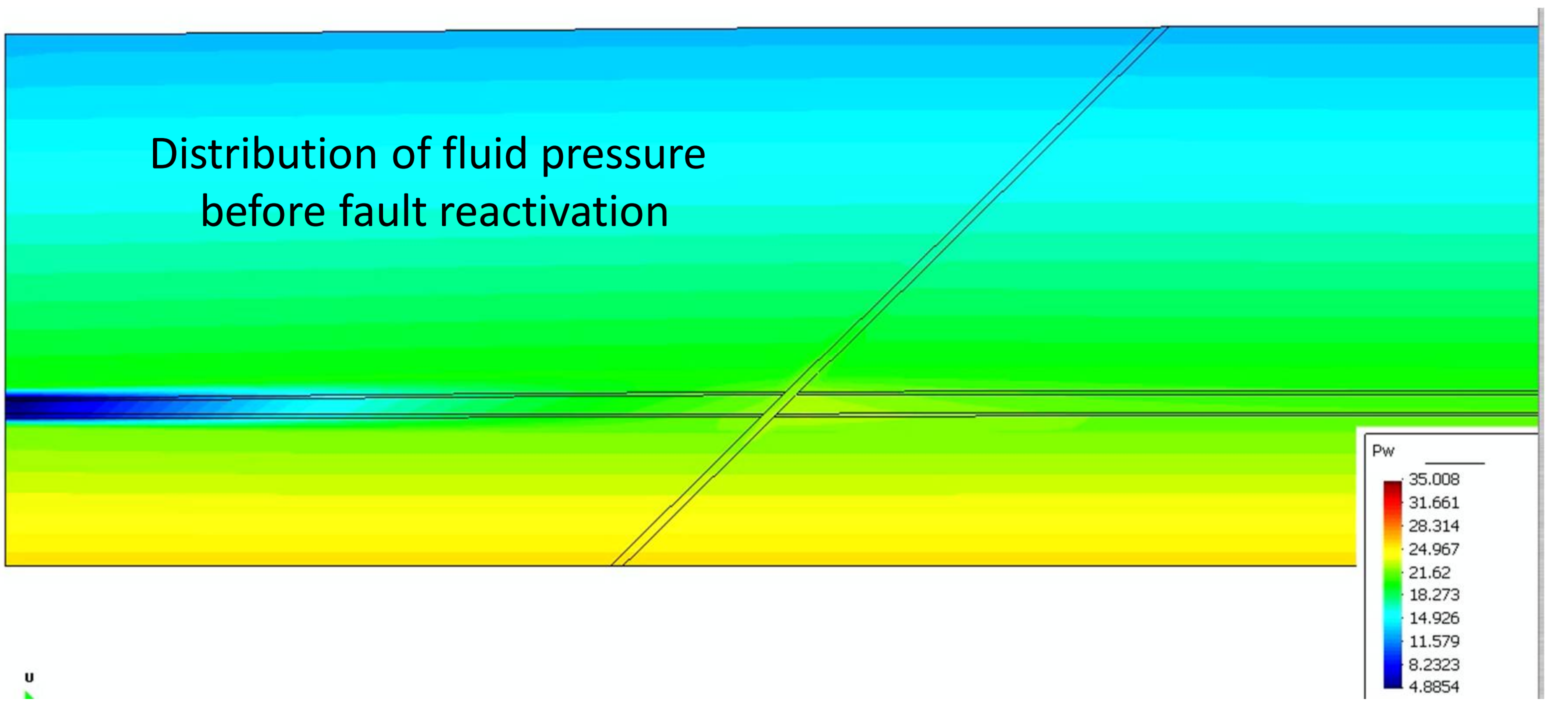

Distribution of fluid pressure before fault reactivation

FAULT REACTIVATION MECHANISM

$$\boldsymbol{\sigma} = \boldsymbol{\sigma}' + p_f \cdot \mathbf{I}$$

$$d\boldsymbol{\sigma}' = \mathbf{D} \cdot d\boldsymbol{\varepsilon}$$

$$\nabla \boldsymbol{\sigma} + \mathbf{b} = \mathbf{0}$$

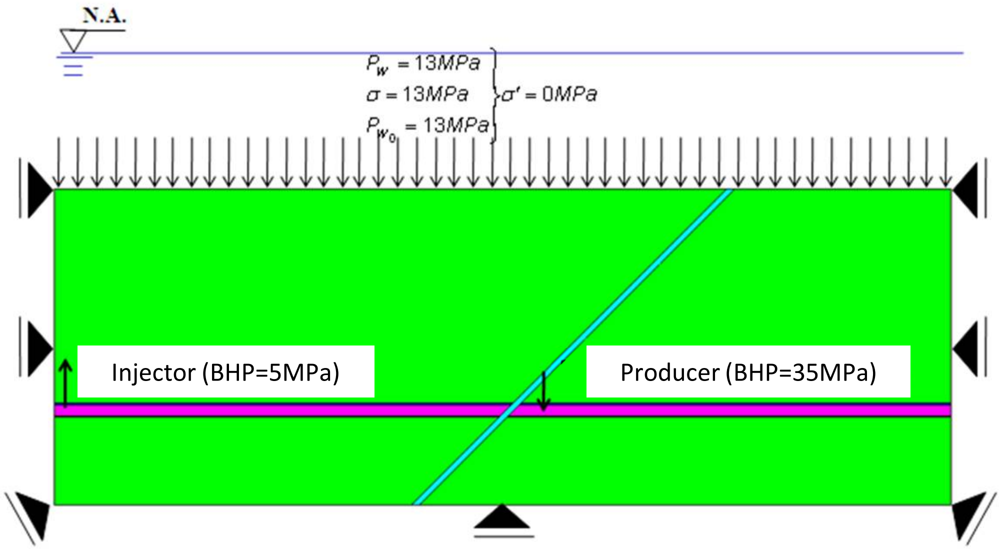

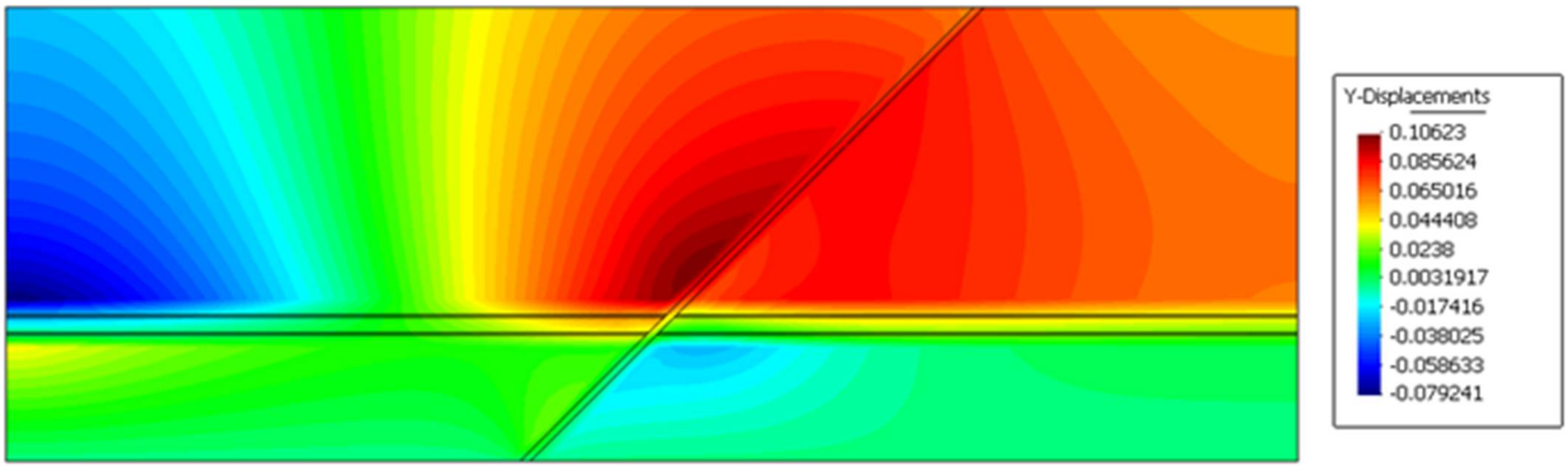

FAULT REACTIVATION MECHANISM

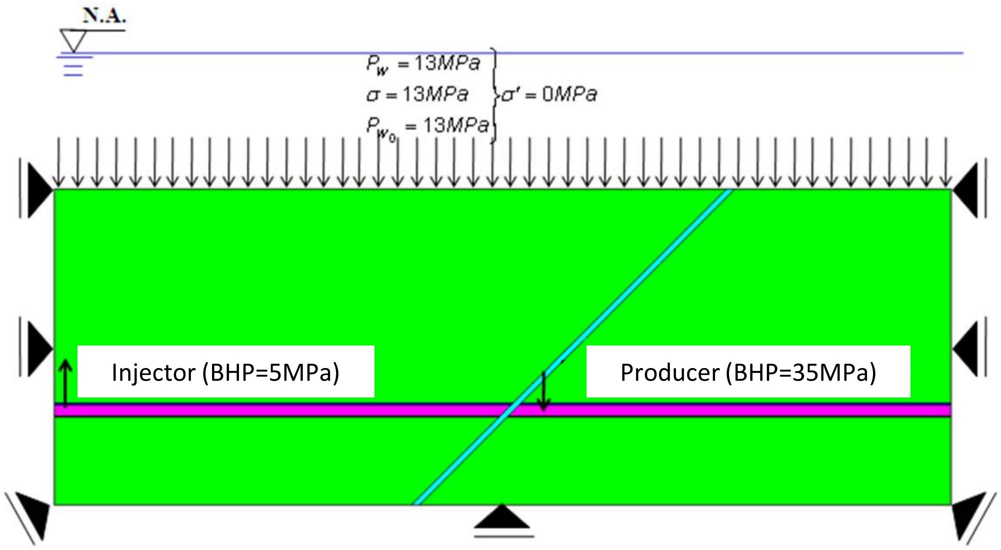

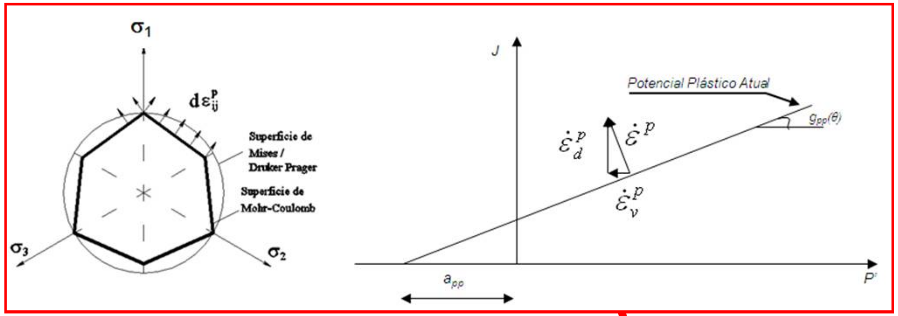

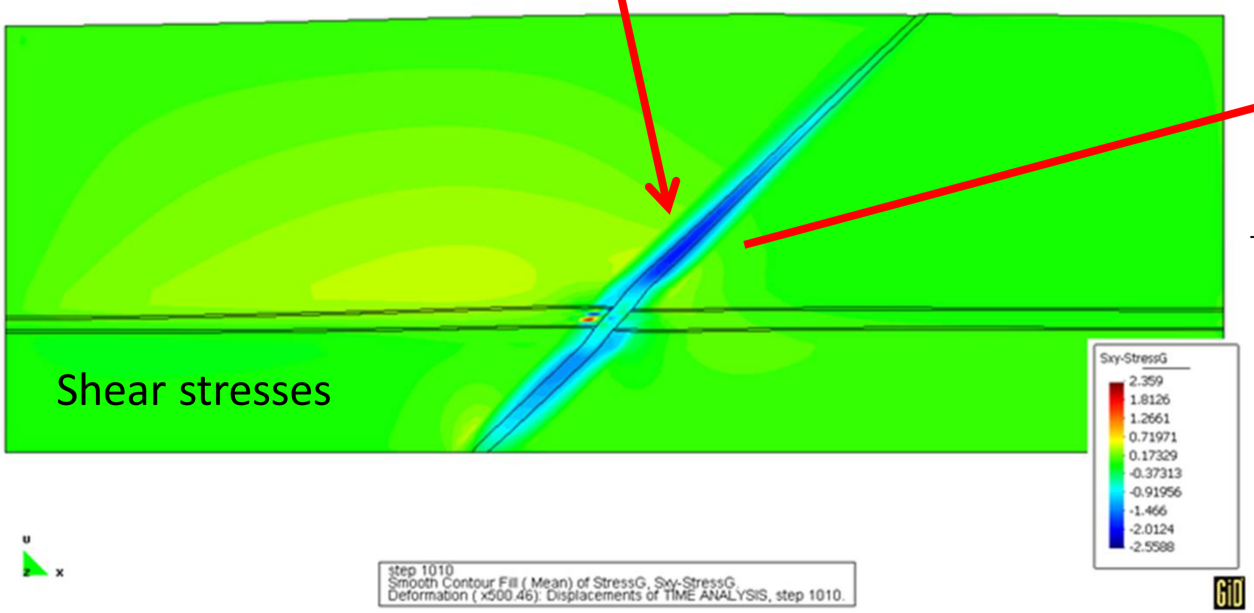

Dilatancy:

$$\frac{d\phi}{dt} = \underbrace{\frac{(1-\phi)}{\rho_s}\frac{d\rho_s}{dt}}_{\text{rock compressibility}} + \underbrace{(1-\phi)\frac{d\varepsilon_v}{dt}}_{\text{deformable porous media (geomechanics)}}$$

$$\mathbf{k} = \mathbf{k_i} \exp[b(\phi - \phi_i)]$$

(more permeable medium)

FAULT REACTIVATION MECHANISM

dilatancy:

$$\varphi \uparrow \quad \Rightarrow \quad \mathbf{k} = \mathbf{k_i} \exp\left[b\left(\varphi - \varphi_i\right) \right] \quad \uparrow$$

$$q_\alpha = -\mathbf{k} \frac{k_{r\alpha}}{\mu_\alpha} \left(\nabla p_\alpha - \rho_\alpha \mathbf{g} \right)$$

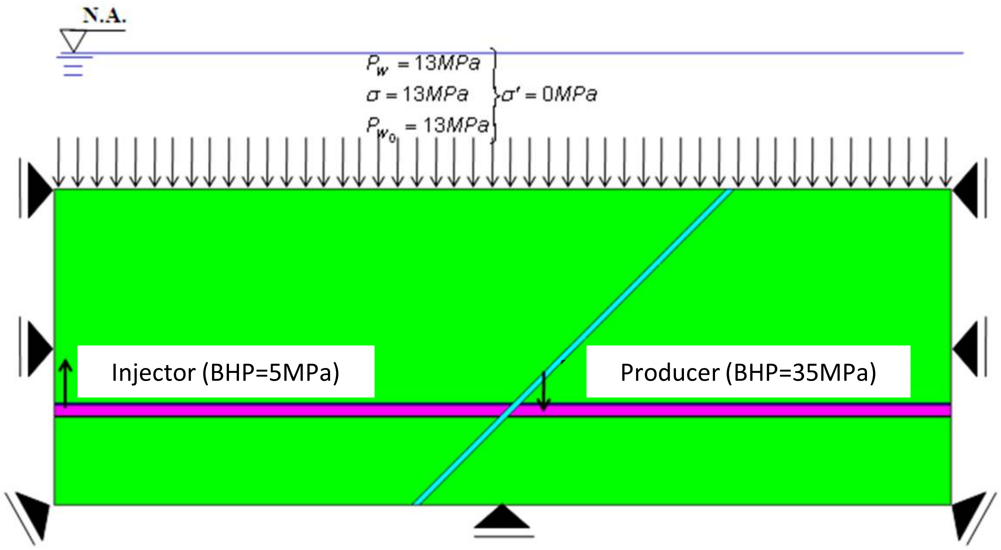

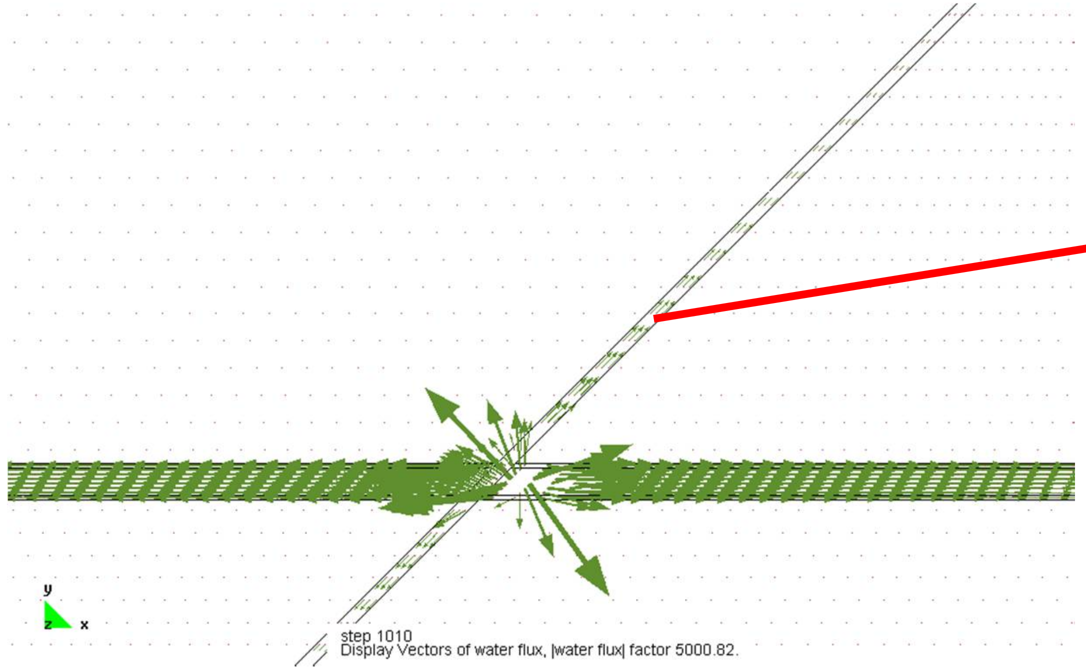

Fault reactivation:
becomes permeable

FAULT REACTIVATION MECHANISM

dilatancy:

$$\varphi \uparrow \quad \Rightarrow \quad \mathbf{k} = \mathbf{k_i} \exp\left[b\left(\varphi - \varphi_i \right) \right] \quad \uparrow$$

$$q_\alpha = -\mathbf{k} \frac{k_{r\alpha}}{\mu_\alpha} \left(\nabla p_\alpha - \rho_\alpha \mathbf{g} \right)$$

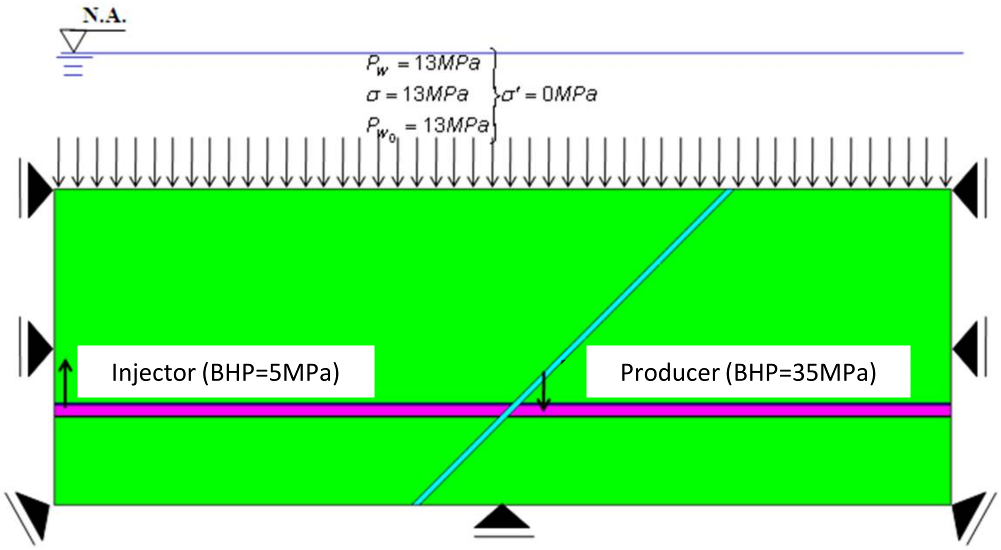

Evolution of fluid pressure: ★

Evolution of shear plastic strain in the fault: ★

FAULT REACTIVATION MECHANISM

dilatancy:

$$\varphi \uparrow \quad \Rightarrow \quad \mathbf{k} = \mathbf{k}_{\mathbf{i}} \exp\left[b\left(\varphi - \varphi_i\right)\right]$$

$$q_\alpha = -\mathbf{k}\frac{k_{r\alpha}}{\mu_\alpha}\left(\nabla p_\alpha - \rho_\alpha \mathbf{g}\right)$$

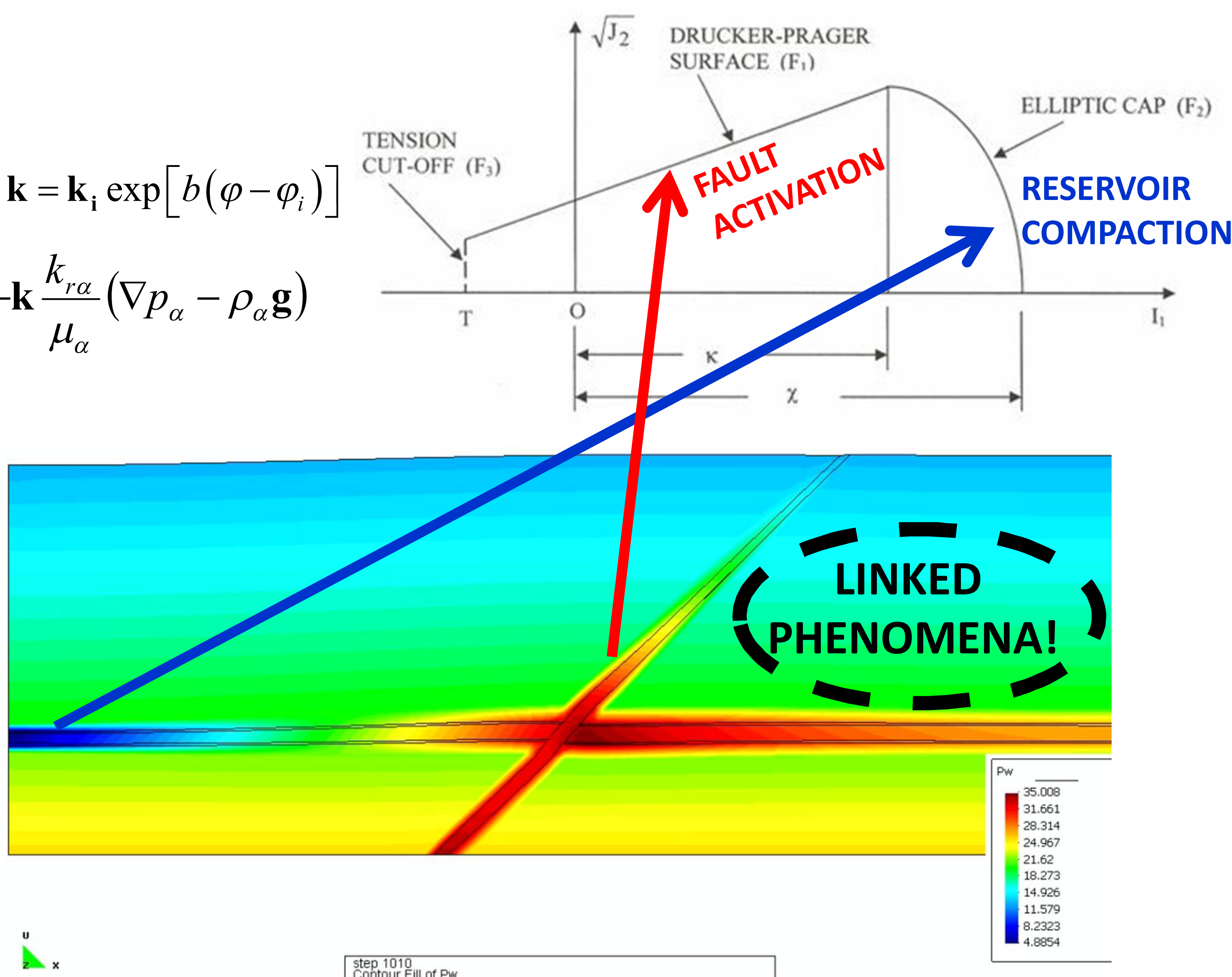

FAULT REACTIVATION

- Influence of a number of factors:

  - Base 2D Case and sensitivity analysis.
    Influence of constitutive laws: evolution of permeability;
    fluid compressibility.

  - Influence of geometry: 3D modeling ;
    faults and wells interactions.

  - Caprock integrity: hydraulic fracturing.

FAULT REACTIVATION
Petroleum Engineering

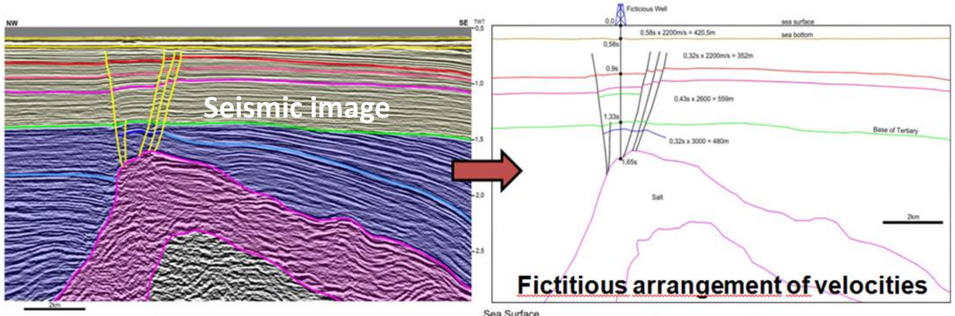

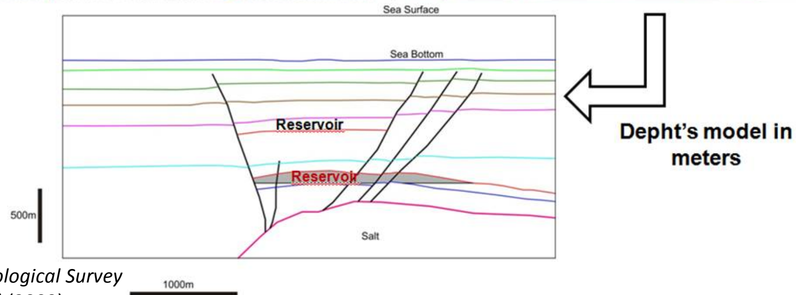

G.S.C. (Geological Survey of Canada) (2009) *Lithoprobe Seismic and Magnetotelluric Data Archive Geoscience Data Repository.* (htpp://gsc.nrcan.gc.ca).

In oil reservoirs with fault reactivation possibility, definition of maximum bottom hole pressure of the injectors during waterflooding can only be safely conducted based on a coupled hydro-geomechanical analysis tool with realist modeling of the constitutive behavior of the materials.

MAXIMUM BHP?

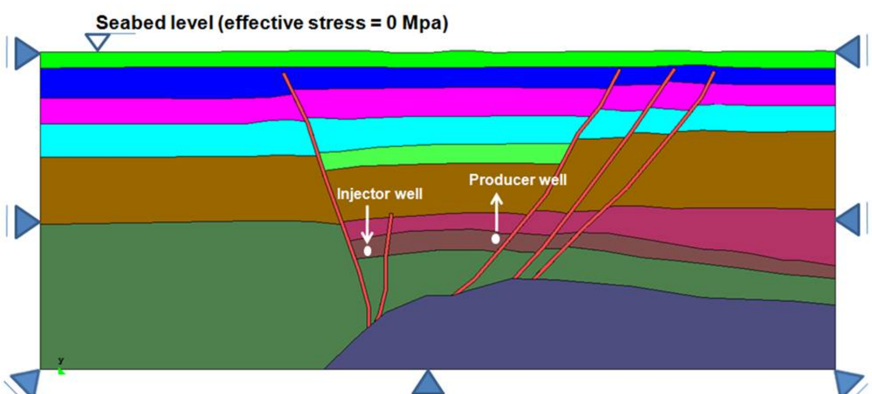

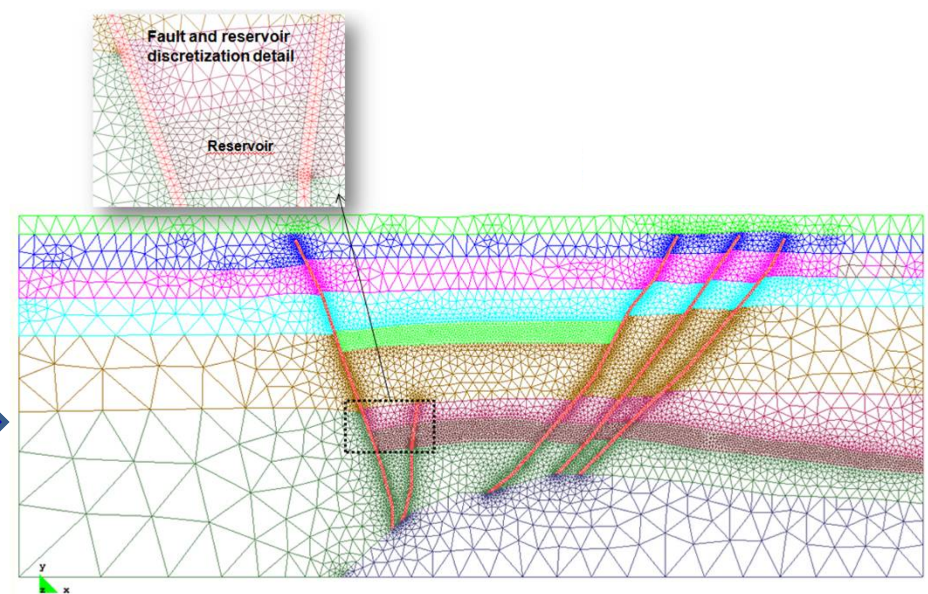

FAULT REACTIVATION
Petroleum Engineering

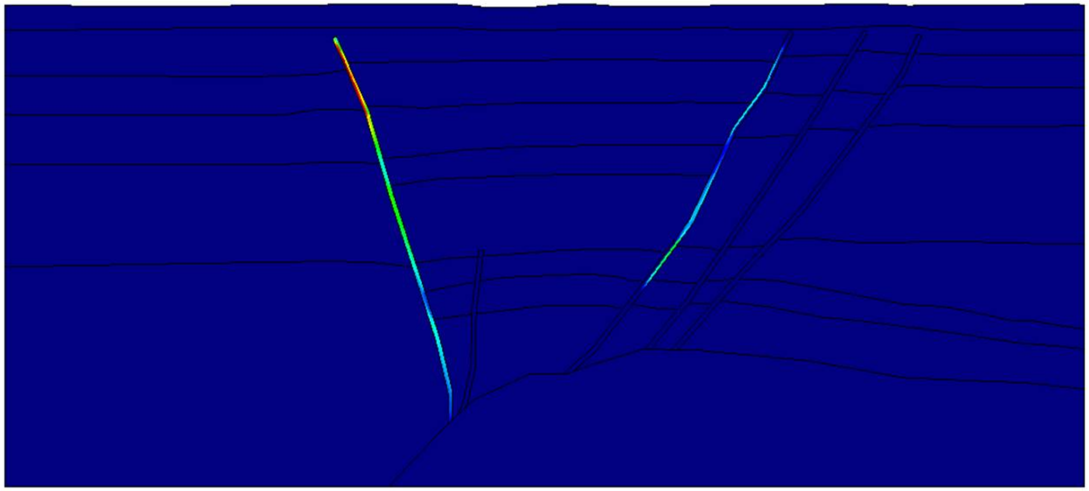

In oil reservoirs with fault reactivation possibility, definition of maximum bottom hole pressure of the injectors during waterflooding can only be safely conducted based on a coupled hydro-geomechanical analysis tool with realist modeling of the constitutive behavior of the materials.

MAXIMUM BHP?

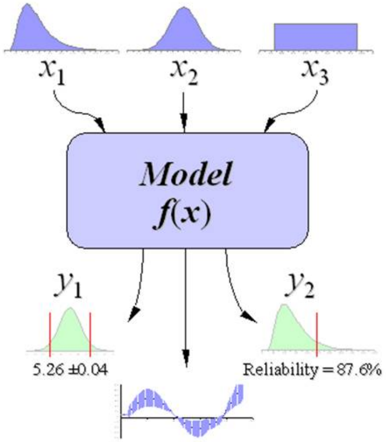

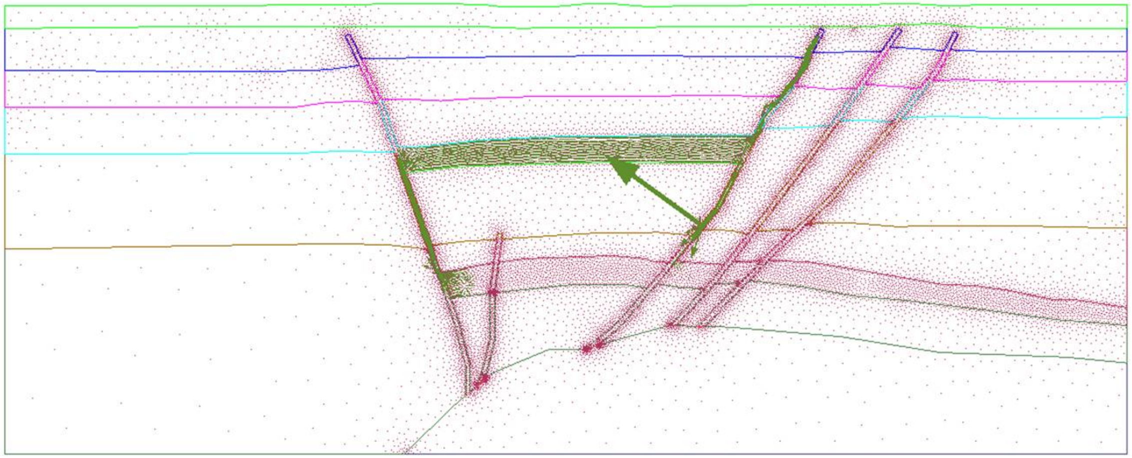

Finite Element Analysis of Fault Reactivation:

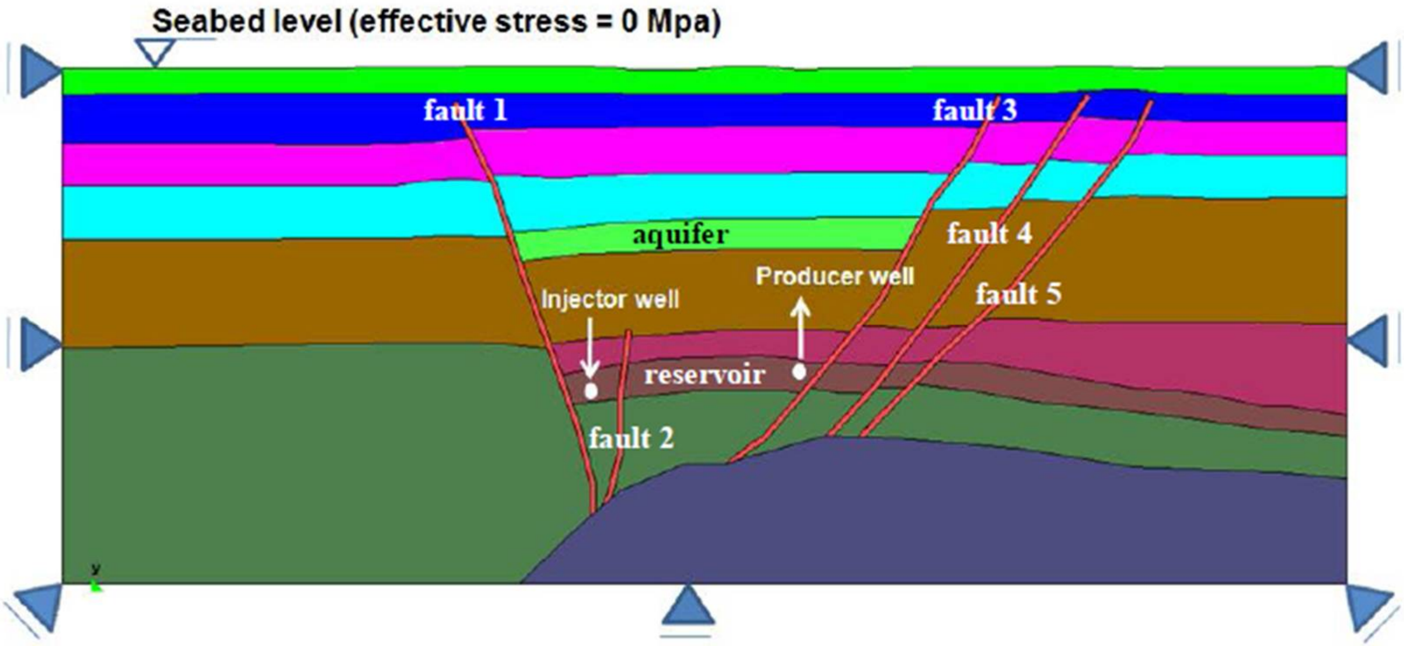

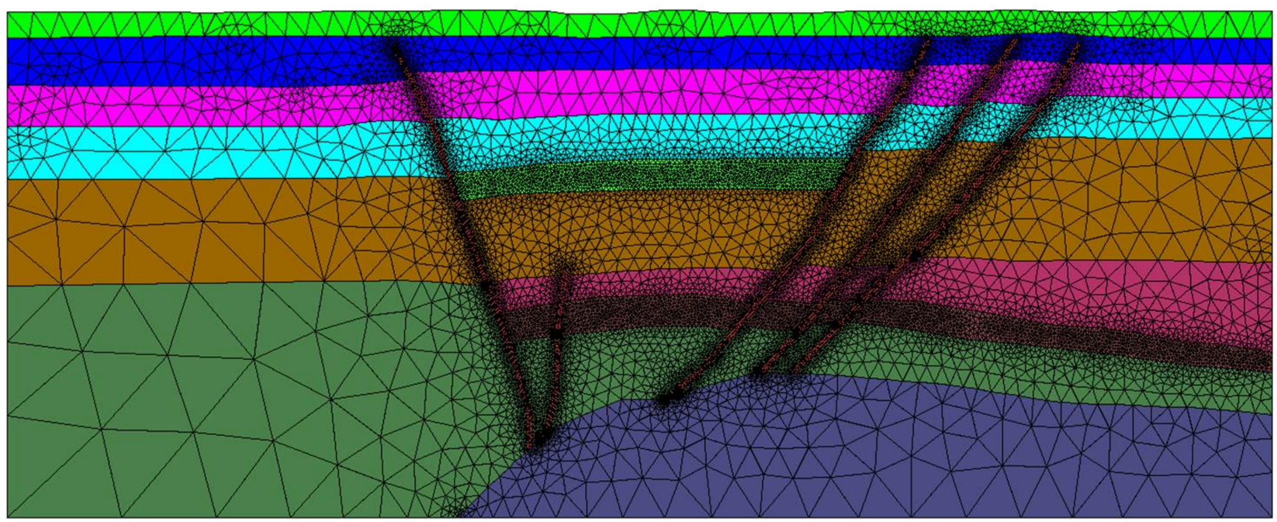

MOHR COULOMB

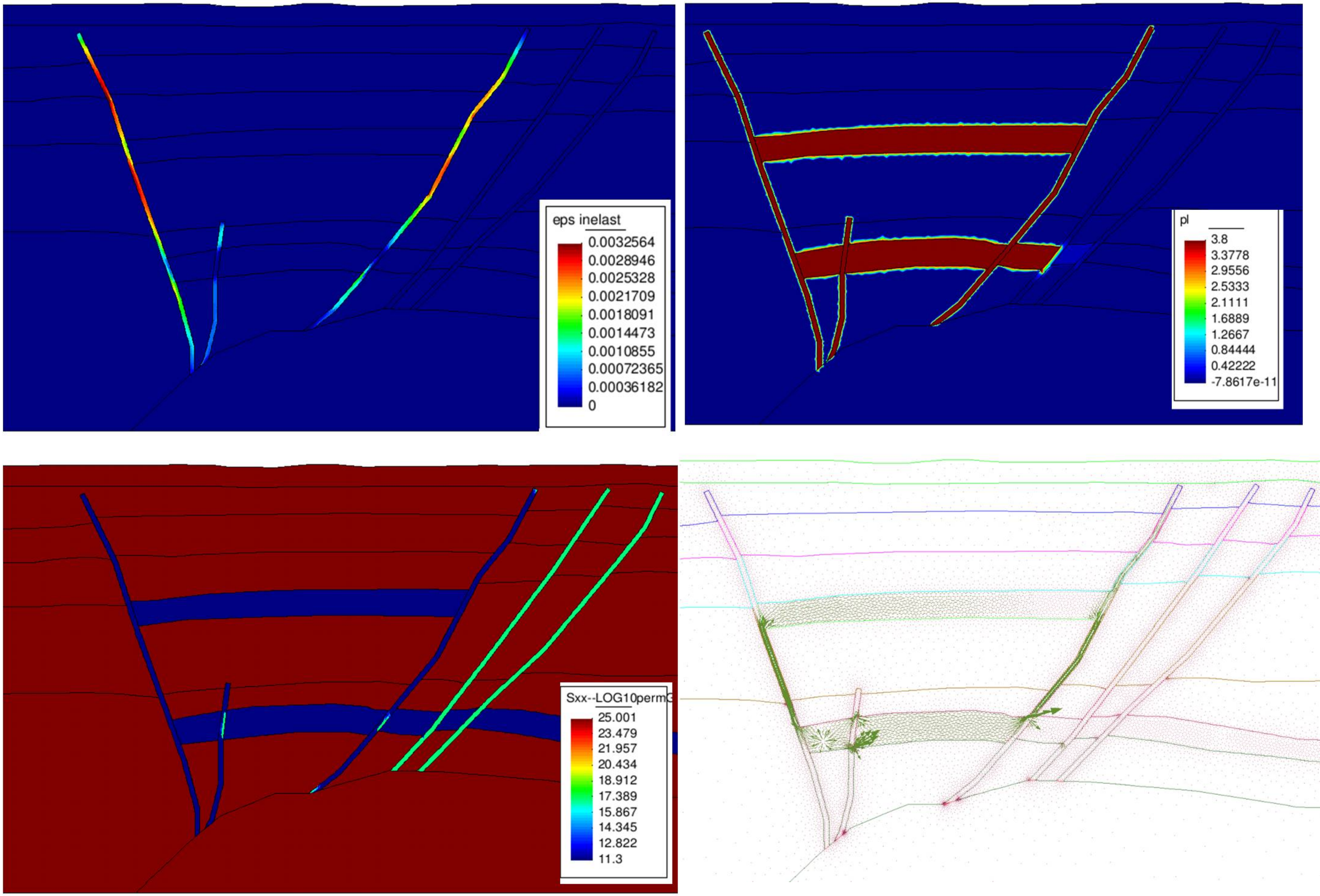

MOHR COULOMB

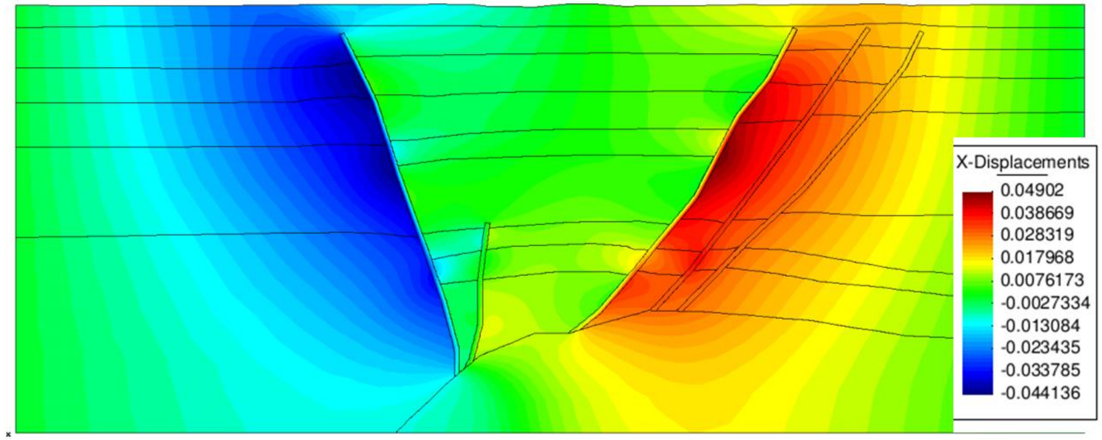

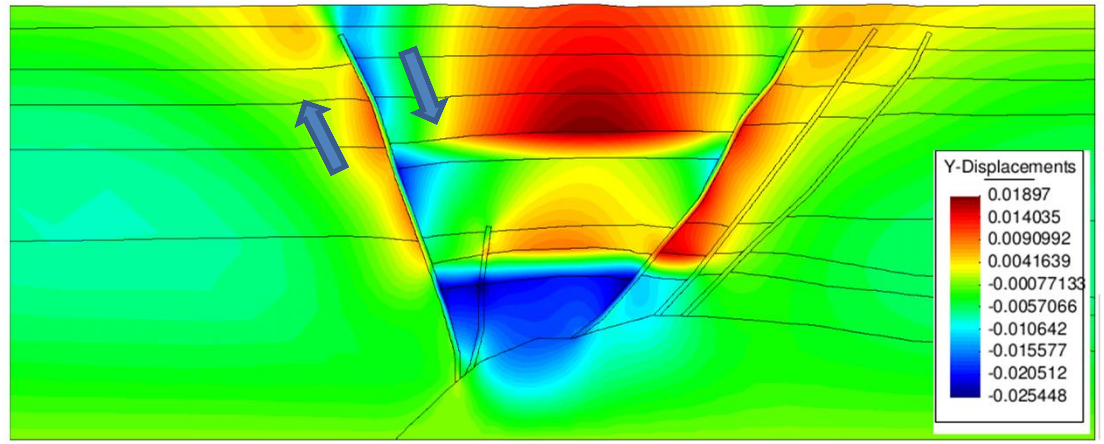

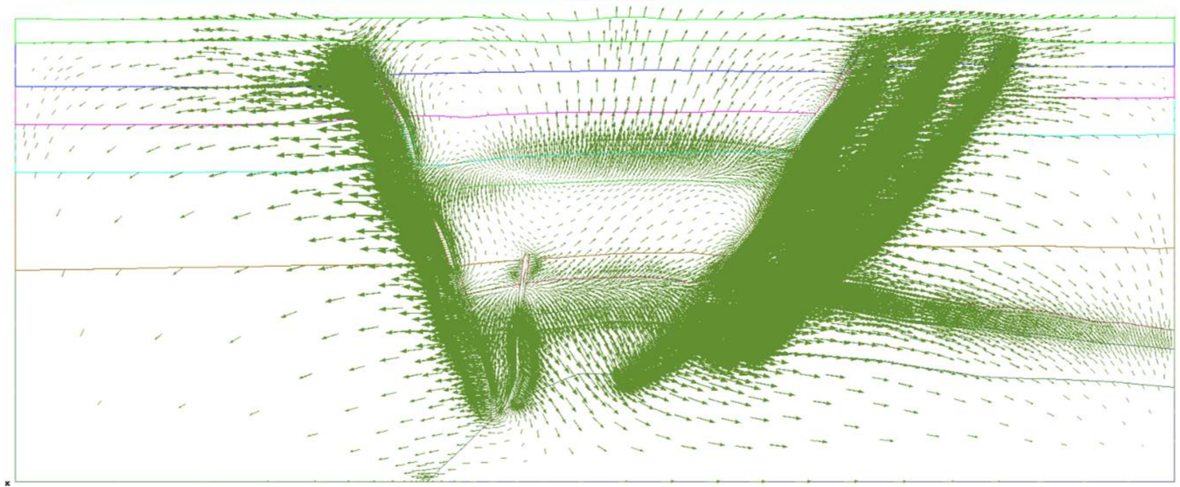

FAULT REACTIVATION

UFPE

PETROBRAS-UFPE Project:

‘Coupled Hydro-geomechanics simulation of fault reactivation’

Researchers:

UFPE: Leonardo Guimarães, Igor Gomes, Nayra Vicente, Renato de Almeida

PETROBRAS: Leonardo Cabral

Other aspects studied:

- Influence of initial stress state (stress anisotropy).
- Uncertainty analysis of fault parameters.

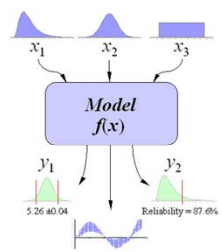

- Fault with different layers of materials.

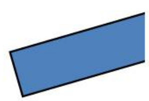

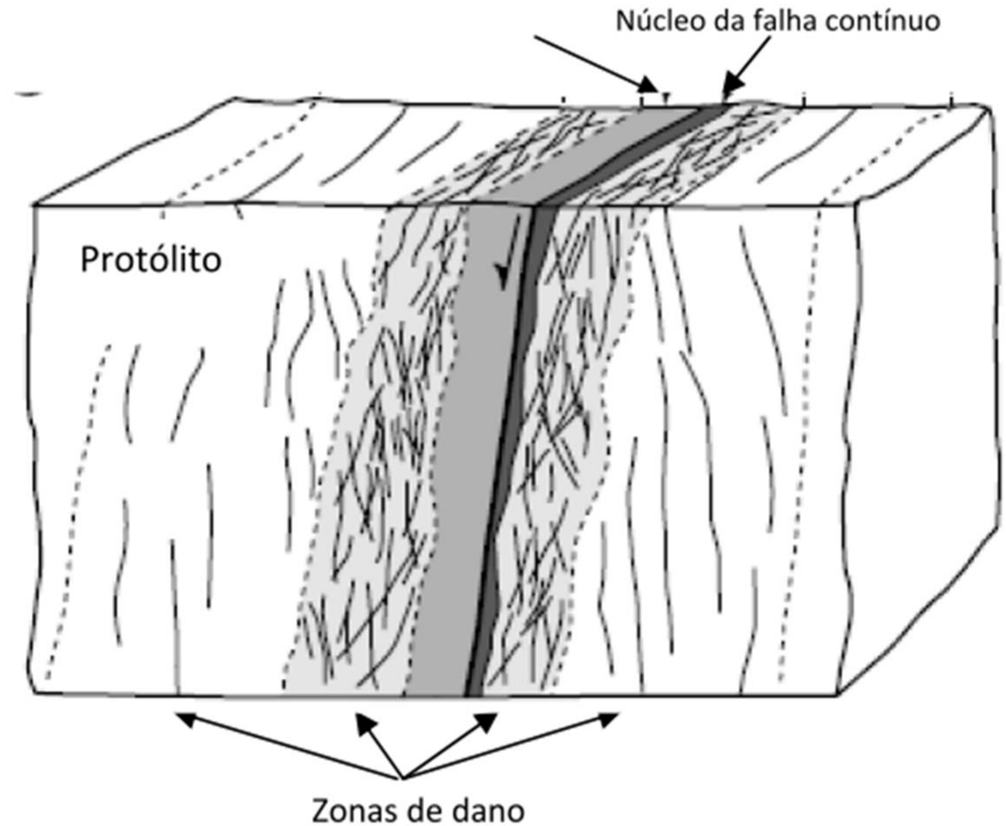

FAULT REACTIVATION

Nuestro Colciencias

<u>PETROBRAS-UFPE Project</u>:

‘Coupled Hydro-geomechanics simulation of fault reactivation’

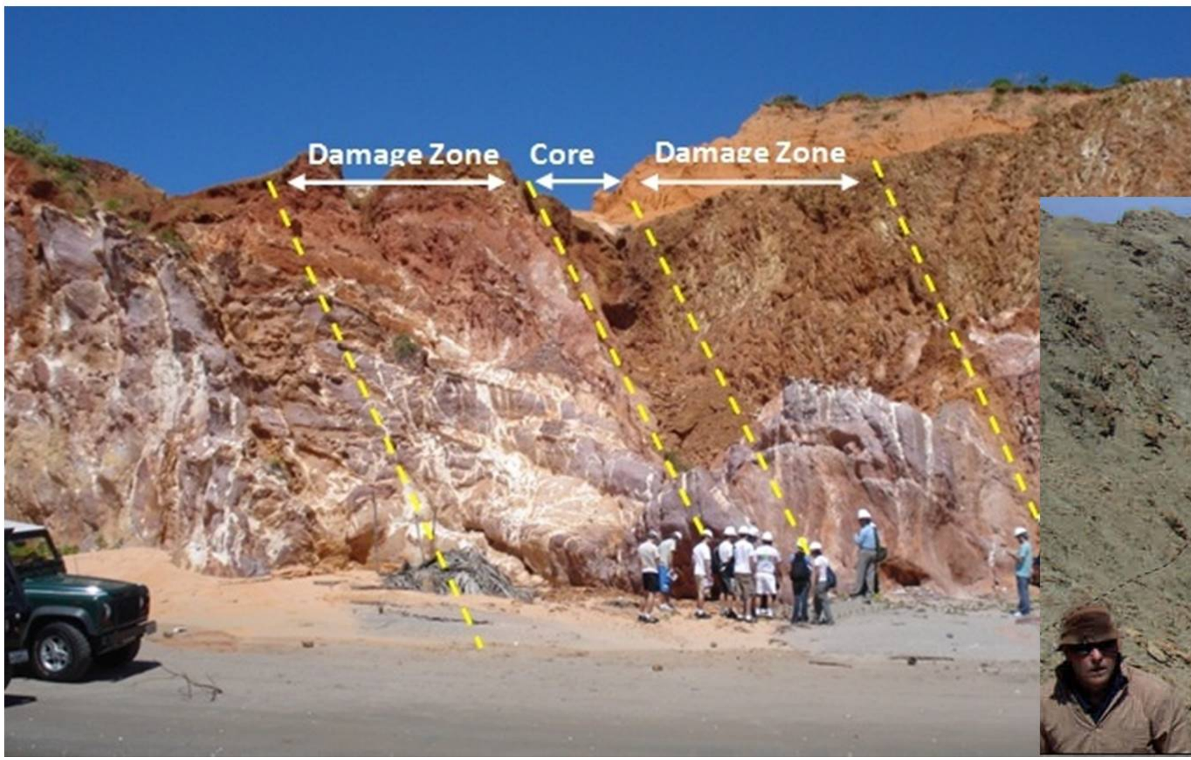

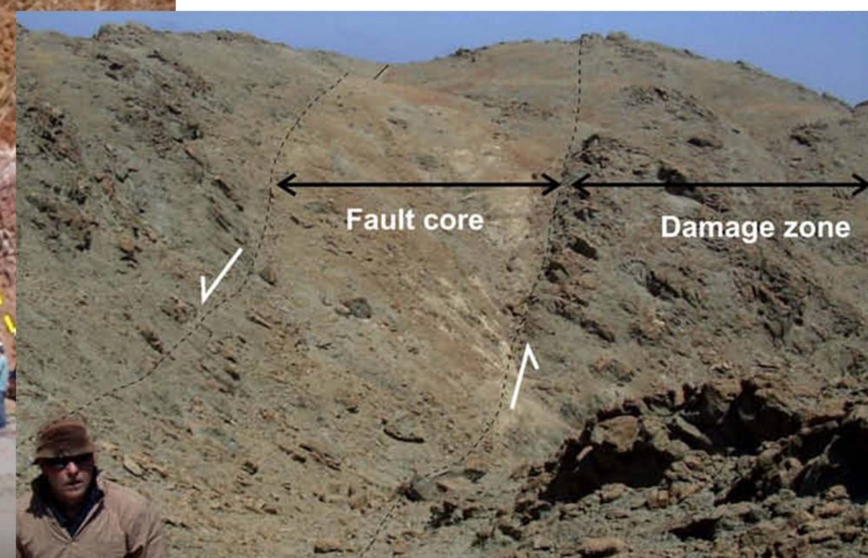

Geological fault reactivation considering damage zones

✓ **Numerical Hydro-Mechanical Modelling of Fault Reactivation Composed by Different Zones – Fault Core and Damage Zones.**

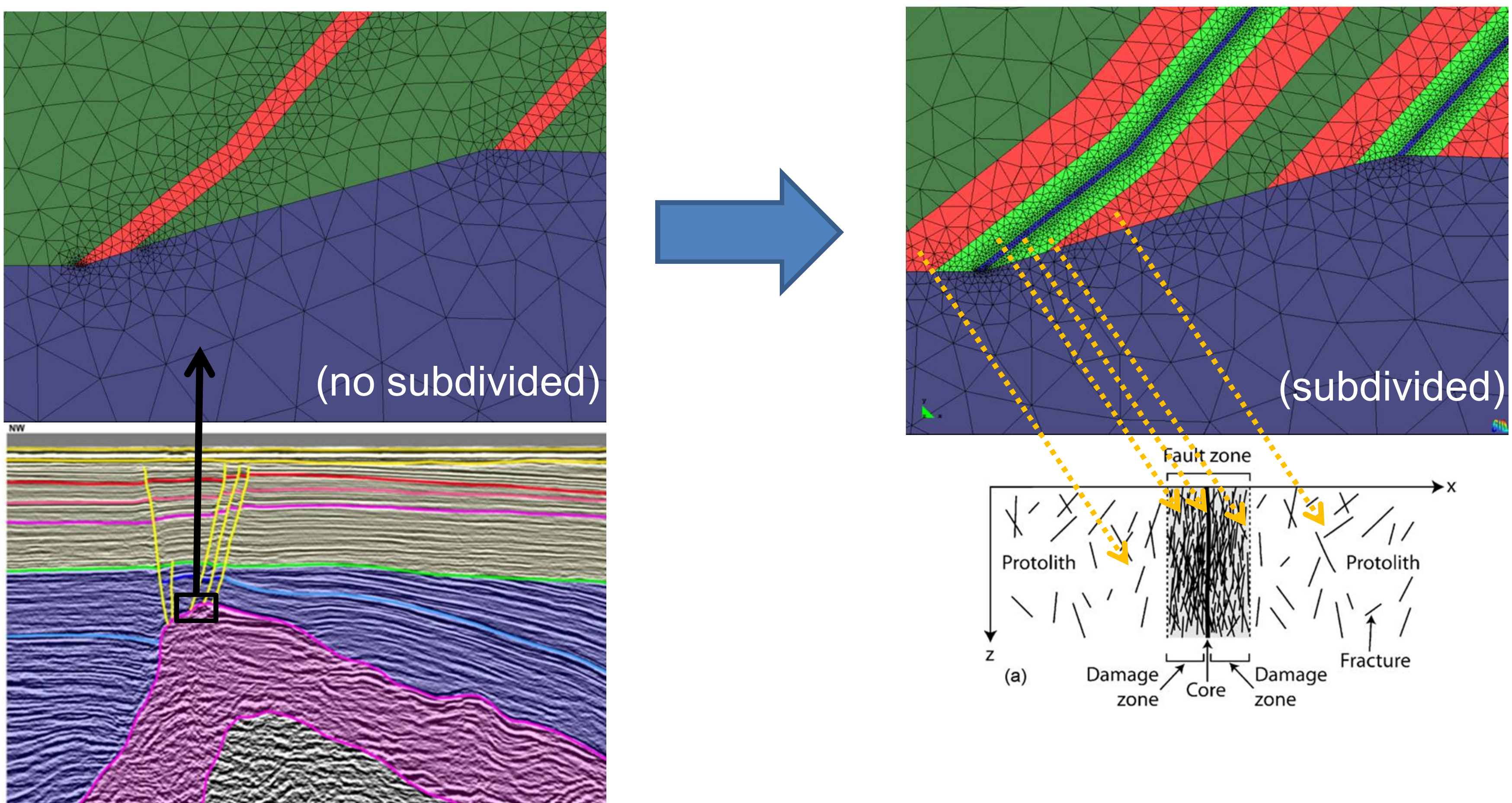

Geological fault reactivation considering damage zones

✓ **Numerical Study of the Influence of Filling Material Stiffness on the Fault Reactivation Mechanism.**

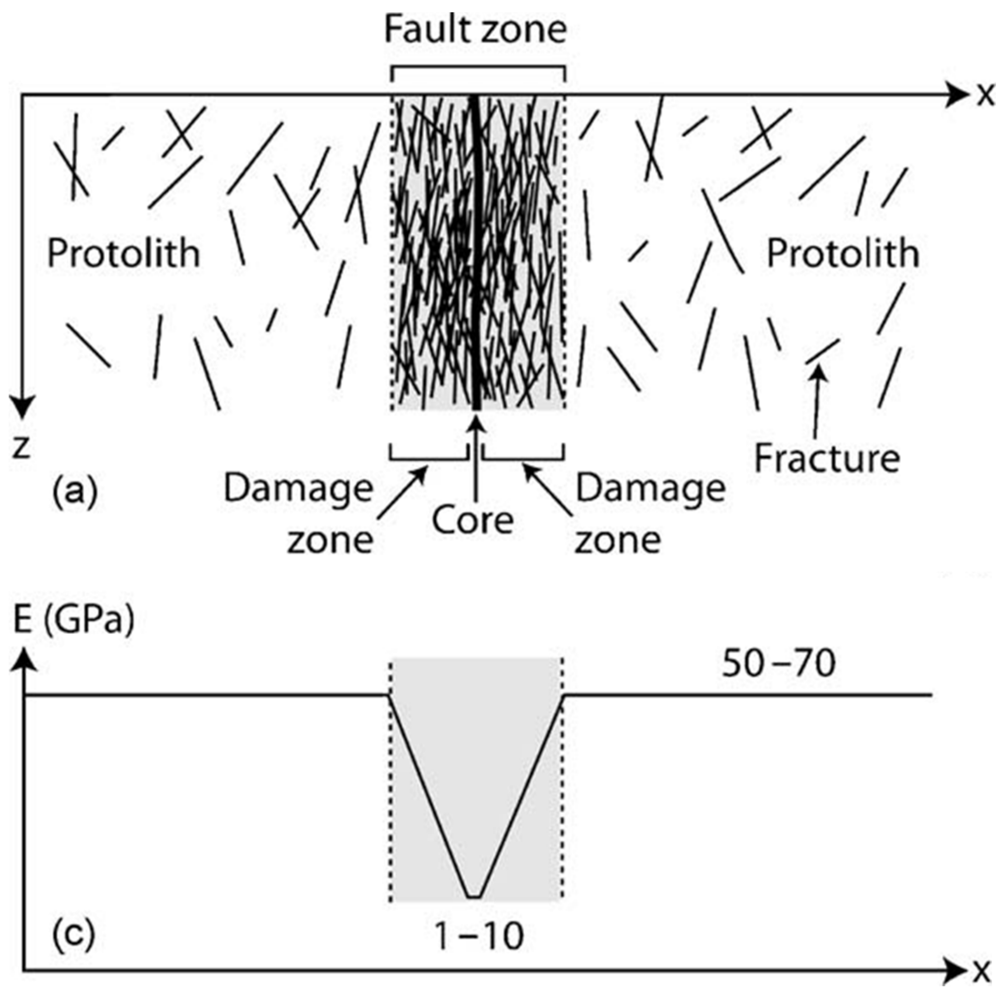

(Constantin *et al*, 2004)

Geological fault reactivation considering damage zones

✓ **Coupled Hydro-mechanical Modelling of the Permeability Change of Sealing Faults in Oilfield Exploitation.**

-HM modeling;
-HMC modeling: filling material dissolution.

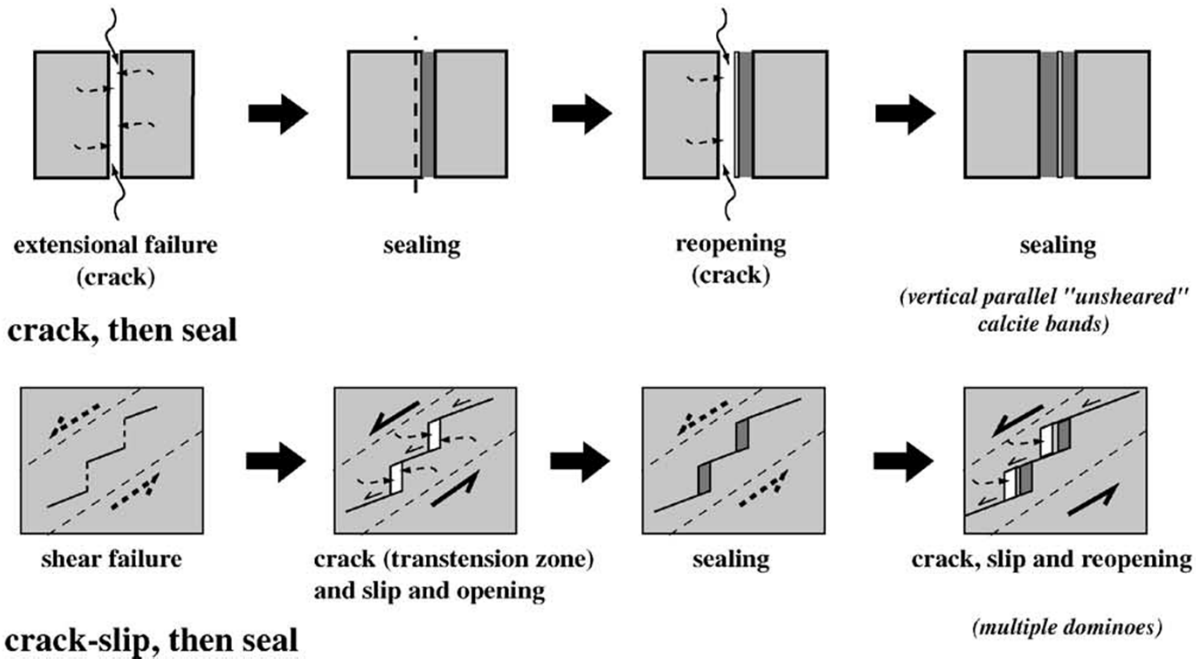

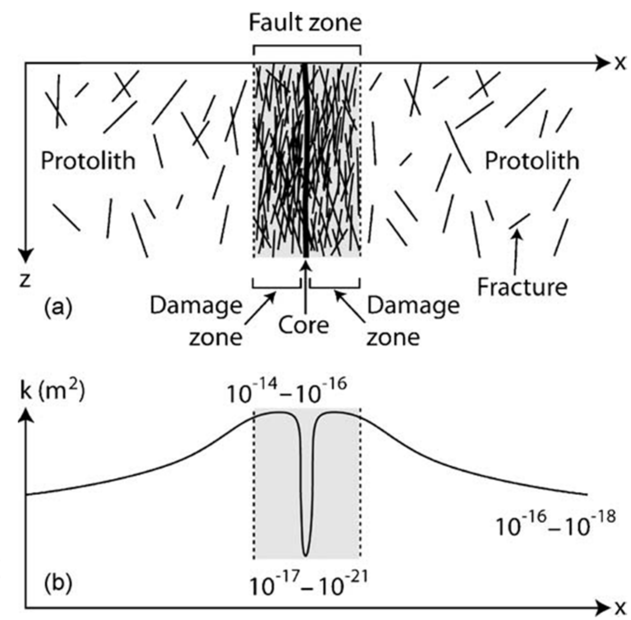

(Mitchell and Faulkner, 2009)

RESULTS

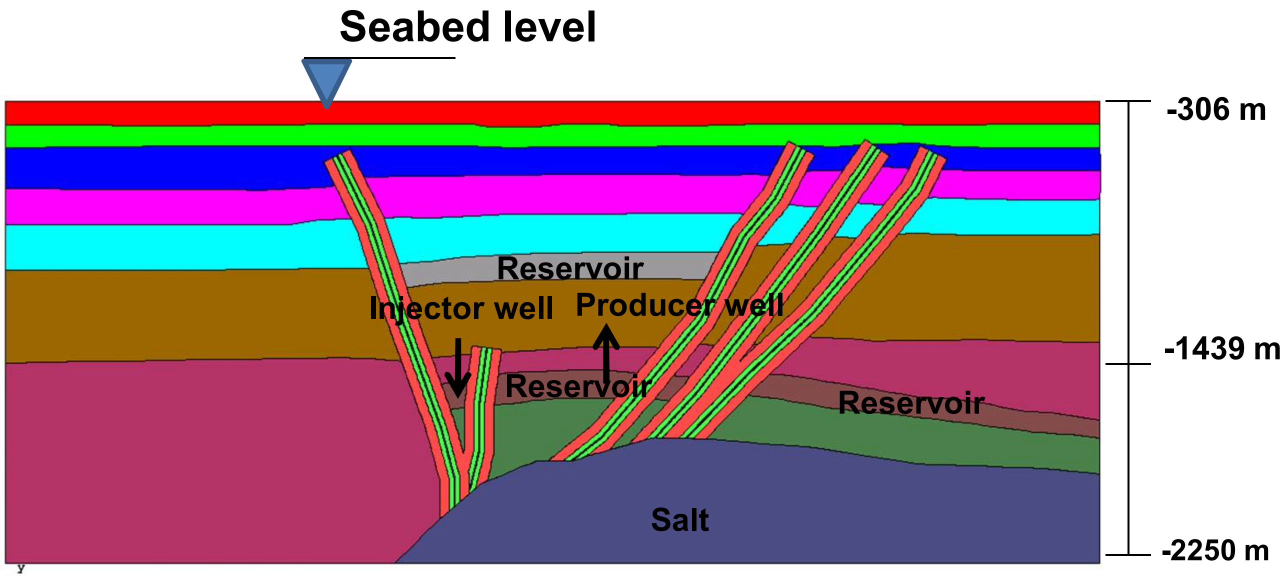

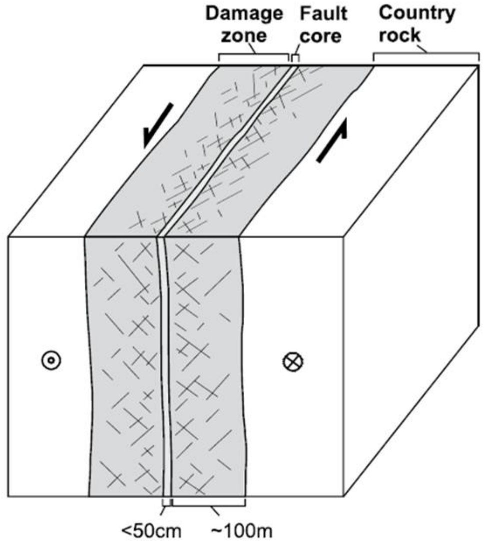

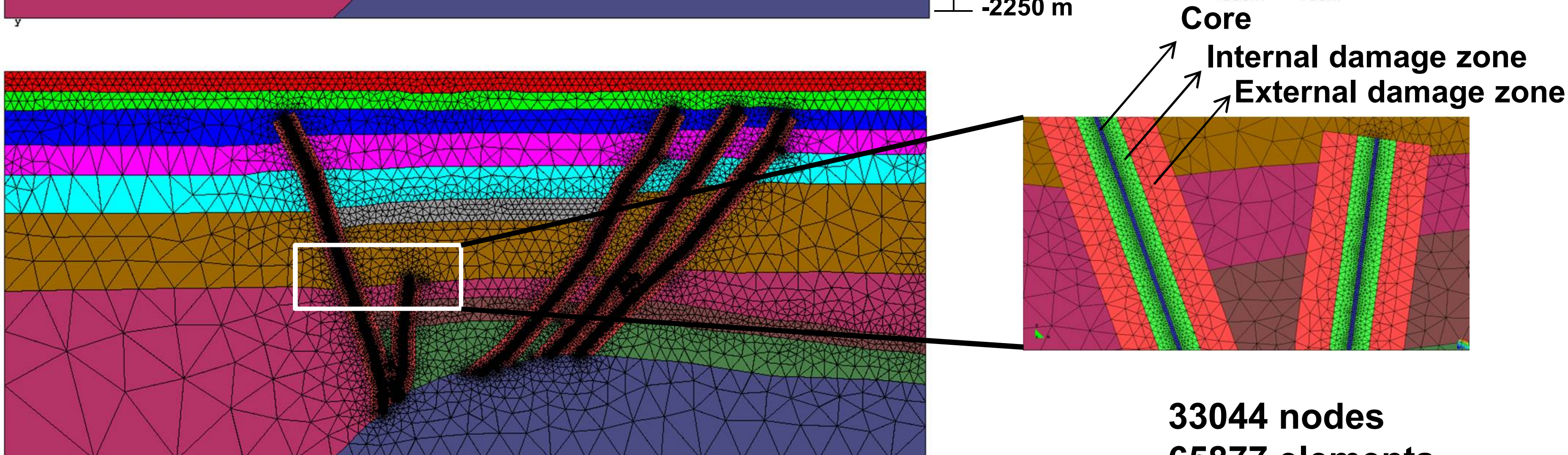

33044 nodes
65877 elements

RESULTS

	Material Properties			
Fault elements	Young Modulus (MPa)	Coesion (MPa)	Friction Angle (°)	Permeability (m²)
External damage zone	7000	3.25	23	$5x10^{-21}$ m²
Internal damage zone	6000	2.5	23	$5x10^{-20}$ m²
Core	8000	4.0	23	$5x10^{-22}$ m²

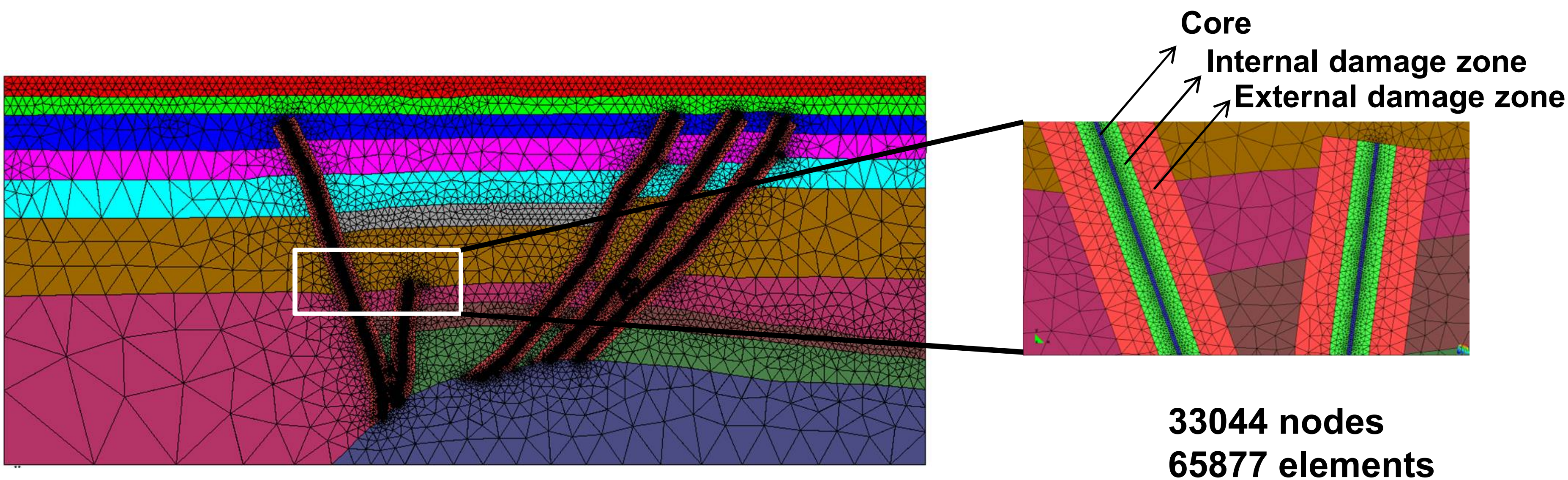

33044 nodes
65877 elements

RESULTS

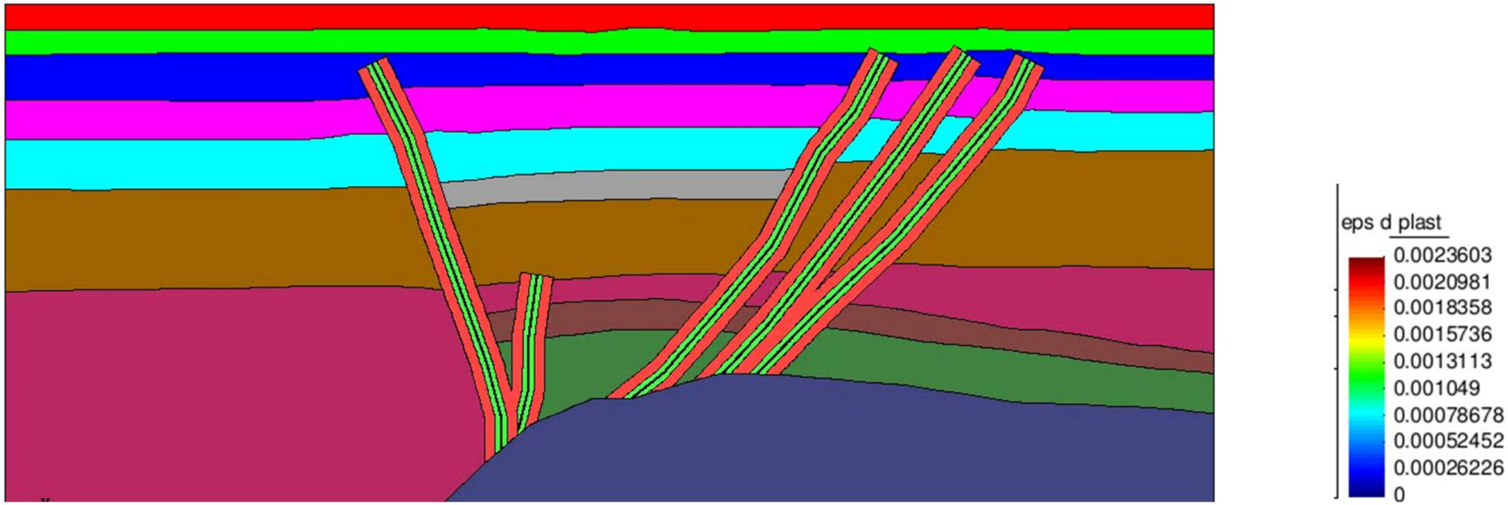

Parameters of Sensitivity :

-Coesion and friction angle;
-Stifness;
-K0, Poison Ratio;
-Shear plastic strain limit;
-Fluid compressibility;
-Permeability;
-Anisotropy;
-Mechanical constitutive model;
-Wellbore position;
...

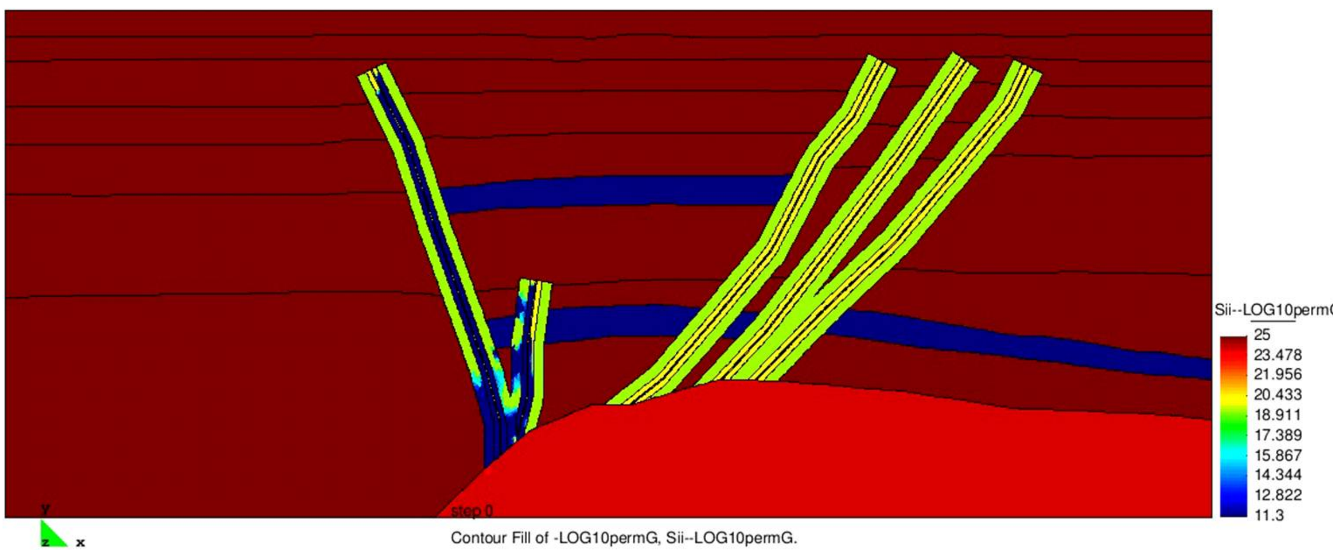

RESULTS

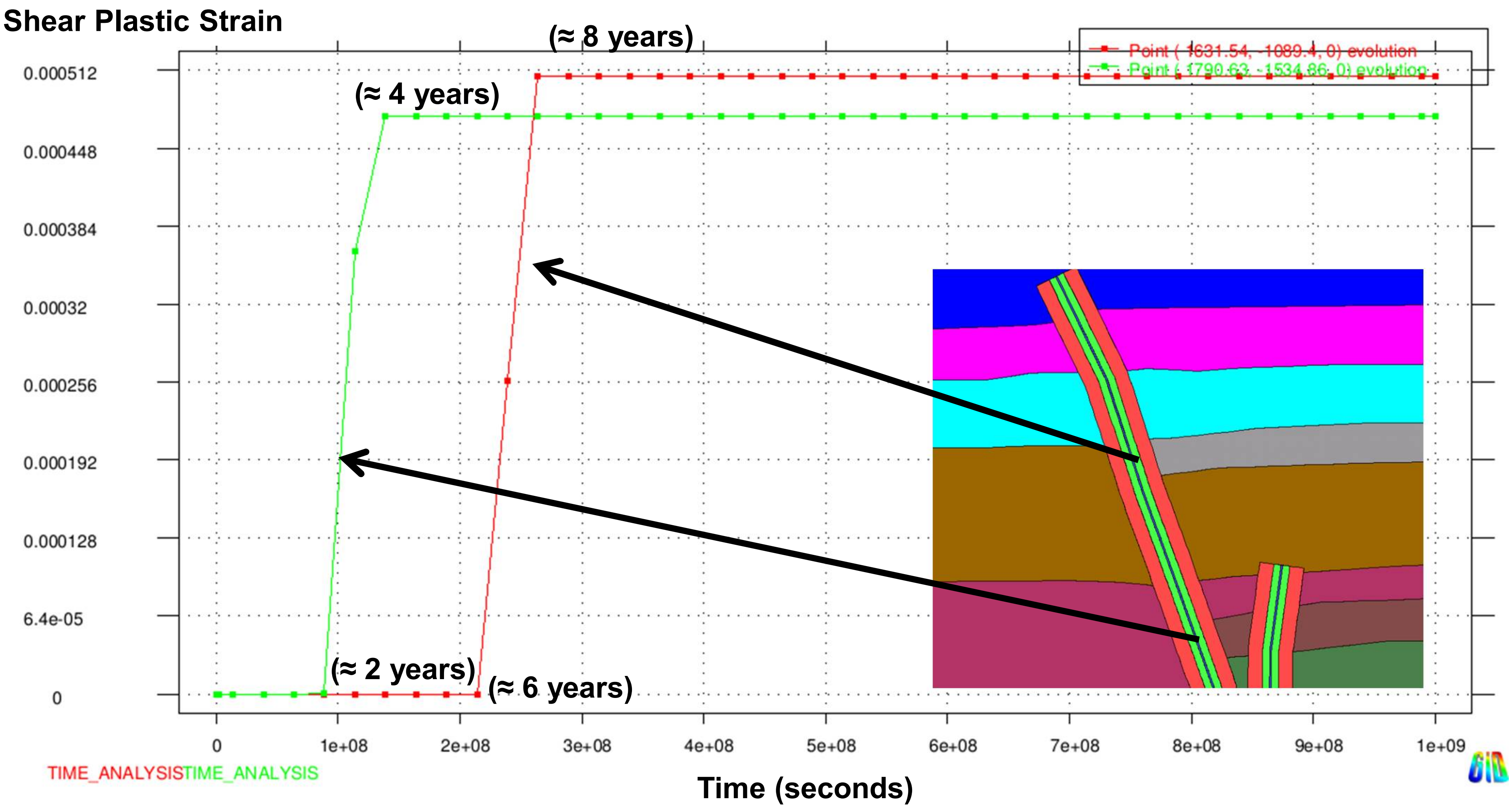

Shear Plastic Strain
(≈ 8 years)
(≈ 4 years)
(≈ 2 years)
(≈ 6 years)
Point (1631.54, -1089.4, 0) evolution
Point (1790.63, -1534.86, 0) evolution
0.000512
0.000448
0.000384
0.00032
0.000256
0.000192
0.000128
6.4e-05
0
0
1e+08
2e+08
3e+08
4e+08
5e+08
6e+08
7e+08
8e+08
9e+08
1e+09
TIME_ANALYSISTIME_ANALYSIS
Time (seconds)

RESULTS

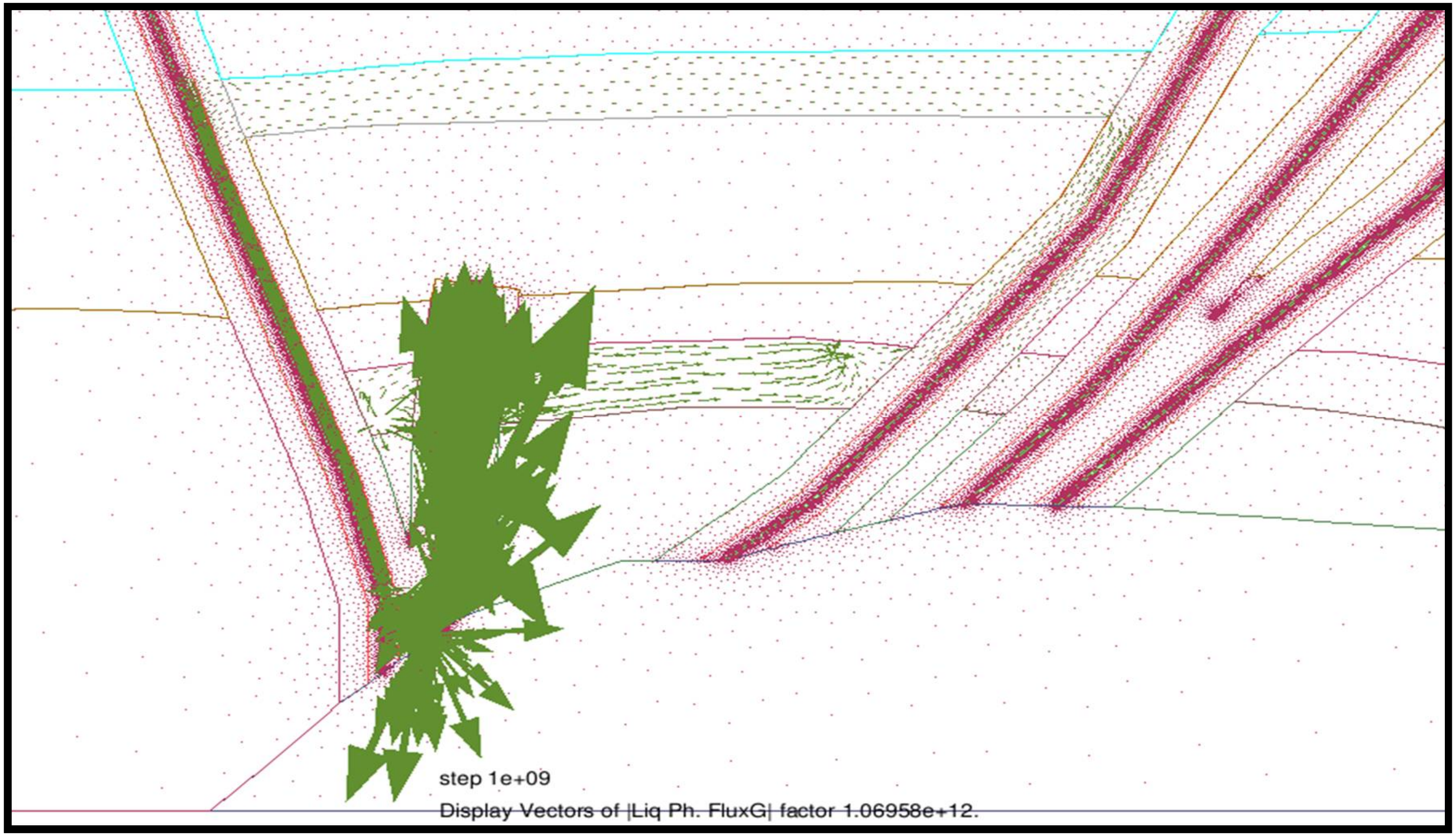

RESULTS

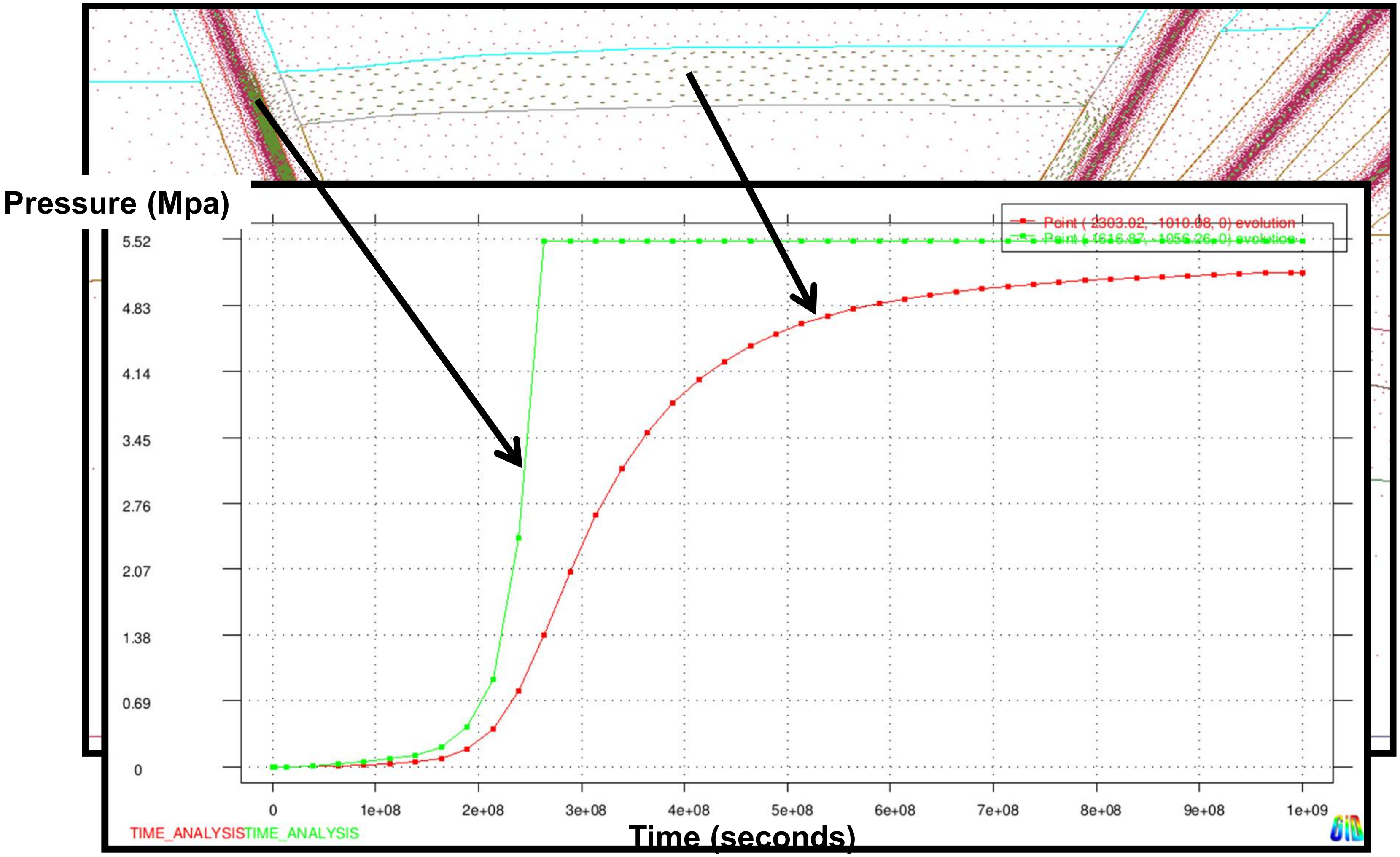

Pressure (Mpa)
5.52
4.83
4.14
3.45
2.76
2.07
1.38
0.69
0
0
1e+08
2e+08
3e+08
4e+08
5e+08
6e+08
7e+08
8e+08
9e+08
1e+09
Time (seconds)
TIME_ANALYSISTIME_ANALYSIS

RESULTS

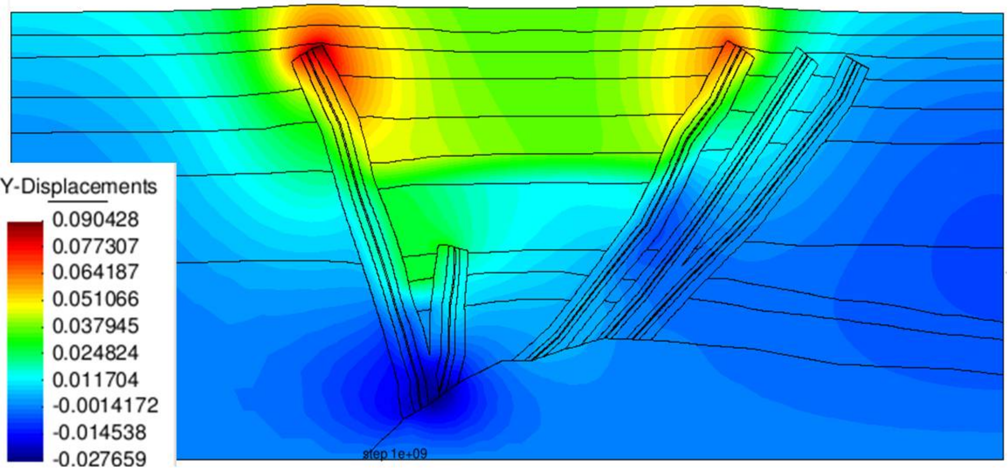
Y-Displacements
0.090428
0.077307
0.064187
0.051066
0.037945
0.024824
0.011704
-0.0014172
-0.014538
-0.027659
step 1e+09

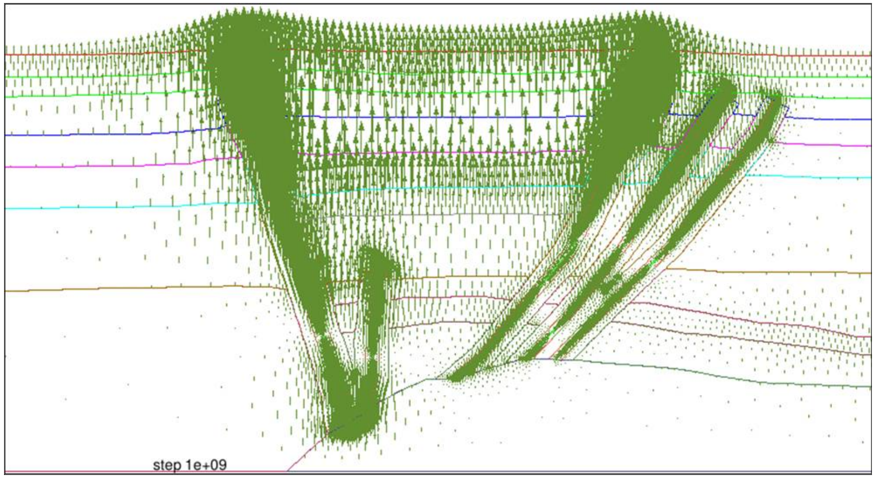
step 1e+09

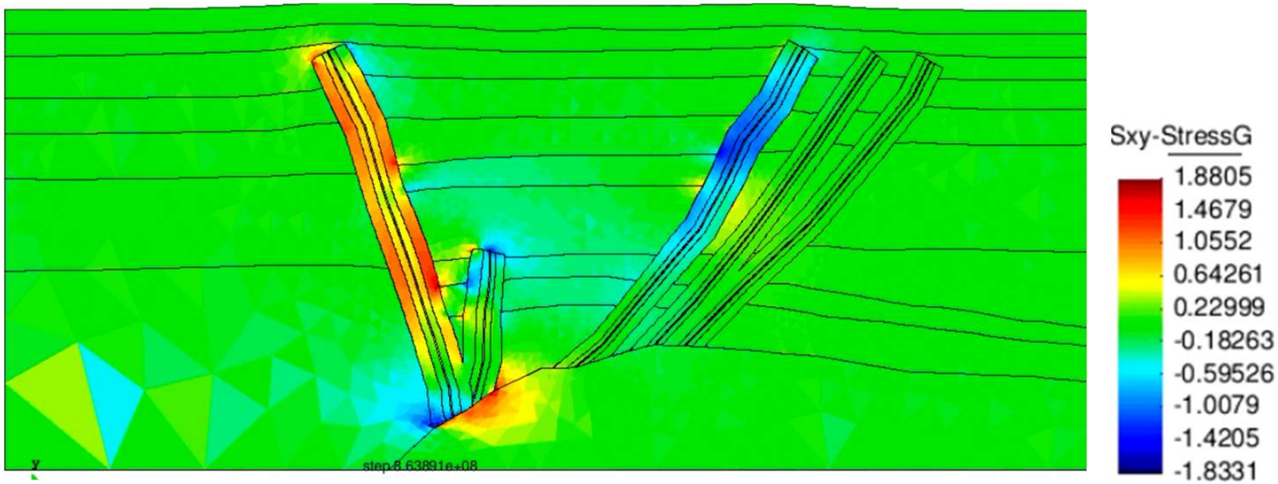
Sxy-StressG
1.8805
1.4679
1.0552
0.64261
0.22999
-0.18263
-0.59526
-1.0079
-1.4205
-1.8331
step 8.63891e+08

RESULTS

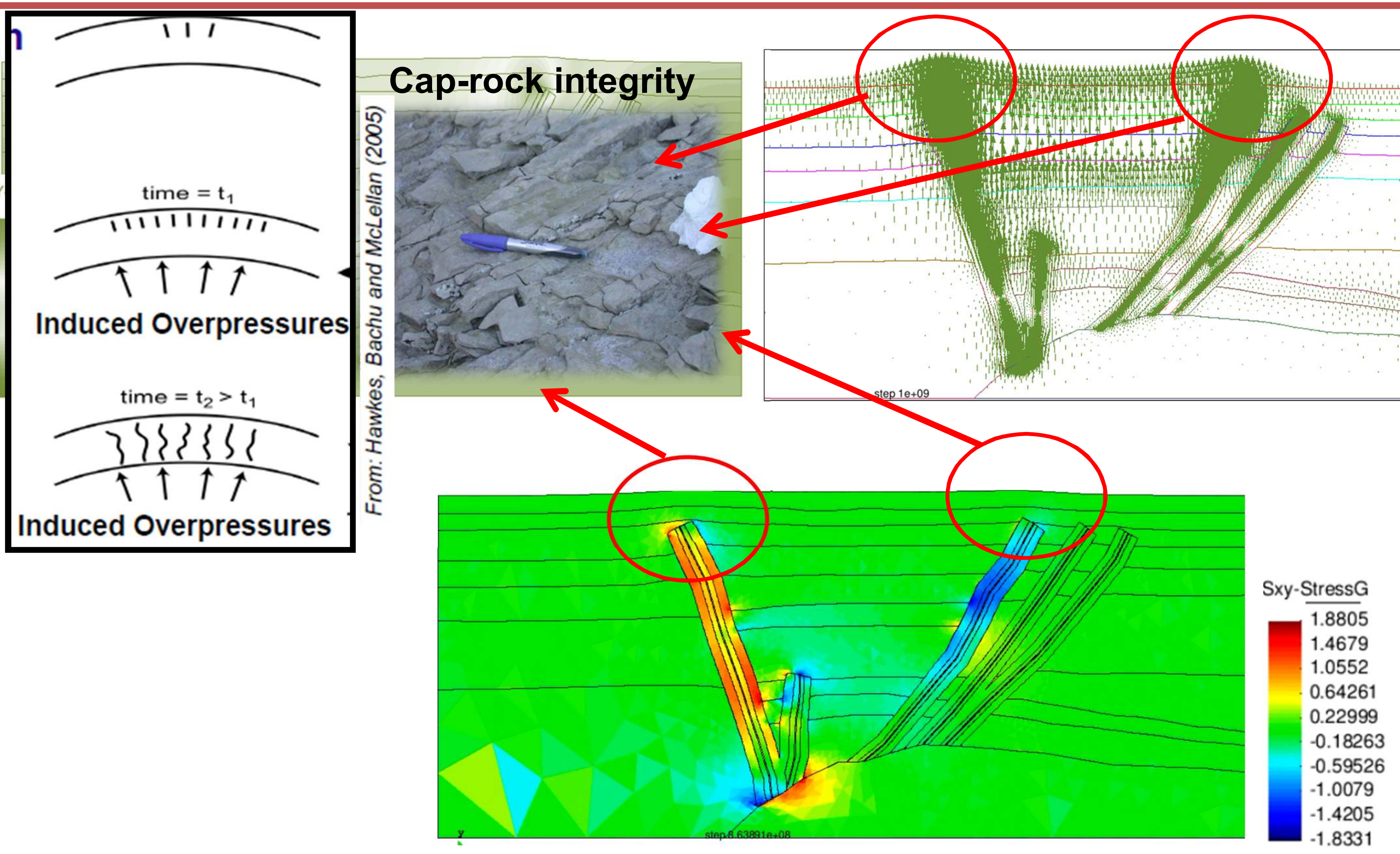

time = t_1
Induced Overpressures
time = $t_2 > t_1$
Induced Overpressures
Cap-rock integrity
From: Hawkes, Bachu and McLellan (2005)
step 1e+09
Sxy-StressG
1.8805
1.4679
1.0552
0.64261
0.22999
-0.18263
-0.59526
-1.0079
-1.4205
-1.8331
step 8.63891e+08

RESULTS

	Material Properties			
Fault elements	Young Modulus (MPa)	Coesion (MPa)	Friction Angle (°)	Permeability (m²)
External damage zone	7000	~~3.25~~ 2.7	23	$5x10^{-21}$ m²
Internal damage zone	6000	2.5	23	$5x10^{-20}$ m²
Core	8000	4.0	23	$5x10^{-22}$ m²

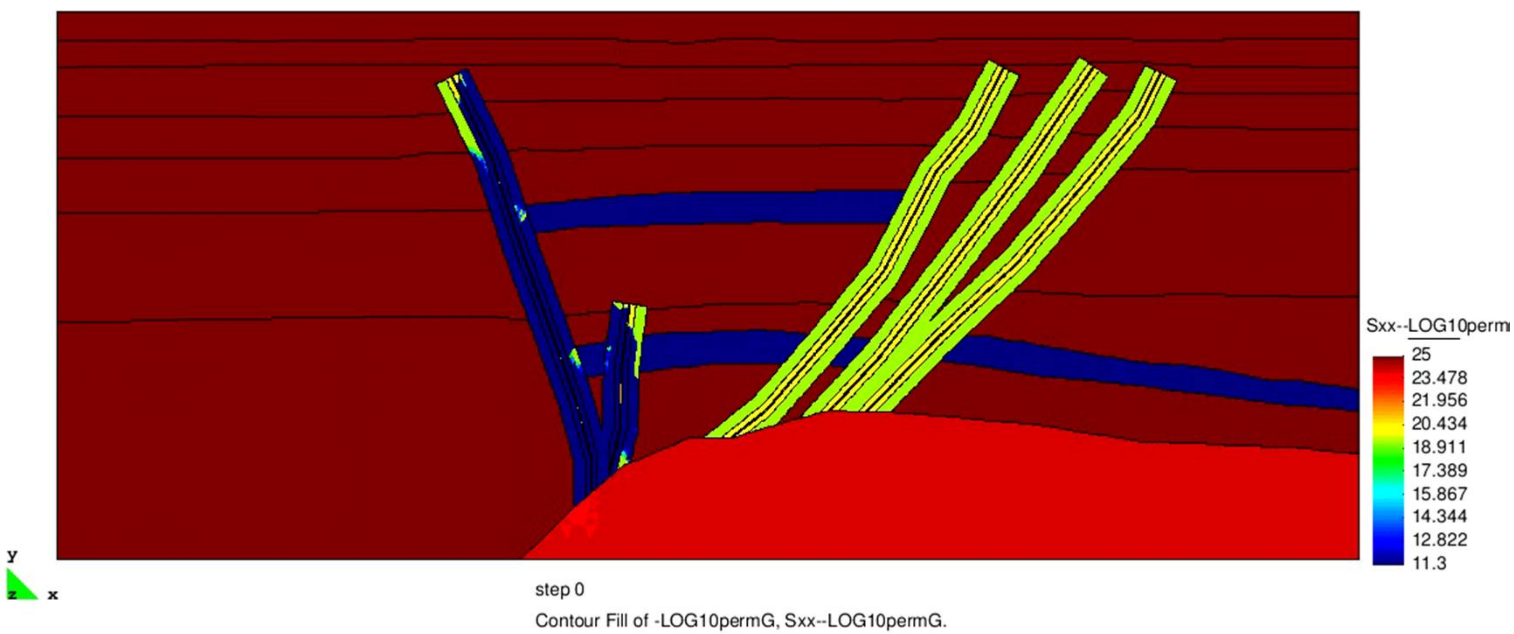

RESULTS

	Material Properties			
Fault elements	Young Modulus (MPa)	Coesion (MPa)	Friction Angle (°)	Permeability (m²)
External damage zone	7000	~~3.25~~ 2.7	23	$5x10^{-21}$ m²
Internal damage zone	6000	2.5	23	$5x10^{-20}$ m²
Core	8000	4.0	23	$5x10^{-22}$ m²